Effect of market fuel variation and cetane improvers on CAI combustion in a GDI engine

by

Kevin David Cedrone

B.A.Sc., Honours Mechanical Engineering
University of Waterloo (2008)

Submitted to the Department of Mechanical Engineering
in partial fulfillment of the requirements for the degree of

Master of Science in Mechanical Engineering

at the

MASSACHUSETTS INSTITUTE OF TECHNOLOGY

June 2010

Author .....
Department of Mechanical Engineering
May 7, 2010

Certified by .....
Wai K. Cheng
Professor of Mechanical Engineering
Thesis Supervisor

Accepted by .....
David Hardt, Professor of Mechanical Engineering
Chairman, Department Committee on Graduate Theses

Effect of market fuel variation and cetane improvers on CAI combustion in a GDI engine

by

Kevin David Cedrone

Submitted to the Department of Mechanical Engineering
on May 7, 2010, in partial fulfillment of the
requirements for the degree of
Master of Science in Mechanical Engineering

Abstract

There is continued interest in improving the fuel conversion efficiency of internal combustion engines and simultaneously reducing their emissions. One promising technology is that of Controlled Auto Ignition (CAI) combustion. The lack of direct combustion control makes control of CAI combustion challenging. Practical implementation of CAI an engine, the engine's behaviour must be predictable. This work investigates the impact of market fuel composition variation and cetane improver additives on CAI combustion in a gasoline direct injection (GDI) engine.

The test fuels were blends of different commercial refinery products, containing hundreds of hydrocarbon species. The blends were selected to vary Research Octane Number (RON), olefin content, and aromatic content. The blends were chosen based on a market fuel study done by the project sponsor, and subsequent research conducted at MIT.

Cetane number improvers are diesel fuel additives used to shorten ignition delay in Diesel engines. Di-tert-butyl ether (DTBP) and 2-ethylhexylnitrate (2EHN) were added in concentrations of 4800ppm and 2000ppm respectively to one of the test fuels in an attempt to extend the low load limit (LLL) of CAI operation.

Fuel type was found to have a modest impact on the CAI operating range. Valve timing was largely capable of compensating for the changes observed. Neither cetane additive had any significant impact on CAI operation. GDI allowed the use of a split injection strategy involving a pilot injection during negative valve overlap (NVO) recompression, before the main injection during the intake stroke. This strategy, employed at low loads, resulted in heat release during the NVO recompression, which advanced and stabilized main combustion process. At higher engine speeds, the split injection strategy resulted in lower indicated fuel conversion efficiency.

Thesis Supervisor: Wai K. Cheng
Title: Professor of Mechanical Engineering

Acknowledgements

I would like to thank my thesis advisor Professor Wai Cheng. I have learned a great deal from you in the lab and in the classroom. I am becoming a better scientist, engineer and researcher with each passing day thanks to your support and guidance. I have enjoyed the freedom and opportunity to develop my own ideas and research strategies and I look forward to working with you over the next few years.

I would like to thank Ford Motor Company and BP, without whose sponsorship this research project would not have been possible. Special thanks to Tom Kenney of Ford for the effort and expertise he shared in the early stages of my project. Thanks to Brad VanDerWege of Ford for insightful suggestions and ideas shared during the execution of the project. Thanks also go to Samir Chahine of BP for the time and input you shared during all phases of the project.

I would be remiss if I did not acknowledge the Sloan Automotive Lab staff. My time in the lab so far has been helped along by the efforts of Janet Sabio, Karla Stryker and Thane DeWitt. Special thanks to lab technician Raymond Phan for practical design advice and lightning-fast, bulletproof fabrication. Thanks to Boston Volvo and Lee Volvo in Wellesley, MA for help with parts and tools for my engine. I want to thank Leslie Regan, Joan Kravit and Una Sheehan in the Mechanical Engineering Graduate Office for their tireless efforts, they have made my time in MechE at MIT incalculably easier.

I want to thank my fellow Sloan Automotive Lab students past and present. My days at MIT were made easy by the likes of RJ Scaringe, Craig Wildman, Vince Costanzo, Vikram Mittal, Alex Sappok and Iason Dimou who all offered help around the lab, advice on setting up an engine from scratch and advice on qualifying exams. Special thanks to Eric Senzer, Emmanuel Kasseris and Justin Negrete for spit-balling research ideas, lending a hand, holding a wrench, sharing coffee and offering moral support while I pushed myself and my engine to the limit.

Finally I would like to thank my family and friends for their support during my time at MIT.

This page intentionally left blank

Contents

This page intentionally left blank

List of Figures

This page intentionally left blank

List of Tables

This page intentionally left blank

Chapter 1

Introduction

As a leading portable power source for outdoor appliances, backup generators and transportation applications, the internal combustion engine (ICE) plays a vital role in modern life Amidst growing concerns over climate change and increasingly demanding fuel economy and emissions standards there is renewed interest in improving efficiency and emissions performance of automotive ICEs. One promising technology for improving the common 4-stroke ICE is Controlled Auto-Ignition (CAI), sometimes also called is Homogeneous Charge Compression Ignition (HCCI).

CAI is an alternative to conventional diesel fuelled Compression Ignition (CI) and gasoline fuelled Spark Ignition (SI) engines. In many ways CAI resembles a sort of hybrid between these two conventional operating modes and has been demonstrated on hardware intended for each. Compared to conventional engine operation, CAI has demonstrated the potential for drastically lower emissions of oxides of nitrogen (NO_x) and particulate matter with efficiency superior to SI engines, and on par with CI engines. [1]

1.1 Conventional SI and CI engines

In a typical cycle of an SI engine, a fresh charge of fuel and air is inducted and compressed before the spark ignites the charge. Stringent emissions standards require after-treatment of engine exhaust. Hence for reasons relating to exhaust after-

treatment, the fuel-air mixture is usually stoichiometric and contains some recirculated exhaust gases from a previous cycle. Whether the fuel is injected in the intake runner, so-called Port Fuel Injected (PFI), or directly into the combustion chamber, Gasoline Direct Injection (GDI) the charge is usually homogeneous at the time of combustion. A turbulent flame expands outwards from the spark plug, consuming the fuel-air mixture and converting it to product gases. The hot, high-pressure gases are expanded to convert their thermal energy into mechanical work. Engine power output is proportional to fuel input. Since the ratio of fuel-to-air is fixed by emissions after-treatment requirements, the supply of air must be restricted (i.e. throttled) in order to vary the power output.

In a typical cycle of a CI engine, a fresh charge of air only is inducted and compressed. At the opportune moment, fuel is injected into the cylinder and it ignites in a diffusion flame. The fuel and air combust wherever they meet in the correct proportions. It resembles a blowtorch flame and is essentially stationary spatially compared with the travelling flame in an SI engine. The heat released from the flame increases the temperature and pressure in the cylinder. Globally throughout the combustion chamber there is excess air (i.e. combustion is lean) but because the fuel ignites almost instantly there is insufficient time for complete mixing and numerous zones of rich combustion produce soot and subsequently high particulate emissions. The combination of high temperatures and excess air also result in NO_x emissions that are higher for CI than SI engines. As in an SI engine, hot product gases are expanded to convert thermal energy of the working fluid to mechanical work.

CI engines utilize a diffusion flame so they do not require a mixture with a narrow range of fuel to air ratio. Hence CI engines do not throttle the intake of air and instead vary both fuel and fuel-air ratio to control engine output. The lack of throttle losses is part of the reason for their comparative efficiency advantage over SI engines, especially at low loads.

1.2 Auto-ignition and knock

CI engines gain a comparative efficiency advantage over SI engines from their lean charge and higher compression ratio. The lean charge results in a higher specific heat ratio for leaner CI fuel-air mixtures. The fuel-air mixture in an SI engine cannot be compressed as much as the air-only charge of a CI engine because of a phenomenon known as knock.

Knock is the auto-ignition of the fuel-air mixture in the combustion chamber that has not yet been consumed by the flame. The flame front in an SI engine burns and expands outwards at a finite rate. As it burns, it is heating and compressing the fuel and air mixture that have not burned yet, the end gas. If the temperature and pressure of this mixture get high enough and there is sufficient time for the chemical reaction, the mixture will ignite and combust before the flame can consume it. Once initiated, the auto-ignition process (of converting fuel and air to products) is considerably faster than the flame-combustion process. Thus the remaining end gas reacts almost instantaneously, and there is a corresponding spike in the heat release and pressure rise rates. Heat release occurs so quickly that the surrounding gas cannot equilibrate the pressure fast enough and acoustic standing waves are created in cylinder. This yields a characteristic pinging or knocking noise.

Every SI cycle is a sort of race then, between the consumption of fuel and air by an orderly turbulent flame, or the unruly auto-ignition of a parcel of not-yet-reacted fuel and air mixture. Considerable effort is expended in SI engine operation to avoid engine knock due to its harsh noise and potentially damaging effects on mechanical components in the engine. Gasoline-based fuels are formulated to lengthen their ignition delay time and hence their resistance to engine knock. Diesel fuels are formulated to have a short delay time, but just long enough to permit mixing of fuel with the air in cylinder.

CAI is a controlled version of the auto-ignition phenomenon. Knock is dangerous in SI engines because it occurs in the late stages of combustion when temperatures and pressures are already very high and a sudden pressure spike is very undesirable.

In CAI, the charge is usually lean and diluted with exhaust residuals to limit the heat release and reaction rate and consequently the pressure rise, and pressure rise rate. The dilute charge burns at lower temperatures leading to lower NO_x emissions. As shown in Fig. 1-1 the rapid nearly-volumetric reaction more closely approximates the ideal Otto-cycle than a standard SI cycle; thus more work can be extracted in the expansion process. CAI emissions are low enough to permit the combustion of a lean and dilute mixture so no intake throttle is necessary. As with CI combustion, this confers an efficiency advantage over SI engines. Owing to the dilute, lean mixture, higher compression ratios are available compared to SI engines. [1]

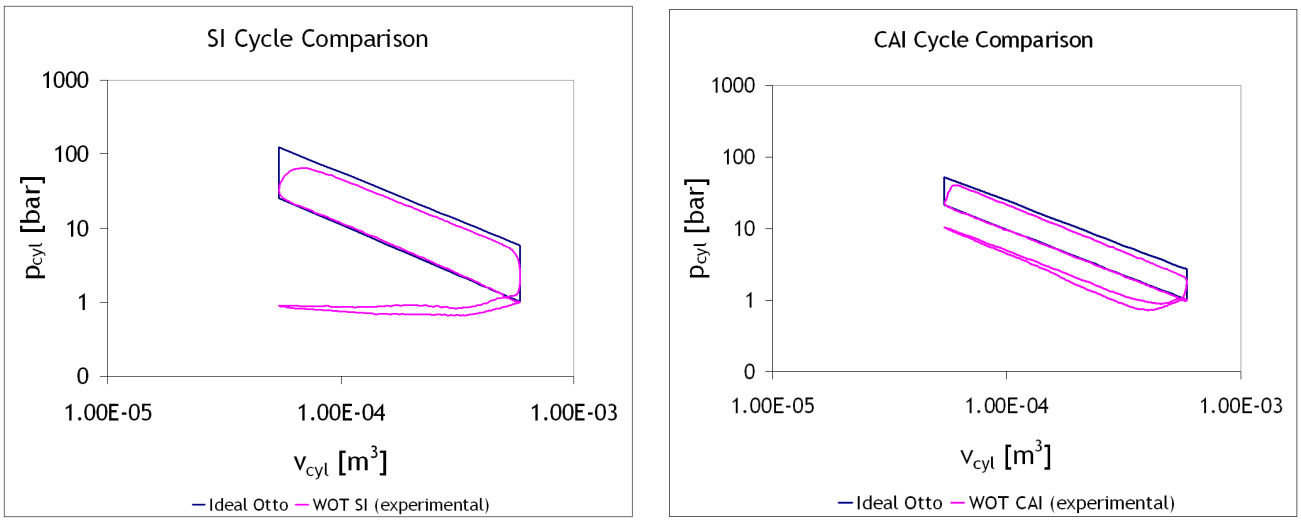

(a) Comparison of ideal Otto cycle and SI cycle

(b) Comparison of ideal Otto cycle and CAI cycle

Figure 1-1: P-V diagram comparison for ideal Otto, and experimental SI and CAI cycles.

1.3 CAI theory of operation

The in-cylinder charge of fuel and air must be brought to a sufficiently high temperature and pressure for a certain period of time before autoignition will occur. In general, higher temperature and pressure result in a shorter ignition delay. However, based on the underlying chemical kinetics, the minimum temperature and pressure required and the ignition delay vary as a function of the fuel and mixture compo-

sition. The dependence is complex and even ambient conditions like humidity have been show to influence autoignition behaviour. Hence, lacking direct combustion control like spark timing in SI or fuel injection timing in CI engines, CAI engines are more susceptible to fuel chemistry effects in determining the timing of combustion.

To control autoignition in a practical CAI engine, the temperature, pressure and composition of the charge must be controlled. Many mechanisms have been proposed. Some strategies include variable compression ratio (VCR) engines, fast thermal management (i.e. variable intake air heating) and the use of exhaust residuals to preheat the incoming charge. Exhaust residuals may be used via exhaust gas recirculation (EGR) or trapped residuals by early exhaust valve closure and negative valve overlap (NVO). Positive valve overlap refers to operation where the exhaust valve closes after the piston reaches top dead centre (TDC), while the intake valve opens before TDC. Hence negative valve overlap occurs when the exhaust valve closes before TDC and the intake valve opens after TDC. Symmetric NVO occurs when the exhaust valve closes the same amount before TDC as the intake valve opens after TDC. Generally this results in the least amount of pumping work although there are potential benefits and limitations that might suggest the use of asymmetric valve timing. Early EVC and NVO are used to trap residuals and preheat new charge in the present work. Fig. 1-2 shows the large NVO used by CAI cams compared to the small positive overlap used to improve scavenging in typical SI operation. Using combustion products from previous cycles to pre-heat reactants for subsequent cycles has a few additional implications. Residuals act as a diluent to reduce in-cylinder oxygen concentration. This can retard chemical reactions, depress reaction rates and hence limit HRR and PRR. Using trapped residuals also increases the engines dependence on its temperature/pressure history since the results of the previous cycle remain in-cylinder and are carried over to subsequent cycles. As will be elaborated later, CAI combustion faces certain operational limitations. CAI has been proposed for use in certain limited areas of the operating envelope and conventional SI or CI elsewhere. Such mixed-mode engines require the use of high residual gas fractions (RGF), typically around 30-70% by volume, meaning the engine displays a much stronger dependence on its history

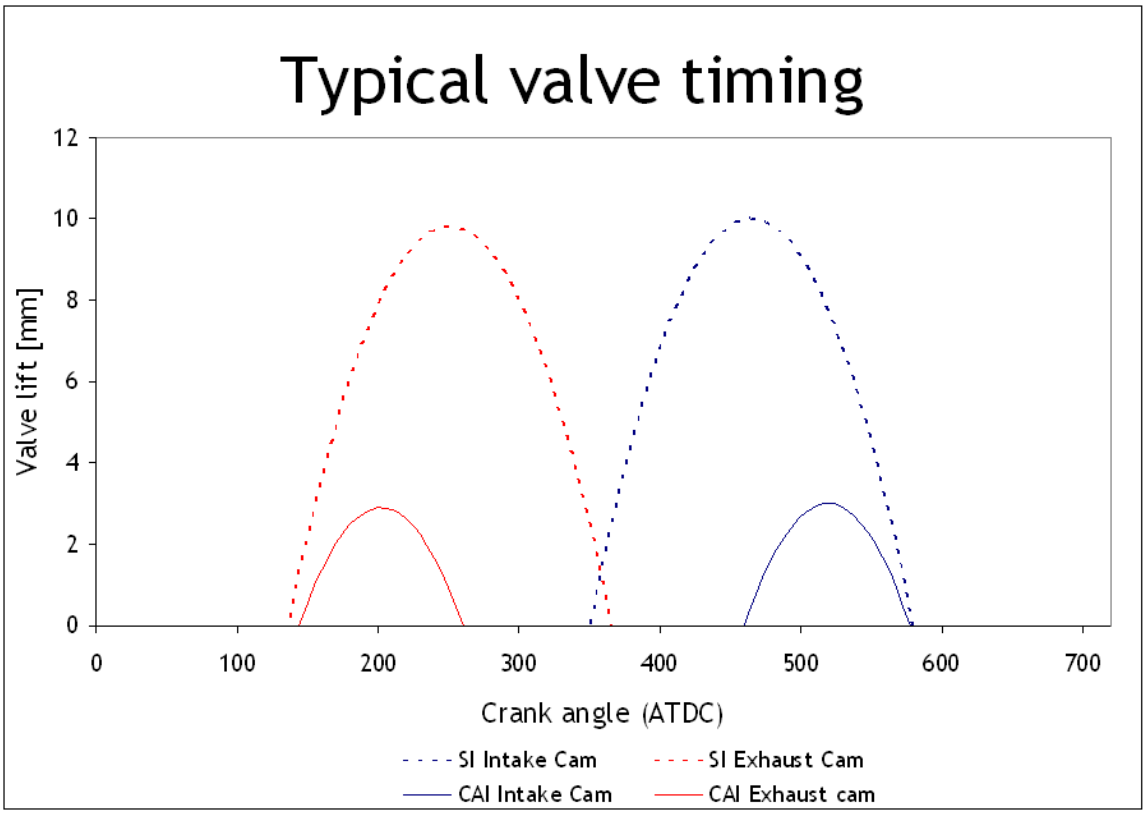

Figure 1-2: Typical cam timing and lift for SI and CAI mode with NVO

than conventional SI or CI engines. Also, such a high RGF significantly reduces the volume and density of fresh charge. The resultant decrease in volumetric efficiency reduces the power density of the engine.

Some implementations of trapped-residual CAI tailor their fuel injection strategies to achieve a spatially stratified charge, to control the local autoignition properties. Some of these implementations use a spark plug and actually realize partial flame propagation before bulk auto-ignition. Other variants use spark-assist to jump-start autoignition in the absence of an actual pre-mixed flame.

Pre-heating the charge widens the combustible limits so leaner charges can be burned. Although dilution with residuals lowers the specific heat ratios, lean charges have a higher specific heat ratios. Since autoignition is the objective of CAI and not a constraint, higher compression ratios can be used than with SI. These increases in specific heat ratio and compression ratio increase the efficiency of the engine.

1.4 Limitations of CAI

1.4.1 Emissions

CAI is not without problems. Lean dilute mixtures burn at low temperatures, which can lead to higher unburned hydrocarbon (UHC) and carbon monoxide (CO) emissions compared with conventional engines. For maximum fuel-conversion efficiency and engine stability, the fuel-air charge must react at the appropriate time, that is the challenge is to control combustion phasing of CAI. Early phasing (before the piston reaches top center) will increase the heat loss and therefore decrease efficiency. Late phasing will slow down the chemistry as expansion cools and potentially quenches the reacting mixture.

1.4.2 Control

Conventional SI and CI engines exert direct control over the start of combustion through the timing of spark and fuel injection respectively. CAI has no such direct control over the initiation of combustion. The in-cylinder temperature, pressure and mixture composition determine combustion phasing. As such CAI combustion is more difficult to control than conventional combustion. Many approaches have been investigated for controlling CAI combustion phasing including variable compression ratio, fast thermal management and intake air heating, and dual-fuel use.

1.4.3 Load limits

The restricted load limits are arguably the most serious practical limitation on CAI technology. In order for auto-ignition to occur in the engine, the fuel-air mixture charge must reach a specified temperature and pressure. In many practical implementations hot residual gases from a previous cycle are used to preheat the incoming charge for the next cycle. RGF is used to control engine output (load). A high RGF means less fuel and air to react, and hence a low load. A low RGF means more fuel and air and hence a high load.

The Low Load Limit (LLL) arises as follows. At progressively lower loads, less fuel is injected and less heat is released which leads to progressively cooler product gas temperatures. Hence although the RGF increases the temperature of the residuals decreases and eventually the overall thermal content of the RGF is insufficient to preheat the new charge and combustion is unstable. The instability arises because a single misfire will yield unburned fuel, a portion of which is trapped with the RGF which enriches the following cycle whose residuals will be hot. The cycle following that will only release heat from the normal amount of fuel and its heat release will result in cooler exhaust. Unstable combustion is not tolerable for passenger vehicles for which Noise, Vibration and Harshness (NVH) considerations limit the instability. If RGF is further increased and fuelling further decreased combustion will be impossible and persistent misfires will result.

There are two possible High Load Limit (HLL). The first is a similar to the LLL. As load increases, fuel and air increase and RGF decreases. More fuel and air means more heat release and hotter products. Although product temperatures are increasing, RGF is decreasing and eventually the overall thermal content of the RGF is insufficient to preheat the new charge. In GDI engines, the thermal energy for evaporating fuel comes from the in-cylinder charge. Hence at higher loads, more fuel must be evaporated and the thermal requirement increases.

Heat release increases with fuel amount. By their very nature, the autoignition reactions are very fast and their reaction rates generally increase at higher temperature. Hence an increase in fuel amount increases the Heat Release Rate (HRR) and Pressure Rise Rate (PRR) as well. The heat release increases the temperature and pressure of the charge so PRR scales with HRR. Excessive PRR can lead to mechanical failure, but before that it usually leads to ringing much like conventional engine knock. Hence this NVH concern constrains the HLL of CAI engines in vehicle applications.

The HLL and LLL both decrease as engine speed increases. At high engine speed there is less heat transfer from the in-cylinder charge. Hence the charge retains more of its enthalpy. Near the HLL the higher temperatures mean a higher HRR, then to

meet a given PRR constraint the fuel mass must be reduced at higher engine speeds. At the LLL the higher temperatures arising from reduced heat transfer mean that less enthalpy from trapped residuals is required. Hence the engine could run more diluted with less fuel and and at a lower load. These limitations restrict the operating range of CAI combustion for transportation applications.

1.4.4 Combustion stability

Because the CAI combustion behaviour depends critically on the state and amount of trapped residuals from the previous cycle, combustion stability (as measured by the cycle-to-cycle torque fluctuation) is particularly severe at the boundary of operation. Instabilities are long lived compared to SI combustion because of the higher RGF used for CAI combustion.

1.5 Multi-mode SI-CAI engines

The operational capabilities in terms of load and engine speed of a CAI-only engine are probably inadequate on their own for on-road application. As an alternative, engines that use a combination of SI and CAI have been proposed. Such an engine would operate in CAI combustion mode when possible, but switch to CAI at very low loads and very high loads. SI operation is least efficient at low to mid loads due to throttling losses. By using CAI combustion in these parts of the operating regime, a vehicle equipped with a mixed-mode engine could realize fuel economy improvements of up to 20% depending on the driving cycle. [1, 2]

This approach is attractive because SI operation is typically quite inefficient at low loads. In an SI engine the equivalence ratio is usually fixed at stoichiometric due to requirements of after-treatment device so a change in load necessitates a change in fuel and due to fixed stoichiometry, a proportional change in air as well. Reduced air intake in SI engines is almost universally met through intake throttling, although recently some engines utilize advanced valvetrain concepts capable of throttleless air metering. Intake throttling increasing the pumping work the engine must do to intake

air. At very low loads, this pumping work can be a significant fraction of the engine output and so overall engine efficiency decreases at low load. SI operation is also inefficient at low speed and high load when spark must be retarded to avoid knock. The more generous the knock margin in the engine operating strategy, the greater the inefficiency at low speed. Fig. 1-3 superimposes the CAI operating limits (i.e. the closed polygon inside which robust CAI operation is possible without excessive noise) on a schematic of the SI operating limits (i.e. essentially any point that is underneath the bold curved line) showing the limited operating regime of CAI combustion for this engine. CAI is typically significantly more efficient within its operating range than SI is at those same speeds and loads. Then CAI combustion, which is most efficient and

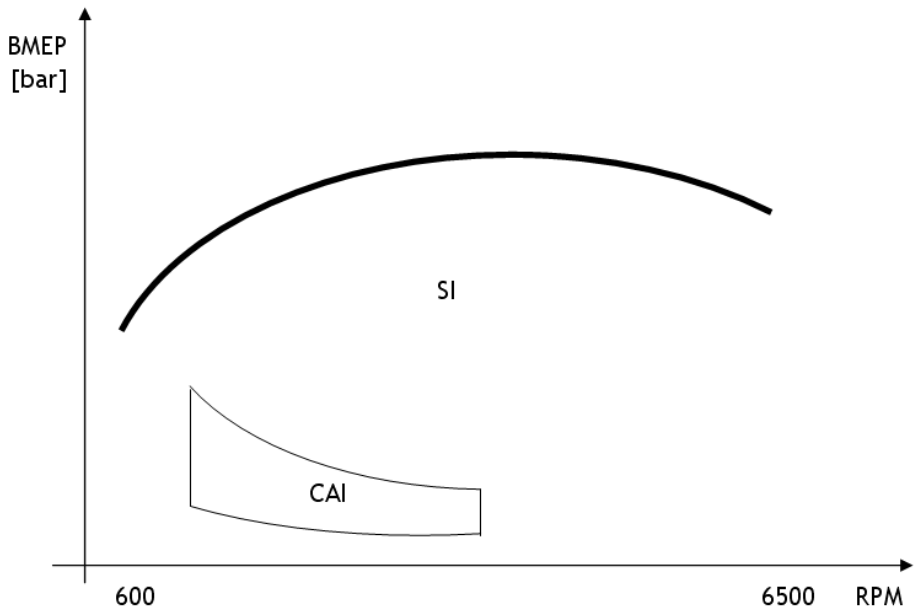

Figure 1-3: Typical CAI and SI engine load limits

only practically viable at low speed and load, seems a good match for SI combustion.

One drawback of SI-CAI mixed mode operation is that the vehicle would still require a three-way catalyst for exhaust after-treatment in SI mode. Also even though the lean/dilute charge of CAI combustion is amenable to higher compression ratios, SI operational requirements to avoid knock limit the compression ratio and hence the ultimate efficiency potential of CAI combustion. The final drawback is the requirement

for an engine mode-switch control strategy.

Load extension concepts

Various proposals to extend the load limits of CAI combustion have been investigated. They include variable compression ratio, combinations of EGR and boosting, charge stratification and mixture preparation, specialized fuels or dual fuel injection systems. The focus of this work is on characterizing the impact of fuel composition on the location and nature of the load limits, not specifically extending those limits. [3–13]

1.6 Previous research phases

In a practical multi-mode SI-CAI engine, it is desirable to maximize the time spent operating in the CAI operating mode because the SI operating mode is least efficient at low and part loads. To accomplish this requires the highest HLL and lowest LLL possible and an engine control strategy capable of operating as close to those limits as possible. This means accounting for potential differences in engine behaviour and load limit location that may arise due to the engine's dependence on ambient conditions, fuel chemistry and other operating parameters.

Here arises the practical motivation for investigating the CAI operating mode. In two previous phases of the present project, efforts focused on identifying engine operating parameters of interest and characterizing its dependence on engine operating parameters.

1.6.1 Bulk parameters on load limits, engine operation

Using a modified PFI engine, Morgan Andreae examined the impact of ambient conditions like humidity and intake air temperature on engine operation. His study evaluated variable valve timing as a means of compensating for ambient conditions. Andreae's study also investigated the impact of market fuel composition on CAI engine operation. He concluded that fuel type had only a small impact on the operating

range. [14]

The current work focuses on an engine with gasoline direct injection (GDI). Hence mixture preparation, charge cooling and the role of charge motion and mixing is expected to be different. This is expected to be particularly relevant for fuel blends with ethanol whose latent heat of vaporization is approximately four times greater than gasoline. It is expected that injection strategy might permit extension of the low load limit.

1.6.2 Fuel effects on PRR and load limits

The load limits of rapid PRR at high load and misfire (failed combustion) at low load are the result of chemical reaction rates being too fast or too slow respectively. Hence it is not surprising that fuel chemistry, which is highly influential in determining reaction rates, has been shown to affect the operational limits of engines using CAI combustion.

Nathan Anderson completed the second phase of research which comprised a more detailed study of the HLL. Anderson's work characterized engine behaviour near the HLL using three fuels including emissions of oxides of nitrogen (NO_x). Two primary reference fuels (PRF60, PRF90) and a third fuel with extremely low aromatic and olefin (ELAO) content. For the PRF60 fuel operation at high loads was constrained by excessive noise quantified by pressure rise rate (PRR), for PRF90 and ELAO fuels, the PRR increased with load to an acceptable maximum then decreased eventually leading to misfier. Therefore high load operation was constrained by ignition failure. [15]

1.7 Project focus

The main objective of this work is to characterize the effect that variation in market fuel composition has on CAI engine operation for an engine equipped with GDI. A secondary objective is to characterize the effect that cetane improving fuel additives have on load limits. A major aim of this work is to validate and generalize the

conclusions of previous phases of the BP-Ford-MIT HCCI research project using an engine equipped with modern technologies.

1.7.1 Market fuel variation

Conventional gasoline is a blend of hundreds of species of hydrocarbons and additives such as detergents. The source of the oil, details of the refining and blending processes all impact the fuel's final composition. Fuel composition also varies seasonally. For example gasoline producers increase the volatile content of gasoline in winter months to improve cold-weather starting. Fuel composition also varies geographically. For example, California enforce strict limits on volatile organic compounds (VOCs) and gasoline blends with high ethanol content are more widely available in Minnesota than elsewhere.

Fuel energy is converted to thermal energy through the combustion process, after that the engine mechanically extracts enthalpy from the combustion products. The details of the combustion process such as timing and duration will be different for each fuel because the reaction pathway is different for different for each component of the fuel. Unfortunately, detailed reaction mechanism models only exist for a limited number of pure hydrocarbon fuels to say nothing of the complicated blends used as market fuels. However, from the perspective of practical combustion, there is a limited number of combustion characteristics that really matter. Combustion phasing and duration are the chief parameters of interest. Other fuel properties such as density, heating value and enthalpy of evaporation are important too but they can be obtained separately from detailed kinetic models.

Many researchers have investigated the impact of different fuels on CAI combustion. Most previous work focuses on pure hydrocarbon species or simple binary or ternary mixtures thereof. Relatively few researchers have evaluated how realistic fuel blends impact CAI combustion. During a previous phase of the study, project sponsor BP provided a fuel survey to decide which fuel properties showed high variability in the market. The survey was based on data from 1999 to 2005 including approximately 27000 fuels from the US gasoline market. The properties of interest

for the previous matrix were Reid Vapor Pressure (RVP), Research Octane Number (RON), aromatic content, olefin content and ethanol content. The fuel matrix was subsequently updated for this study. The main properties of interest for this matrix are RON, aromatic content, olefin content and additives. Follow-up work with fuel blends containing oxygenates ethanol and butanol is planned.

There are a few different reasons that triggered a fuels inclusion in the test matrix. Fuels were included to test engine sensitivity to fuel properties that vary within the present fuel market, and that have been shown to exert influence on CAI combustion. This explains the fuels with variable olefin and aromatic content, components which have different autoignition behaviour than straight chain and saturated hydrocarbons. Another reason is to test potential future fuel blends and additives for influence. This explains the blends with cetane improvers, elaborated below.

RON is tested because it is the market-standard descriptor of autoignition behaviour. In SI engines, fuels display sufficiently different auto-ignition properties that manufacturers prescribe minimum fuel performance criteria usually in terms of a minimum RON. This allows them to devise a control strategy with reference to a predictable knock limit. Analogously, fuel auto-ignition behaviour is an important consideration for practical SI-CAI multi-mode operation. A few options exist for engines that display significant fuel sensitivity. One is a conservative control strategy that seeks to maintain operation in whatever regions exist where the engine is fuel insensitive. Another strategy is to make the engine fuel-aware and explicitly modify the control strategy on a per-fuel basis.

1.7.2 Cetane-number additives

In addition to a matrix compiled to explore market variation, two test fuels are added to explore the potential to extend the low load operating limit even further, particularly at low engine speed. Such an extension would reduce or potentially eliminate the need for inefficient SI operation at low loads.

Both fuels are based on the low RON fuel in the market fuel matrix. One fuel gas 2000ppm 2-ethylhexyl nitrate (2EHN) added and the other has 4800ppm di-

tert butylperoxide (DTBP). These additives are normally used as cetane number improvers in diesel fuel. The cetane number of a diesel fuel is a measure of the time between the start of its injection and the start of combustion. A higher cetane number indicates a shorter delay.

These additives are thought to lower the low load limit by advancing low temperature heat release and increasing reactivity at the low temperatures characteristics of the LLL. It is also expected that these additives may increase reactivity at high temperatures and hence decrease the HLL as well. This would shift the entire CAI operating range down to lower loads.

The use of diesel fuel additives in gasoline may appear curious but as engine technology has evolved, fuel formulations have evolved as well. Although CAI is a sort of hybrid between SI and CI combustion, it has certain important distinguishing characteristics that imply that neither gasoline or diesel is an optimal fuel on its own.

Spark assist

For consistency and purposes of comparison with related work done with this engine at Chalmers University, CAI operation was spark assisted. This means that spark was activated during CAI combustion cycles. [16] Spark assisted CAI has been widely used in other research labs, particularly during SI-CAI mode switch. [12, 13, 17–21] Despite extensive study, its role is not well understood. Considering that for typical spark assisted spark timing the lean and dilute charge is not hot enough for premixed flame propagation. It is noted in the present work that engine stability, misfire recovery and low load limit were improved with spark assist.

This page intentionally left blank

Chapter 2

Experimental Apparatus

2.1 Test engine

All experiments were conducted on a modified prototype engine based on the B6324S Volvo production engine. It is a naturally aspirated, 3.2L inline 6-cylinder, dual overhead cam, 24-valve gasoline engine. This engine can be found in on-road use in the Volvo V70 and Volvo XC90 after the 2008 model year. Major modifications completed by Ford of Europe include gasoline direct injection (GDI), fitting a cylinder pressure transducer and installation of additional active valvetrain components. The engine was subsequently modified at MIT for operation with only one cylinder firing. The remaining cylinders are motored. Table 2.1 contains some of the engine's geometric parameters.

Table 2.1: Engine geometry

Displacement [cc]	532
Bore [mm]	84
Stroke [mm]	96
Connecting rod [mm]	147
Compression ratio	10.8

2.1.1 Control

The engine is controlled using 2 desktop computers executing code developed at MIT. The user controls a master computer and inputs fuel injection timing, fuel injection pulse width, spark timing, spark dwell, intake cam timing, exhaust cam timing, intake cam profile selection and exhaust cam profile selection. The master computer controls a slave computer on which the engine control code is executed. The code permits multiple fuel injections and accepts separate input for timing and duration of each injection. All inputs can be changed in real time as desired. Separate hardware cut-off switches to interrupt fuel and spark signals before they reach the engine. These means are installed for safety and testing sparkless CAI operation.

2.1.2 Engine components

Active valvetrain

The intake camshaft of the production engine incorporates variable valve timing (VVT) by means of a hydraulic camshaft phasing unit. The experimental engine was modified to include a nearly identical VVT unit on the exhaust camshaft as well. Intake and exhaust cam phasing are continuously variable with a range of approximately 60 CAD. The phase angle is controlled by an electrohydraulic valve that regulates oil pressure within the hydraulic phaser. Greater oil pressure results in more advanced valve timing. When the system is not energized the camshafts and valve timing return to their fully retarded default timing. Table 2.2 lists the fully retarded timing from which the valve timing may be advanced. Figure 2-1 shows the default valve timing from which the valve timing may be advanced. With the given default timing in CAI and the 60 CAD range of valve advance, symmetric negative valve overlap (NVO) is possible in CAI operating mode when EV advance is less than approximately 42 CAD.

If a desired cam position is outside of the 60 CAD range of the valve phaser, the default position can be adjusted mechanically within the engine to allow the desired position to be reached. The control is accurate to within +/- 1 CAD. The feedback

Table 2.2: Basic valve timing and lift (cam phasers inactive)

	SI Cams		CAI Cams	
Valve lift [mm]	**Maximum**	**Reference**	**Maximum**	**Reference**
IV lift	10	0.70	3.0	0.35
EV lift	9.8	0.65	2.9	0.25

	SI Cams		CAI Cams	
Timing from [CAD ATDC$_{compr.}$]	**Zero lift**	**Ref lift**	**Zero lift**	**Ref lift**
IVO	345	390	440	462
IVC	660	620	602	580
EVO	94	136	166	184
EVC	410	366	318	300
IVO duration	315	230	162	118
EVO duration	316	230	152	116

control on cam phasing is executed once per cycle, and the resolution on the cam position measurement is 1 CAD.

The production version of the engine is fitted with a variable valve lift system via cam profile switching (CPS) on the intake camshaft only. The experimental engine was modified to include this variable valve lift system on both intake and exhaust camshafts. The intake and exhaust sides of the system operate independently but identically so the mode of operation will be described for one side only.

Each camshaft incorporates two distinct sets of cam lobe profiles. Cam profile selection is achieved with a special hydraulic tappet. Conventional engines have a single cam lobe making contact with a simple, solid tappet. In this engine, each valve has three cam lobes arranged with one wide central profile and two identical, thinner outer profiles flanking the inner profile. These profiles mate with a tappet that has independent inner and outer (i.e. annular) contact surfaces that can be locked together with internal locking pins. The position of the locking pins is controlled by an electro-hydraulic actuator on the engine, and a return spring in the tappet. In the default position the tappet is unlocked and the inner hydraulic tappet makes contact with the central cam lobe, transmitting its lift and duration to the valve. In this configuration the outer (annular) tappet can move coaxially with, but independent

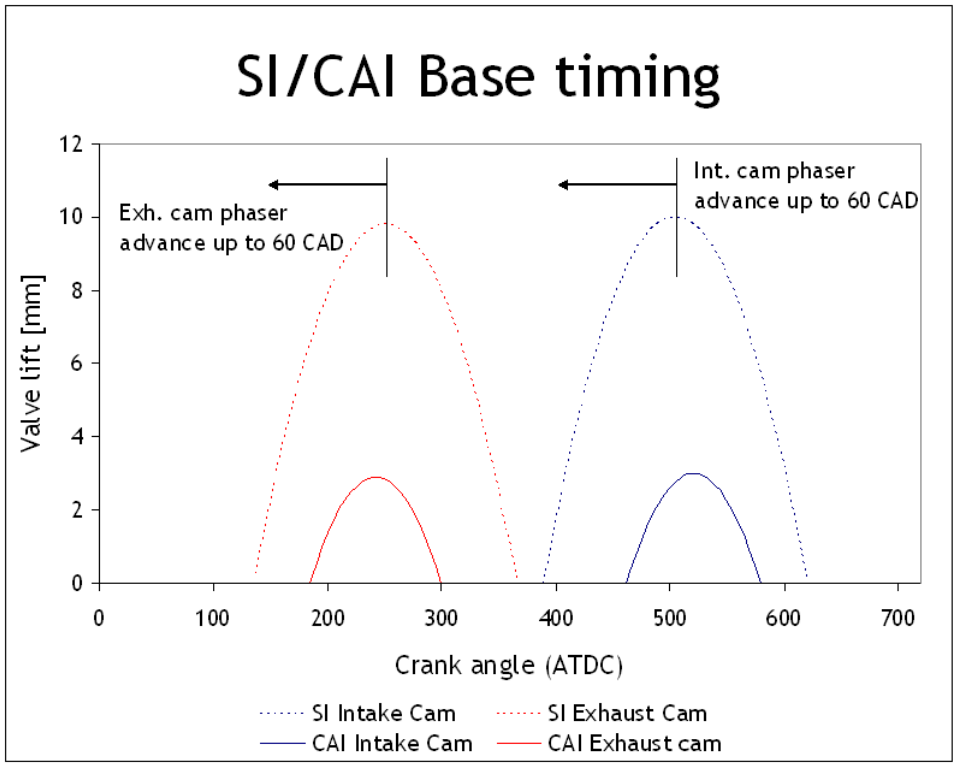

Figure 2-1: Default valve timing for SI and CAI operating modes

of the inner tappet, that is without transmitting its motion to the valve. However, when the system is active and the locking pin is in place, the inner and outer tappets are locked together and only the outer profile is transmitted to the valve. In the production engine the inner cam profile is the default, and the taller outer profiles are used when the system is active to provide greater valve lift. The high lift cams are used to reduce pumping losses at higher engine speeds. In the experimental engine the default is the outer profiles which provide high lift, long duration valve events for SI operation. When the system is active, only the inner profile is transmitted which is a low lift, short duration cam profile for CAI operation.

For the purposes of CPS, cylinders are divided in banks of three. To reduce wear on the switching mechanism, profile switches must be scheduled such that a switch is requested shortly before all of the valves in the given bank are closed. Since the experimental engine was run with only one firing cylinder, only one bank of intake cylinders and one banks of exhaust cylinders required attention. In both cases, the

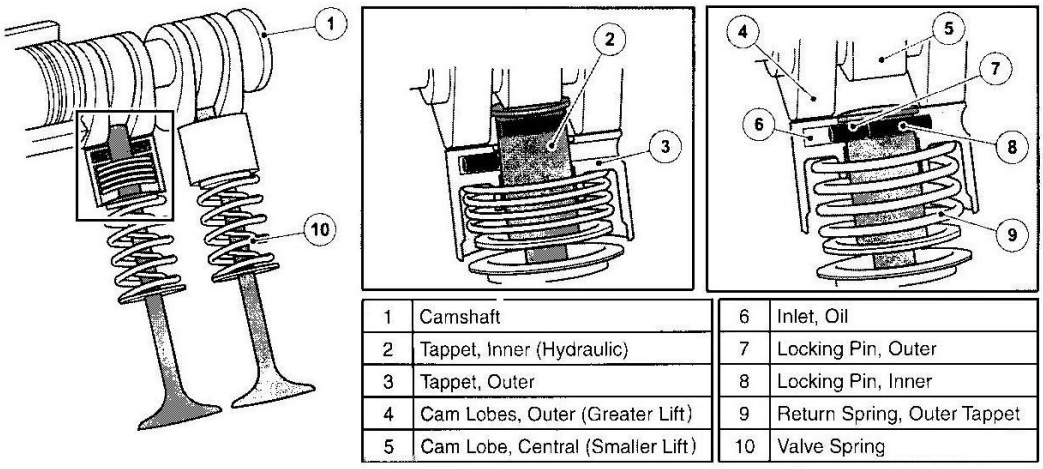

1	Camshaft	6	Inlet, Oil
2	Tappet, Inner (Hydraulic)	7	Locking Pin, Outer
3	Tappet, Outer	8	Locking Pin, Inner
4	Cam Lobes, Outer (Greater Lift)	9	Return Spring, Outer Tappet
5	Cam Lobe, Central (Smaller Lift)	10	Valve Spring

Figure 2-2: Schematic of production CPS components

bank included cylinders 1, 2 and 4.

Intake and exhaust

A custom intake manifold was fabricated for the one firing cylinder. The manifold had ports for measuring manifold air pressure and temperature approximately 5 cm from the intake port. The intake was modular and allowed the installation of a manual throttle valve and damping tank, and a 5kW intake air heater. In the most common configuration only the intake air heater and sensors were fitted to optimize heater response time and air temperature control precision. Air flow to the five motored cylinders was filtered, but not otherwise throttled or conditioned.

A custom stainless steel exhaust manifold was fabricated for the one firing cylinder. The runner for the fired cylinder included ports for the measurement of exhaust temperature and pressure. Downstream of the sensor ports was an exhaust damping tank with a port for emissions sampling. The exhaust had throttle valves for simulating the back pressure of the close-coupled catalytic converters found on the production engine, removed for the present work. The exhaust air from the five motored cylinders was separate from the firing cylinder exhaust.

Fuel system

The GDI fuel system operates at a pressure of 12 MPa [1740 psig] driving one multi-hole solenoid-controlled injector per cylinder. The prototype engine had an integrated gear-driven precision lobe pump. In the interests of simplifying fuel purge procedures and reducing control requirements that pump was removed from the engine. An alternate design using high pressure gaseous N_2 in a hydraulic accumulator to pressurize fuel was used instead. Comparable systems are already operating reliably on other engines in the Sloan Automotive Laboratory at MIT. To reduce switching time and improve testing throughput, two parallel high pressure systems were employed, one for the base fuel and the other for the test fuel.

Each high pressure cylinder is supplied by a low-pressure fuel replenishment system comprising a pump, filter and various purge ports. All components were selected for compatibility with ethanol and butanol. Moreover, separate filter elements were procured for each fuel to minimize sources of cross-contamination between fuels. Figure 2-3 shows a schematic view of the fuel systems.

Fuel injector pulse width demands are sent from the slave computer to a Volvo-proprietary injector driver responsible for the high peak, low-hold injection pulse that actually drive the injector. Pressure is measured before the GDI fuel rail by an OMEGA PX309-3KG5V pressure transducer.

Coolant

All experiments were performed with the engine coolant at 95°C (+/- 2°C). The engine inlet coolant temperature is subject to closed-loop control. An OMEGA CN-7823 PID controller governs an immersion heater in the coolant reservoir and a normally closed solenoid valve controlling city water supply to a counterflow heat exchanger. Engine coolant from the heated reservoir is pumped continuously through the engine whose coolant thermostat was removed.

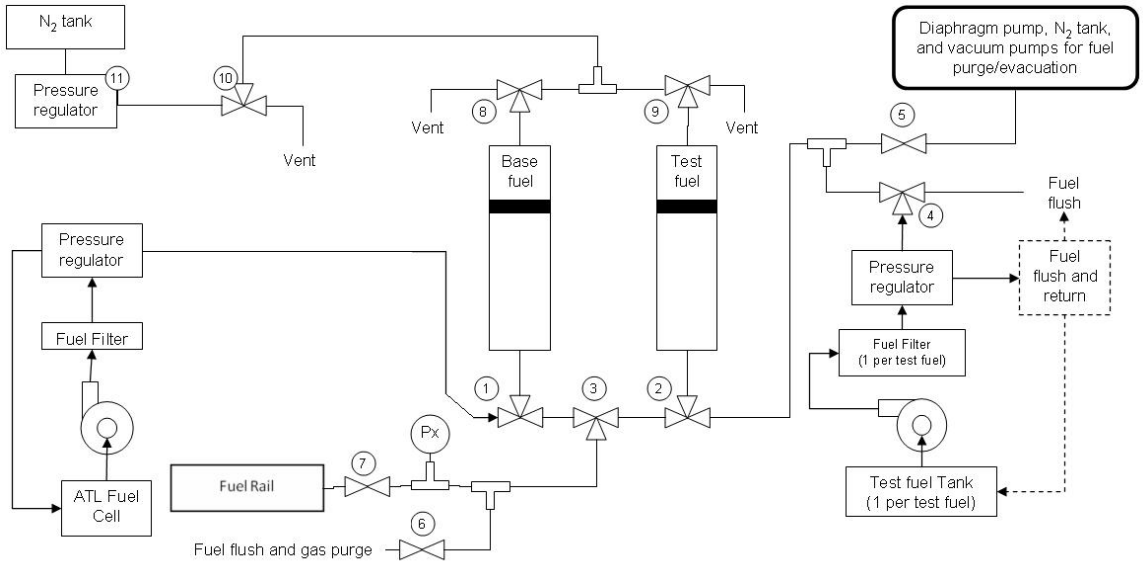

Figure 2-3: Fuel system schematic

2.2 Dynamometer

A 3DSE Dynamatic Co. universal motoring/absorbing dynamometer controlled the speed of the engine and absorbed its power output. The engine's flywheel is connected to an always-coupled clutch, which is mated to a proprietary Volvo output shaft. The dynamometer is coupled to the engine using a custom spool adapter and U-joint shaft with a compliant coupling to damp torque spikes from the engine's single firing cylinder. The 40 hp dynamometer's speed range of 900rpm to 3500rpm was reduced to a safe operating range of 1100rpm to 3000rpm to avoid resonant frequencies due to torsional excitation of the compliant shaft. Although the load cell on the dynamometer was capable of measuring the brake torque output of the engine, the measurement was not accurate enough to be useful, and it was rendered less meaningful by inclusion of friction from the 5 motoring cylinders.

2.3 Data acquisition and measurements

National Instruments hardware and LabView software is used to acquire data from the experimental data onto a desktop PC. Table 2.3 summarizes the sensors and mea-

surements recorded by LabView. Subsequent subsections describe the configuration and operation of each sensor.

Crankshaft position	BEI encoder, $360^{c}irc$ per rev.
Cylinder pressure	Kistler 6053CC60 sensor, Kistler 5010b charge amplifier
Intake pressure (MAP)	Honeywell SA-001-BAC1DE sensor
Exhaust pressure	OMEGA PX209-030A5V sensor
Fuel pressure	OMEGA PX309-3KG5V pressure transducer
Air-fuel ratio	Horiba MEXA 720NO_x combined λ and NO_x sensor
Intake cam timing	OEM intake cam sensor
Exhaust cam timing	Modified OEM intake cam sensor

Table 2.3: DAQ sensor details

2.3.1 Crankshaft position

An optical encoder is installed on the engine and coupled to the crankshaft. The encoder signal is aligned with the engine cycle phasing by analyzing the motoring pressure trace at 2500 rpm. Most data was collected at a rate of once per CAD but pressure data for analyzing PRR_{max} was collected at 100kHz to resolve the high frequency standing waves associated with standing waves in this engine.

2.3.2 Cylinder, intake and exhaust pressure measurements

Intake pressure is measured approximately 5cm upstream of the intake port. Exhaust pressure is measured approximately 10cm downstream of the exhaust port.

In-cylinder pressure is measured with a Kistler 6053CC60 pressure transducer mounted in the cylinder wall. This pressure transducer is a narrow-body, high temperature piezoelectric pressure sensor. Like many pressure transducers, this model of sensor and charge amplifier have an offset drift, therefore the sensor must be pegged to another sensor to obtain the absolute value of the cylinder pressure.

In some cases the pressure signal offset is not critical, i.e. the absolute pressure is not important. For instance, the absolute pressure is not important for determining NIMEP since it is a contour integral over a cycle.

In general for all experiments, the cylinder pressure was set equal to the MAP at BDC of intake stroke. This is common practice in conventional SI experimental engine setups. At BDC intake, the piston is not moving and it is sufficiently late in the intake stroke for pressure equilibration across the intake valve. In the present experimental engine the valve lift and duration of the CAI cams is often too short for this equilibration. Figure 2.3.2 shows a cylinder pressure trace and the MAP trace during one intake event of a CAI cycle, and a similar figure for an intake event of an SI cycle.

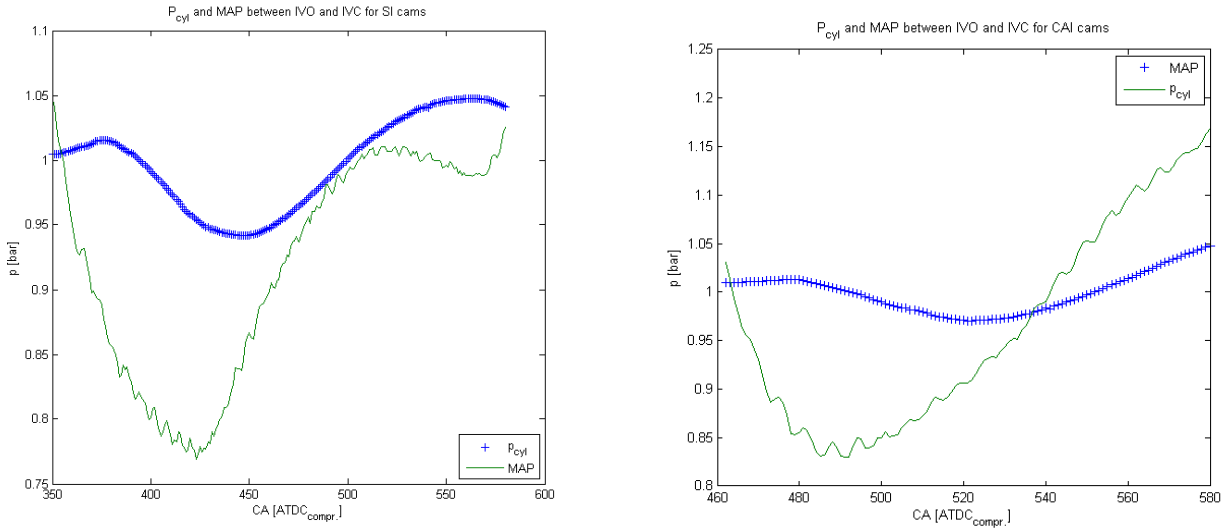

(a) SI intake event

(b) CAI intake event

Figure 2-4: MAP and cylinder pressure during CAI intake event

As noted the pressures do not exactly equalize but the error is usually a small fraction of atmospheric pressure. The error can be bounded by checking that for CAI intake events the cylinder pressure should be less or equal to MAP at BDC. One can also expect a comparable phenomenon to occur during the exhaust stroke. The short duration and low lift CAI valve event does not allow adequate time for complete blow down and pressure equilibration between the cylinder and exhaust manifold. In this case however, it is in our interests to impede the exhaust process to a certain extent, in order to improve residual retention for charge pre-heating. However the the lack of equilibration is why we cannot peg the cylinder pressure transducer to the exhaust

pressure sensor.

2.3.3 Fuel pressure and flow rate

Fuel pressure is measured approximately 15cm upstream of the fuel rail. Fuel flow is not measured directly. An "end-to-end" bench test correlation of fuel injector pulse width demanded by the slave computer and fuel mass actually injected was conducted at numerous injection pressures and pulse widths. The injectors provide linear response between fuel mass and injector pulse width in the range of 0.3ms to 6ms. Below 0.3ms there is some deviation from linear response but it is repeatable non-linearity down to approximately 0.2 ms. Above 6 ms there is some non-linearity due to a decay in fuel supply pressure. A production engine would likely not suffer from this non-linearity, moreover a 5 ms injector pulse width is about the maximum WOT SI fuel requirement of this engine anyway. Fuel mass increases as square root of injection pressure so fuel mass is calculated from injector pulse width as follows:

$$m_{fuel,0} = a_0 + a_1 t + a_2 t^2 + ...$$

Where t is injector pulse width and a_i come from correlation at p_{ref}, then

$$m_{fuel,actual} = m_{fuel,0} \sqrt{\frac{p_{actual}}{p_{ref}}}$$

The influence of in-engine heating on injector behaviour, an effect which is absent in the benchtop correlation, is expected to be minimal. The effect of transient heating of fuel between injections is not expected to appreciably change the fuel flow rate. Several trials during the bench top pulse width correlation were used to assess the accuracy of the calibration method. Sources of uncertainty such as evaporation of fuel (and subsequent loss from the collection vessel), condensation of water from the ice bath were quantified and found to be less than 1% for the test protocol used.

Fuel pulse width correlations for different gasoline test fuels did not differ within the uncertainty of the correlation. Correlations for fuel blends containing ethanol and butanol are expected to differ appreciably from that of gasoline.

2.3.4 Equivalence ratio

Air-fuel ratio or equivalence ratio is measured using a Horiba MEXA 720NO_x combined λ and NO_x sensor. It is installed in a port approximately 15cm downstream from the exhaust port.

2.3.5 Temperature measurements

Intake, exhaust, coolant and ambient temperature data is recorded manually and encoded in the DAQ filenames for each experiment. From there it is included in the data upon post-processing.

2.3.6 Intake and exhaust camshaft signals

Intake and exhaust cam positions are measured using production Hall effect inductive intake cam position sensors. The sensors are installed in the rear of the engine just inboard of the VVT cam phasers. The sensors generate two voltage pulses per revolution of the cam when a metal feature machined into the camshaft rotates past the sensor. This signal is processed by custom designed digital hardware resulting in a digital pulse with the leading edge at BDC of the compression stroke, and the trailing edge at the cam metal tooth passing. The duration of the pulse is used to infer the cam timing. Advancing the cam phasers shortens the duration of the digital pulse. This voltage pulse duration is read by the control software on the slave computer once per cycle.

2.3.7 RGF Estimation

Combustion dynamics are expected to depend on mixture composition. In particular we are interested in the residual gas fraction defined in Eq. 2.1.

$$x_{residual} = \frac{n_{trapped}}{n_{total}} \text{ where } n_{total} = n_{fuel} + n_{air} + n_{trapped} \tag{2.1}$$

We can readily determine the amount of fuel and air in cylinder from injector pulse width and equivalence ratio measurements using Eq. 2.2

$$n_{fuel} = \frac{m_{fuel}}{MW_{fuel}} \text{ and } n_{air} = \frac{m_{air}}{MW_{air}} \text{ where } m_{air} = m_{fuel} \cdot \lambda \cdot (A/F)_{stoich.} \tag{2.2}$$

Fast in-cylinder composition measurements are difficult and sometimes unreliable so in order to characterize the in-cylinder composition, namely $n_{trapped}$, the ideal gas law is used to estimate the amount of residuals trapped in cylinder at EVC according to Eq. 2.3.

$$n_{trapped} = \frac{P_{EVC}V_{EVC}}{RT_{EVC}} \approx \frac{P_{exh}V_{EVC}}{RT_{exh}} \tag{2.3}$$

Parameters on the left hand side of Eq. 2.3 refer to in-cylinder quantities, and parameters on the right hand side refer to the approximate values we substitute. V_{EVC} is the cylinder volume at EVC, found from the engine geometry and crank angle. Because the CAI exhaust cam profile features short duration, low-lift events, the approximation that in-cylinder properties are equal to manifold properties is likely incorrect. However, Wildman's comparisons of actual in-cylinder species concentration show that this approximation is good.[11] The pressure and temperature errors are compensatory and the overall residual gas fraction estimate is good. This approach also ignores possible backflow of residuals into the intake manifold during operation with asymmetric valve timing. In that case mass inducted during the intake event will be a mixture of air and residuals. Back flow would be caused by residual pressure due to incomplete re-expansion from NVO re-compression. For low lift, short duration cams this back flow caused is neglected in the calculation.

Chapter 3

Test fuel matrix and test methods

3.1 Test fuel matrix

The objective of the test fuel matrix is to verify and generalize previous findings about the sensitivity of CAI combustion to market fuel variation and assess whether the same trends apply to an engine with GDI.

Andreae used a 12-fuel matrix to investigate sensitivity to market fuel variation. His results indicate a weak sensitivity to most of the fuel properties tested. [14] For the present work a base fuel representing average market fuel is selected as a baseline. Three fuels are added to the fuel matrix to include variation of properties found to be influential in the previous study (such as olefin content) or market-relevant properties such as RON, i.e. properties known to vary widely in the market.

Three new test fuels are also considered. One is a blend with high olefin content but low aromatic content, and two contain cetane number additives. Except when RON was the property being varied, test fuels are blended to vary the property of interest subject to having a constant RON of 91 and a nearly constant RVP around $7.2 psi$. Fuel properties are summarized in Table 3.1.

Table 3.1: Test fuel matrix

	Base Fuel	**High Olefin**	**High Ol./ Low Ar**	**High RON**	**Low RON**	**Low RON +0.48% DTBP**	**Low RON +0.20% 2EHN**
S.G. at 60°F	0.7429	0.7428	0.7319	0.7485	0.7232	0.7232	0.7232
RON	**91.5**	**91.5**	**91**	**97.4**	**89.4**	**81**	**79.4**
MON	83	83.8	82.3	86.9	84.8	80.6	78.7
R+M/2	87	88	87	92	87	81	79
T10 [°F]	137.6	130	137.1	143.1	150.3	150.3	150.3
T50 [°F]	223.6	207.1	209.8	218.5	222.1	222.1	222.1
T90 [°F]	333	332.4	332.5	337.8	333.1	333.1	333.1
DI	1210	1149	1168	1208	1225	1225	1225
RVP [psi]	7.44	7.78	7.69	7.5	7.31	7.31	7.31
Vol-% Aromatics	**28.6**	**27.3**	**16.7**	**31**	**13**	**13**	**13**
Vol-% Olefins	**10.2**	**17.5**	**17.3**	**10.1**	**5.2**	**5.2**	**5.2**
Vol-% Saturates	**61.3**	**55.2**	**66**	**58.8**	**81.8**	**81.8**	**81.8**
Vol-% Oxygenates	**0**	**0**	**0**	**0**	**0**	**0**	**0**

3.2 Engine operating conditions

All tests are conducted at steady engine speed. Other engine operating parameters are described in Table 3.2 and exceptions to the listed parameters given after the table.

Table 3.2: Engine operating conditions

Parameter	**Value**
Engine speed	1250rpm, 2000rpm and 2500rpm
λ	1.3[1]
$T_{coolant}$	95°C
T_{intake}	80°C
Spark timing	30 CAD BTDC
Valve timing	Symmetric[2]
Fuel pressure	124 bar (1800 psig)
Injection strategy away from LLL	Single, EOI at 50 CAD $ATDC_{exh}$
Injection strategy near LLL[3]	Split 30% pilot and 70% main (mass basis) Pilot EOI at 50 CAD $BTDC_{exh}$ Main EOI at 50 CAD $ATDC_{exh}$

Notes:

1. The air fuel ratio λ=1.3 is selected for purposes of comparison with related work done at Chalmers University.[16] In cases where the seeking of the LLL is constrained by valve timing, valve timing is held at its limit and leaner mixtures are used until the LLL is reached. In general, leaner operation is possible at higher RPM because the combustible limits of the charge are wider due to higher in-cylinder temperatures resulting from reduced heat transfer.

2. Symmetric valve timing is only available up to 42 CAD advance of the EV phaser. Then valve timing is held as close to symmetric as possible, with a 10 CAD sweep for maximum combustion stability based on NIMEP COV.

3. Split injection was found to improve stability and extend the operational limit at low loads. This strategy was chosen for continuity with the work done at Chalmers Univeristy.[16]

3.3 Test Procedure

At the start of each day the engine is preheated using the coolant heating system to ensure consistent and uniform temperatures throughout the engine. At the start of each series of tests, and every time the engine speed is changed a motoring pressure trace is collected to verify the crankshaft encoder offset. Once the engine is firing, time is allotted for temperatures and flow rates to reach steady values before data is collected.

The objective of this study is to characterize the impact of fuel on load limits and engine operating characteristics. To that end, for each fuel, nine operating points are selected comprising three load points at three engine speeds. These nine points shown schematically in Fig. 3-1. Points 2, 5 and 8 in Fig. 3-1 are defined, based on Base Fuel results, approximately half way between the HLL and LLL. This set is done to test a series of consistent load-speed points to better isolate the engine's response to changes in fuel composition.

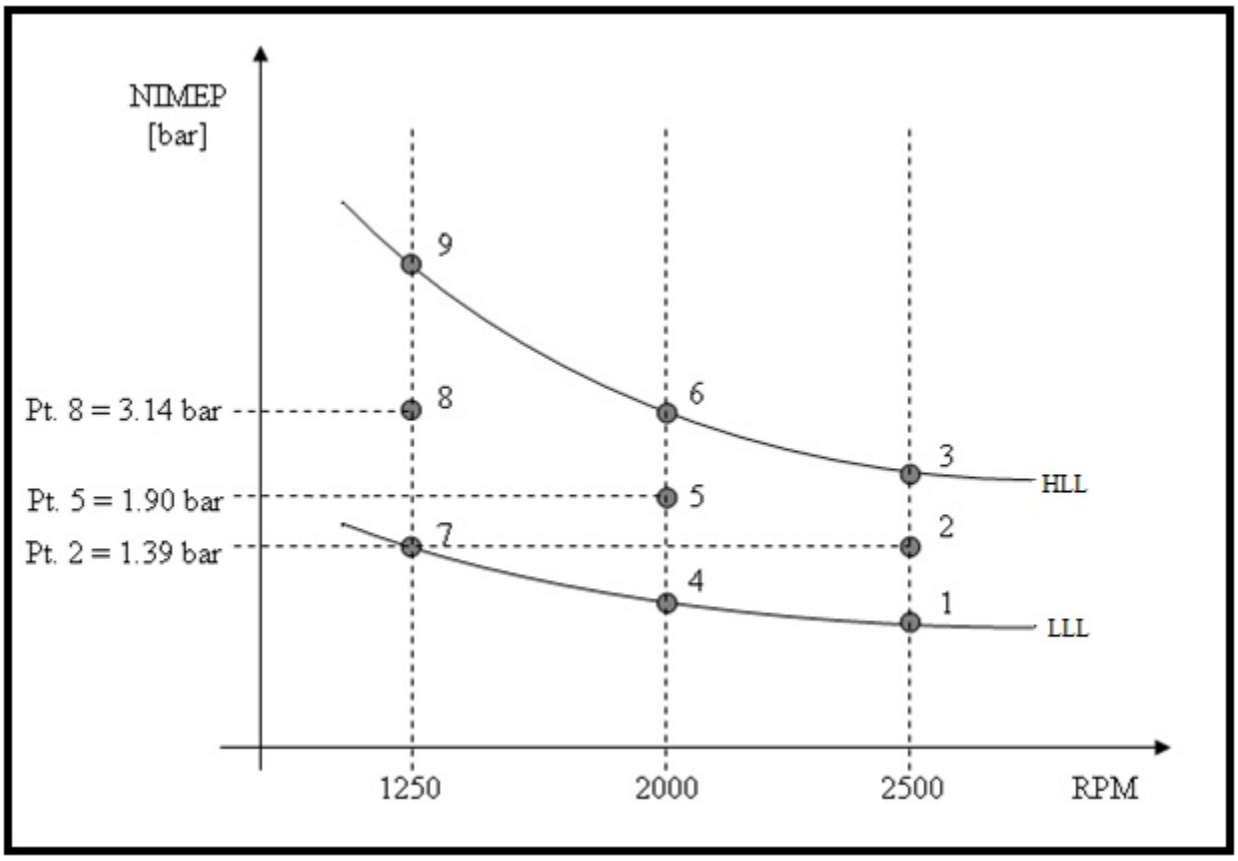

Figure 3-1: Data collection operating points

3.3.1 Load limit criteria

Based on previous CAI research at MIT and elsewhere, it is expected that engine misfire or excessive noise will limit engine operation at high loads. It is expected that misfire and unstable combustion will limit the lowest achievable limit. Therefore three load limit criteria are required.

Misfire criterion

For the present work, misfire is defined as a failed combustion event more than once in the 100 cycles. Further, a misfire condition is declared if, following a failed combustion cycle the engine does not spontaneously recover to a steady state. In a practical sense this limit is imposed because failed combustion drastically increases emissions of unburned hydrocarbons and results in rough engine operation.

Stability criterion

Combustion stability is a consideration for operation near both the high load and low load limits. Although it incorporates many direct combustion variables such as fuel rate and combustion phasing, output torque is a more practical measure of interest. Due to NVH concerns the maximum allowable variability in engine torque is around 3-10%. For the present work, the stability criterion is that COV of NIMEP over 100 cycles is less than 7%.

Engine Noise

Many researchers have attempted to quantify the audible intensity of engine knock and correlate it with. Other measurable engine parameters. Table 3.3.1 contains the knock limit employed by other CAI investigators. As reflected by the range and type

Table 3.3: Selected engine knock criteria from the literature

Research Group	SAE Paper	Knock Criterion	Equivalent dP/dt
AVL	2003-01-0754	2 bar/cad @ 3000 RPM	3.6 MPa/ms
Brunel	2001-01-1030	0.5 bar oscillation on 10% of cycles	
Cosworth	2005-01-0133	6-8 bar/CAD @1500 RPM	5.6-7.2 MPa/ms
GM	2002-01-2859	Ringing Index $(dP/dt)^2/P_{max}$	3 MPa/ms^2
Lotus	2005-01-0157	dP/CAD	
Lund	980787	12 bar/CAD @ 1000 RPM	7.2 MPa/ms
Nippon Oil	2005-01-0138	dP/CAD	

of knock criteria employed, this task of correlating knock is difficult because as an acoustic phenomenon, knock depends on the geometry and prevailing thermal conditions within each engine. At present there does not appear to be a single conventional metric for reporting knock intensity, or correlating the onset of knock. Cheng, Andreae et al developed an inequality that defines an approximate rate of heat release required to create an oscillating pressure wave. [22]

$$\dot{q} > \left(\frac{3\gamma}{\gamma-1}\right)\left(\frac{p}{r/a}\right)$$

Where γ is the specific heat ratio of the gas, p is the gas pressure for a local parcel charge having radius r and local sonic speed a. Then the denominator represents a

local pressure equilibration time scale. Heat release at a greater rate than the left hand side of the above inequality would result in a thermal expansion that cannot be accommodated with acoustic expansion. Hence the local parcel would be pressurized and a pressure oscillation would result.

Heat release rate correlates strongly with pressure rise rate. Indeed the assumption that changes to cylinder pressure arise from either piston motion or heat release allowed Rassweiler and Withrow to develop a crude yet effective method for estimating the apparent heat release and mass fraction burned from pressure and cylinder volume data. This technique remains widely used today. So arises the pressure rise rate as a metric of knock. This criterion has been used previously at MIT and by a number of other CAI researchers and seems to correlate with audible knock. For the present work knock is defined as a maximum cylinder pressure rise rate greater than 5 MPa/ms. That is,

$$\text{PRR}_{max}=(\frac{dP}{dt})_{max} > 5 \text{ MPa/ms}$$

The maximum cylinder pressure rise rate is actually the average of the maximum pressure rise rates of at least 30 cycles, sampled at 100kHz. Pressure rise rate is selected for the physical reasons described above. 5 MPa/ms was selected as a quantitative limit for this work during engine installation and commissioning. It was noted that steady audible SI combustion knock correlated well with that pressure rise rate across a range of speeds from 1200rpm to 2000rpm. Knock occurred at lower pressure rise rates (visible on cylinder pressure trace) but was inaudble or only audible intermittently.

High load limit search

Near the high load limit, data is collected at several points to ensure that the true high load limit is captured. With the engine in a steady state, the load is gradually increased via injector pulse width (i.e. fuel rate) in small discrete steps. Valve timing and injecting timing are varied to hold equivalence ratio and EOI constant as specified in Table 3.2. The engine and measurements are allowed to stabilize before

data collection. LabView calculates instantaneous and 100-cycle average PRR_{max} using CA-resolved pressure measurements. This offers a useful approximation of true cylinder pressure rise rate. At each point, data is collected by LabView for 100 cycles at (1/CA) frequency. Temperatures and steady engine parameters such as valve timing are collected once per point. Near the high load limit, cylinder pressure data is also collected at 100kHz for 3 seconds to evaluate $(dP/dt)_{max}$. The sweep to progressively higher loads is continued until a CA-resolved pressure rise rate of around 6-6.5 MPa/ms. Then load is gradually decreased and a few more points are collected for comparison and assessment of repeatability. The location of the high load limit is determined from cylinder pressure sampled at high frequency during data post-processing.

3.3.2 Interior points

Fuel amount, injection timing and valve timing are varied to achieve the fixed speed and load targets of interior points of the operating envelope. CA-resolved and high frequency pressure data is collected at each point. Sometimes there are numerous possible combinations of operating parameters that can achieve the speed and load target within the constraints of Table 3.2. In practice these configurations are nearly identical in terms of valve timing and fuel rate. In those cases, the configuration whose speed and load results most closely match the prescribed points is manually selected.

Low load limit search

If the fuel amount is gradually decreased from the interior points, load will decrease. At a certain point combustion stability will also begin to decrease as well, that is COV of NIMEP will increase. When this happens, fuel injection is changed to a split injection strategy as specified in Table 3.2. For reasons that will be discussed later in this work, this tends to improve stability at the cost of conversion efficiency and permits operation at lower loads.

Load is gradually decreased in discrete steps subject to the constraints in Table 3.2. Time is allotted after each change for equilibration before data collection begins. Near the low load limit high frequency pressure data is not collected because CA-resolved pressure data is found to be sufficiently accurate. Load is decreased until the load limit criteria defined above are exceeded. As with the high load limit, whenever possible, stable points near the load limit that do not satisfy the criteria are also collected for comparison and trend analysis of engine behaviour on trajectories approaching and exceeding the load limit.

3.4 Data post-processing

Raw data collected by LabView is batch-processed offline using custom code in Mathworks Matlab. It outputs quantities of interest such as load, stability and pressure rise rate as described in the preceding sections as well as estimating residual gas fraction, volumetric and indicated efficiencies. Post processing also involves code based on the Rassweiler-Withrow technique for estimating heat release to estimate combustion phasing and combustion duration.

Chapter 4

Experimental results

The operating point of an engine is specified by load and speed. The load (as measured by the NIMEP) is affected by many factors. For instance, inefficient conversion of a quantity of fuel may result in the same output power at the same speed as efficient conversion of a smaller quantity of fuel. Several factors affect the conversion efficiency such as combustion phasing, combustion duration. The objective of the following chapter is to report and explain the effect of fuel composition on the fundamental physical processes of CAI combustion.

4.1 Basic engine operating characteristics

4.1.1 Operating limits

The operating limits of stable CAI combustion for the base fuel using the test procedures described in the previous section are shown in Fig. 4-1. The engine displays the expected modest decrease of LLL with increasing RPM, and the more rapid decreasing HLL as well. These high and low load limits are used to define interior operating points for comparison of engine operating characteristics at fixed speed and load.

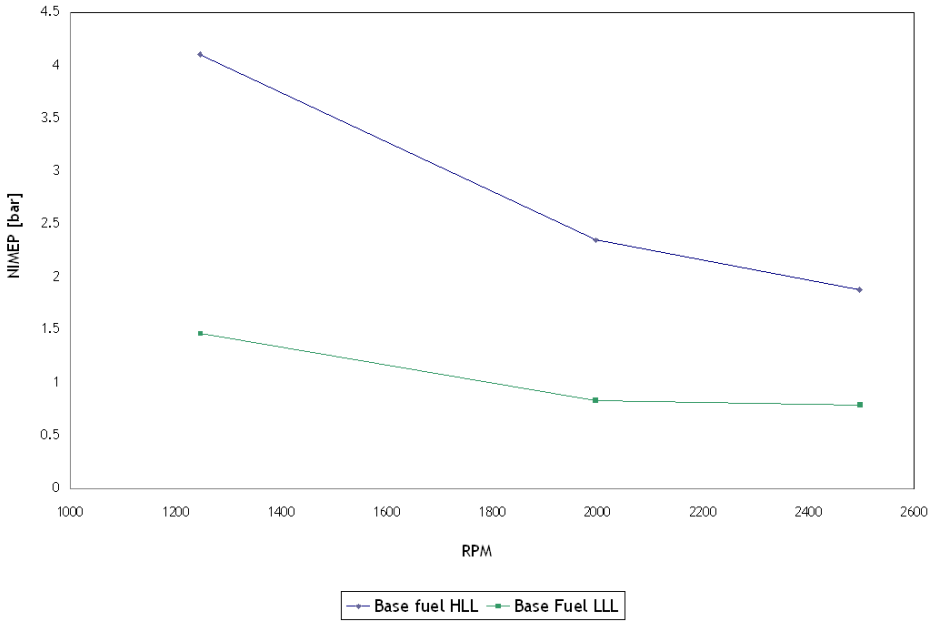

Figure 4-1: CAI operation limits on base fuel

4.1.2 Load control

Stoichiometric SI engine output is largely dependent on volumetric efficiency (VE), which is primarily controlled by the throttle position. Fig. 4-2 indicates that CAI engine output is also proportional to volumetric efficiency. The points shown are interior operating points and operating points near the HLL, that is operating points that use a single fuel injection strategy and all points have fixed $\lambda = 1.3$. This implies that conversion efficiency is approximately constant across a wide range of volumetric efficiency. Engine output is also linear for points with split injection, that is points near the LLL. However operating points with split injection near the LLL form a separate line than for single injection strategy because fuel conversion efficiency changes with the split injection strategy. This effect is likely explained by changes in pumping work and increases in heat transfer losses resulting from the large volume of residuals re-compressed and reactions that may occur during NVO recompression.

These findings imply that load can be controlled by altering the volumetric efficiency of the engine. Although engine speed is known to affect volumetric efficiency, engine speed is not an effective way to control volumetric efficiency and load due to

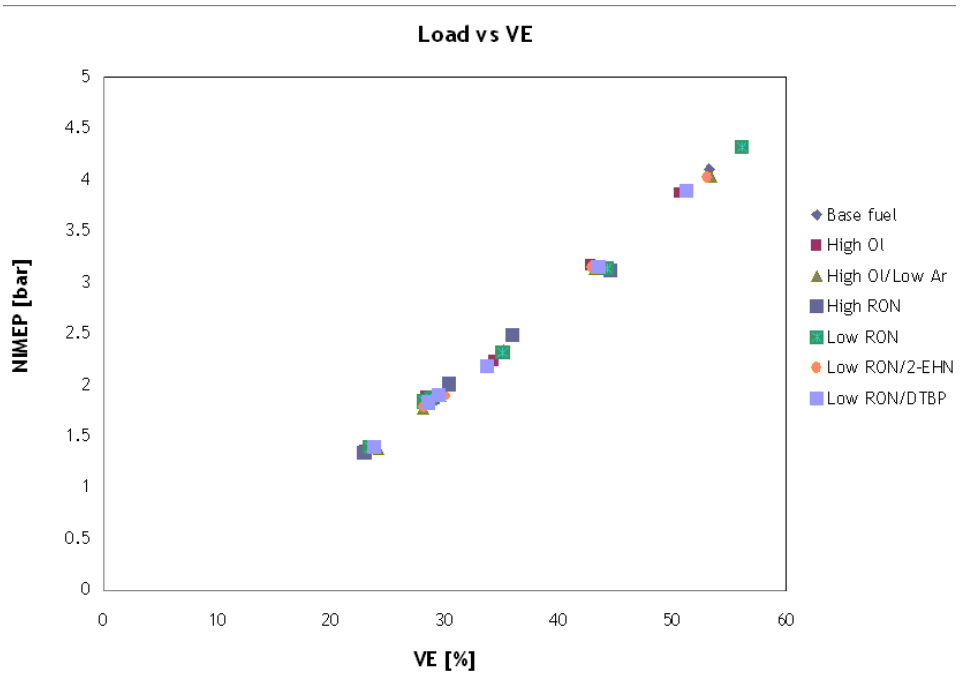

Figure 4-2: Load vs volumetric efficiency for single injection operation

NVH issues associated with rapidly modulated engine speed. This means that valve timing is primary means to control engine output. Significant efficiency improvements are realized by using valve timing to control volumetric efficiency instead of throttling the intake. Despite this advantage, Andreae describes certain beneficial effects on combustion phasing resulting from intake throttling during CAI operation.

Volumetric efficiency can be controlled through exhaust valve timing. Advanced exhaust valve timing traps more residuals. To first order, the greater the amount of trapped residuals the less fresh air that can be inducted. This is verified by Fig. 4-3.

The relationship is slightly more complicated because VE can be affected by the thermodynamic state of the in-cylinder charge at IVO, RPM and injection strategy. Each effect is described below.

The amount of fresh air that may be inducted is determined in part by the state of the charge at IVO. An in-cylinder charge at higher pressure or temperature will admit less fresh air than a cooler or lower pressure charge, and will heat the incoming air and reduce its density thereby reducing VE. Hence higher RGF means higher mean in

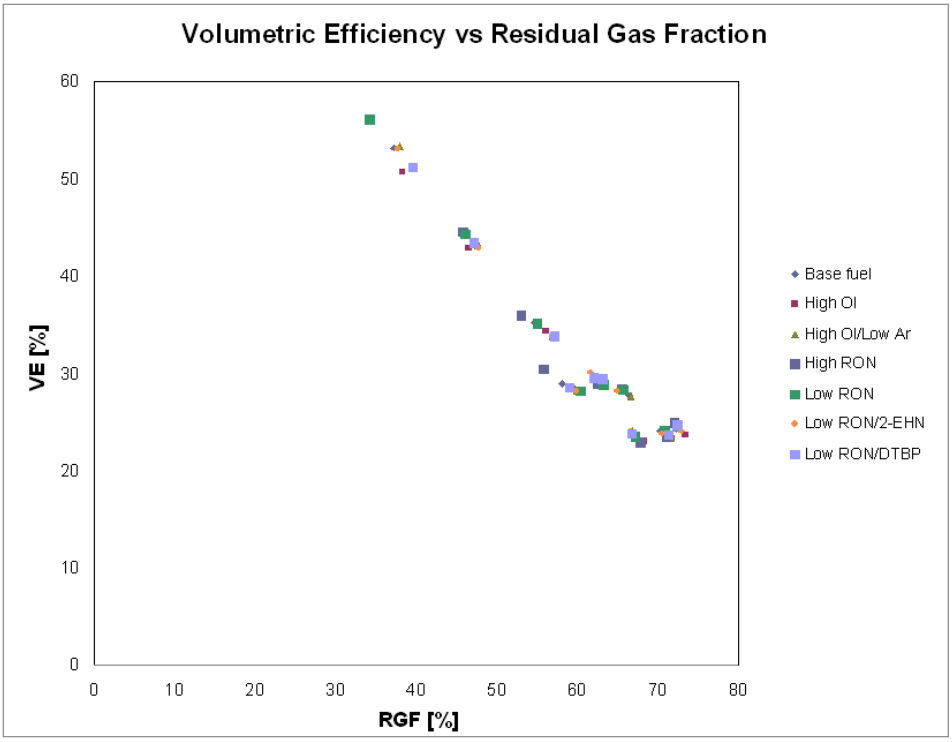

Figure 4-3: Relationship between VE and RGF

cylinder (charge) temperature and reduced charge density, and less volume available for fresh air. The relationship between VE and RGF is complicated by the fact that reduced volumetric efficiency results in cooler residuals (fixed equivalence ratio, less chemical heat release) and greater heat transfer losses during NVO recompression.

Gas exchange processes are impaired at high RPM due to flow losses across already low-lift, short duration valves. Flow losses across the valve affect the intake process more because it has less of a driving force than exhaust blow down. Hence at high RPM volumetric efficiency is lower than it would be for the same valve timing at lower RPM. This result is illustrated in Table 4.1. Two operating points for High RON test fuel at the same stoichiometry and nearly identical valve timing result in a 50% decrease to VE accompanied by only an 18% increase in residual gas fraction. A greater fraction of residuals resulted in a less dense charge of fresh air at IVC even though intake air temperature is fixed at 80°C.

One further complication of engine speed is the impact of Helmholtz resonance on VE. At certain engine speeds, the compression waves created by air in the intake re-

Table 4.1: Effect of RPM on volumetric efficiency, point using high RON fuel

Parameter	Low speed	High speed
RPM	2000	2500
λ	1.31	1.30
EV adv. [CAD]	48	48
IV adv. [CAD]	1	2
Pilot inj. [μs]	0	0
Main inj. [μs]	970	670
m_{fuel} [mg/cycle]	9.0	6.3
VE [%]	33.0	22.9
RGF [%]	57.5	67.9
NIMEP [bar]	2.21	1.34
$\eta_{ind.}$ [%]	29.6	25.6

flecting off the closing/closed intake valve at IVC can be optimized using the geometry of the intake manifold runner such that they reflect and return to the open/opening intake valve at IVO. This improves VE at a particular RPM, and variable geometry intake manifolds can be used to exploit this affect across a range of speeds. For this engine and manifold there appears to be a resonance near 2000 rpm as indicated by the valve timing patterns across all loads at different speeds.

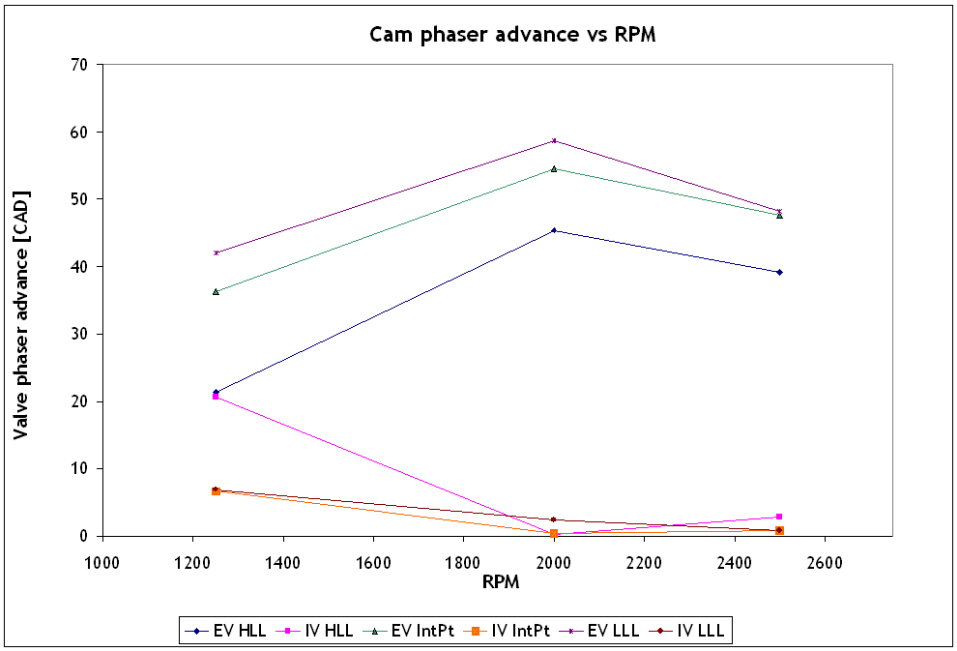

Figure 4-4: Cam phaser advance for different operating points

Table 4.2: Operating point comparison, the role of injection strategy

Parameter	Interior point	Near LLL
RPM	2500	2500
λ	1.30	1.31
EV adv. [CAD]	47	48
IV adv. [CAD]	1	1
Pilot inj. [μs]	0	195
Main inj. [μs]	700	474
m_{fuel} [mg/cycle]	6.5	6.4
VE [%]	23.4	23.2
RGF [%]	67.0	71.6
NIMEP [bar]	1.40	0.71
$\eta_{ind.}$ [%]	25.8	13.4
p_{max} [bar]	28.9	23.0
CA(p_{max}) [aTDC]	6.8	7.3

Table 4.2 shows that injection strategy can impact RGF independently from VE. At the same engine speed and nearly identical valve timing, RGF can increase without an appreciable an impact on volumetric efficiency. Since injected fuel mass is constant, fixed stoichiometry requires equal masses of air in both cases. Then if RGF increases, the fresh air must occupy a smaller volume at IVC since intake air temperature is fixed and equal in both cases. The increase in density means that the charge at IVO must be cooler in the split injection case. This may be the result of charge cooling from evaporation fuel injected in the pre-TDC$_{NVO}$ pilot injection reduced in-cylinder temperatures at IVO. The second possibility is that heat released by reactions during NVO recompression is lost or extracted as useful work. Some reaction or heat loss during NVO recompression is evident from the decrease in max cylinder pressure for the same overall fuel quantity. The timing of the pilot injection can also affect VE and RGF. A sweep of pilot injection timing is completed with fuel amount, valve timing and engine speed held constant. The test is repeated at 1250 rpm and 2500 rpm with substantially similar results. The result is shown in Fig. 4-5. VE decreases as pilot injection advances. If fuel evaporation was cooling the charge one would expect earlier injection would give more time for evaporation thereby improving the charge cooling benefit and improve VE. Since VE decreases we conclude that early pilot injection favours reactions during NVO which reduce reduce VE and output

some useful work.

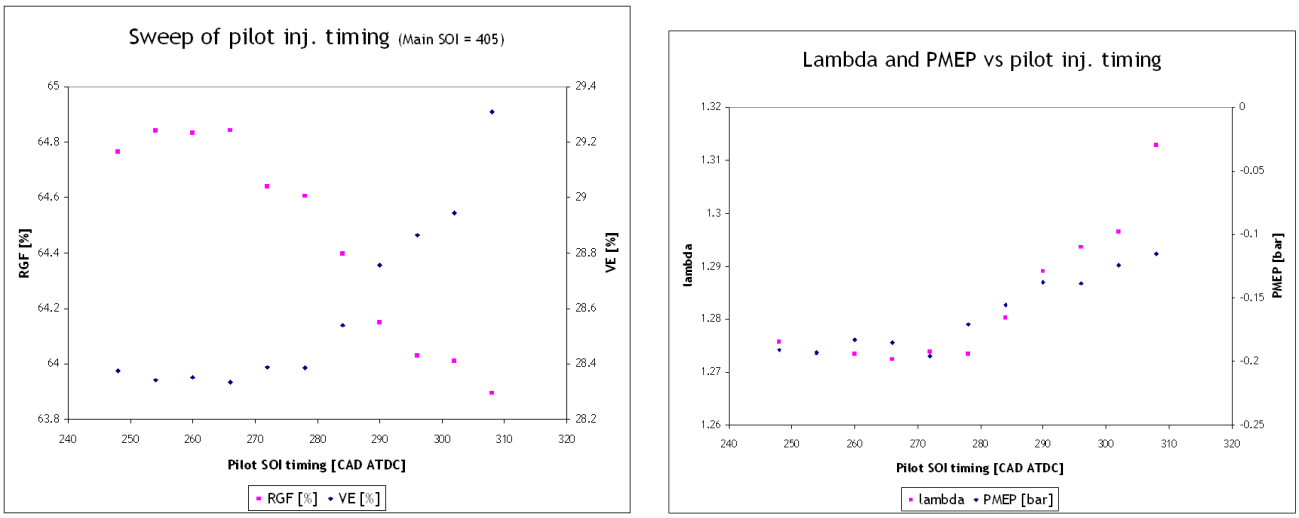

(a) RGF and VE effects

(b) λ and PMEP effects

Figure 4-5: Effect of pilot injection timing on VE, RGF, λ and PMEP.

By testing different main injection times with three fixed pilot injection timings, it is found that VE is far less sensitive to main injecting timing. The trend is that later main injection accompany modest decreases to VE and modest increases to RGF as shown in Fig. 4-6 which are plotted with the same axis limits as Fig. 4-5.

The asymptotic values at for VE, RGF, λ and PMEP hint that the total pilot fuel mass has reacted during NVO. Heat release analysis during the NVO recompression proved inconclusive owing to uncertainty in charge composition and the small magnitude of heat release compared to noise on the pressure trace. The effect of NVO reactions and charge cooling on VE diminish at high engine speed as flow losses across valves dominate the intake process physics of gas exchange.

A coarse sweep of fuel pilot fuel fraction from 0% to 100% by mass reveals diminishing returns in terms of increasing pilot fuel injection and reduction of PMEP. Earlier timing permits greater time for evaporation and mixture homogenization. Evaporation increases the quantity of fuel available for reaction during NVO, but cools the charge. It is not clear what impact fuel stratification has on reactivity. Excessive pilot injection and subsequent evaporative charge cooling may preclude reaction and in the extreme case lead to extinction.

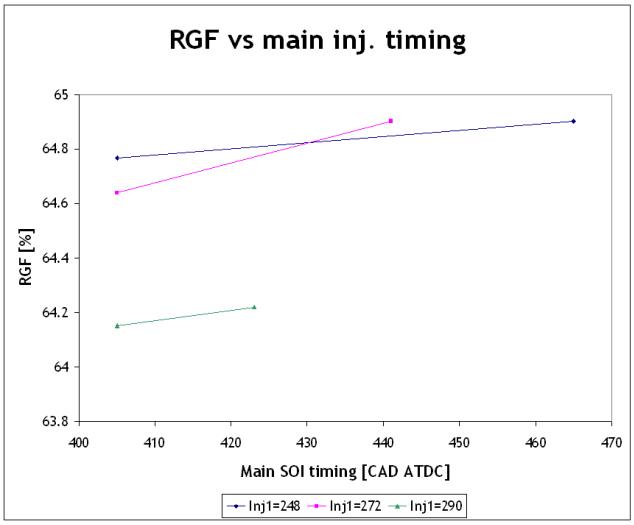

(a) RGF effects

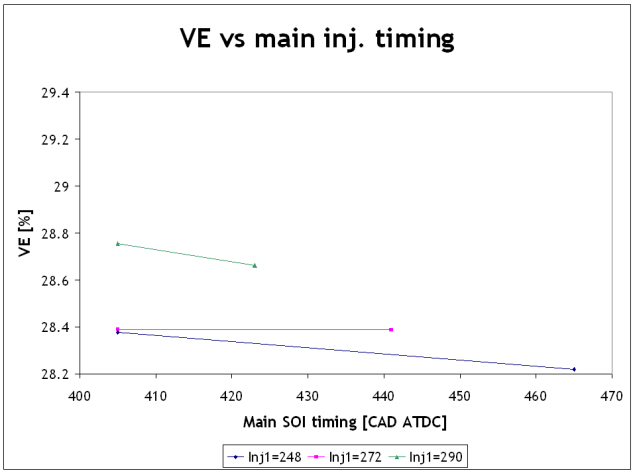

(b) VE effects

Figure 4-6: Effect of main injection timing on VE and RGF.

The above findings indicate that injection strategy can affect volumetric efficiency and load, but that valve timing is the primary means of control. Early commissioning results reveal a linear correlation between VE and EV cam phaser advance. Certain operating points deviate notably from this trend. The above described effect of a split injection strategy at 1250rpm and high RPM flow losses reduce VE. LLL points at higher speed do not suffer VE reductions because there is insufficient time for reaction or evaporation. This will be shown later on a plot of PMEP by operating point and fuel.

Increasing EV cam advance results in earlier EVC and increasing RGF. This behaviour shown in Fig. 4-7 agrees with expectations based on the VE-RGF relationship described above with deviations for high RPM and split injection as expected.

The complex interplay of valve timing and injection strategy result in a linear relationship between load and EV cam phaser advance shown in Fig. 4-8 . The notable deviations are labelled and as with RGF and EV advance, the decrease in VE with RPM decreases NIMEP at high RPM, as does split injection used near the LLL. This opens up interesting control possibilities for modulating load across RPM without changing valve timing or engine speed.

It is observed in Fig. 4-9 that the exhaust gas temperature (EGT) is nearly con-

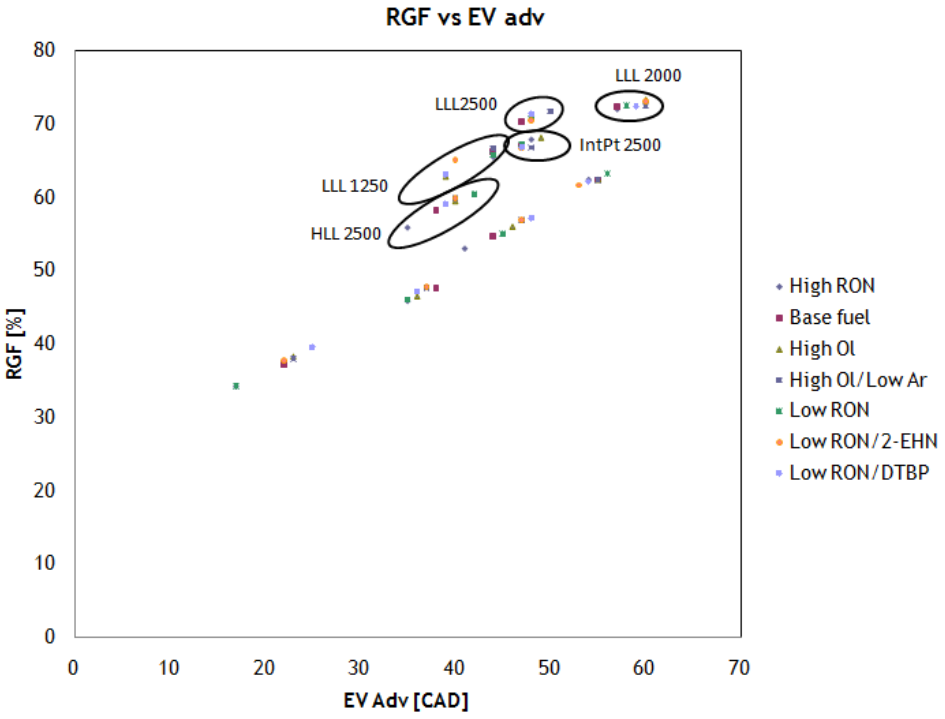

Figure 4-7: RGF versus exhaust valve phaser advance

stant at the LLL for all speeds and fuels. There is a modest decrease in EGT from around 255°C at 1250 rpm to 230°C at 2500rpm. As engine speed increases, heat transfer losses from trapped residuals decrease so their minimum allowable "starting temperature" can be lower while still retaining sufficient thermal energy to initiate autoignition. Excluding points near the LLL, other operating points show an increasing EGT with load explained by the greater chemical heat release from increased fuelling. This trend levels off, almost asymptoticallyan EGT of approximately 450°C. Trapped residuals at this temperature contain sufficient thermal energy that subsequent CAI combustion reactions reach the imposed limit on PRR.

4.1.3 Conversion efficiency

The net indicated fuel conversion efficiency is plotted by fuel and operating point in Fig. 4-10. It appears that indicated fuel conversion efficiency is approximately constant for all fuels at a given operating point. Differences may arise due to variations in combustion duration or combustion phasing. These two factors will be discussed

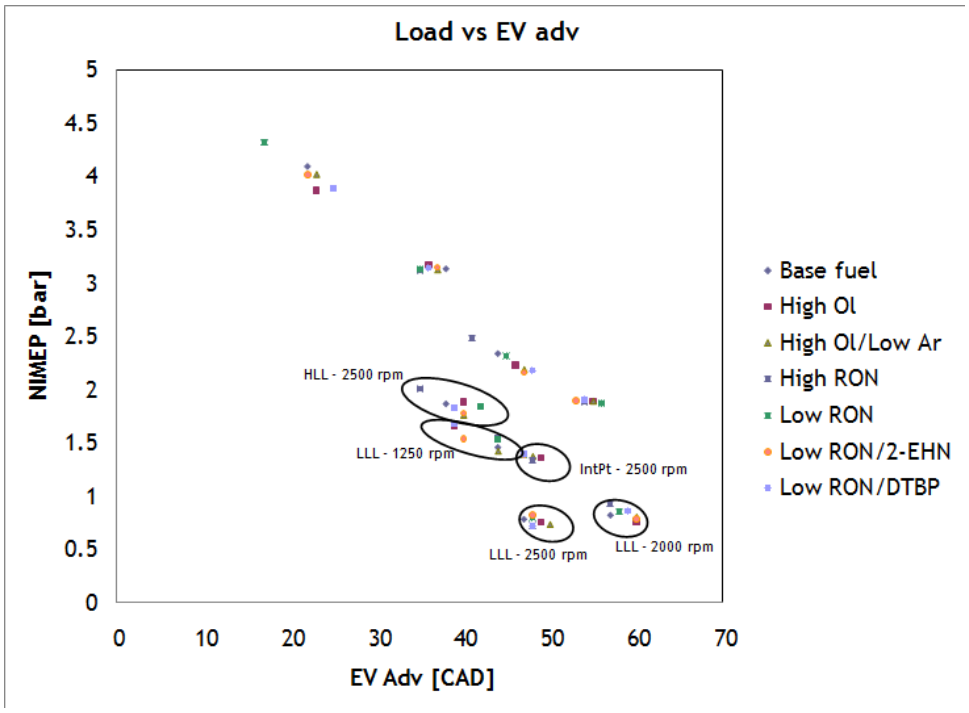

Figure 4-8: Engine output versus EV cam phaser advance

explicitly in subsequent sections. There is a trend of increasing conversion efficiency with increasing load at a particular engine speed for all engine speeds. The decrease in efficiency at higher engine speed comes from increased pumping work. Although pumping work, in absolute terms, remains approximately constant for HLL and interior operating points, the load at those points decreases at high RPM so pumping work represents an increasing fraction of output hence net indicated fuel conversion efficiency decreases.

Fuel conversion efficiency decreases dramatically for split injection except at 1250rpm. The decrease in efficiency cannot be completely explained by the increase in pumping work at 2000 rpm compared to 1250 rpm, since this effect is present at interior point and HLL points as well without the same decrease in efficiency.

The LLL points at 2000 rpm and 2500 pm have asymmetric valve timing and the 1250 rpm does not. The asymmetry results in earlier than symmetric IVO and some back flow from the cylinder to the intake runner. This would require some additional pumping work during the intake stroke required compared to 1250 rpm. This alone is not a satisfactory explanation because the trend in pumping work does not match

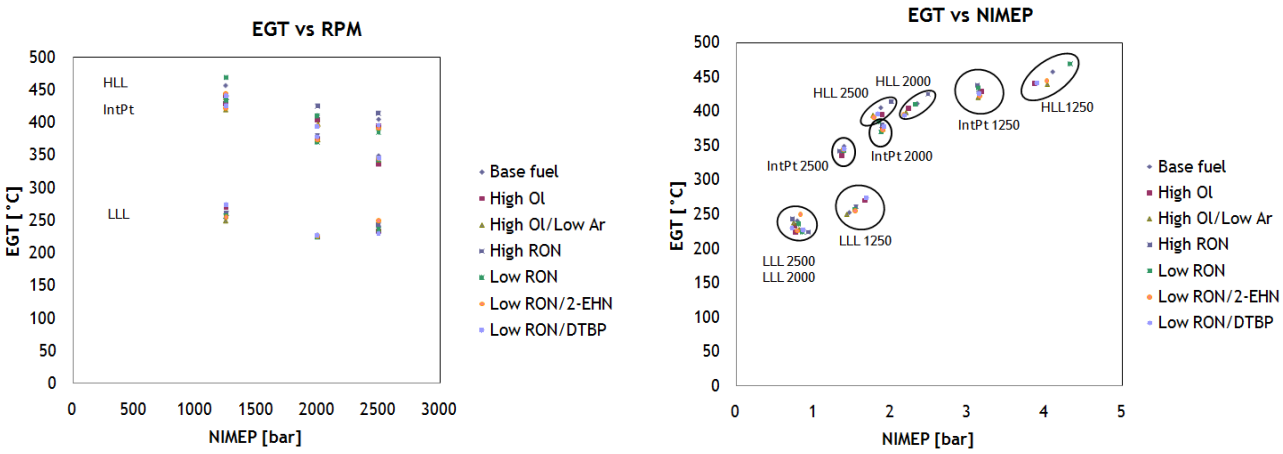

(a) EGT vs engine speed

(b) EGT vs engine output

Figure 4-9: Engine exhaust gas temperature vs load and speed

valve timing.

It is further theorized that the switch to a split injection strategy is responsible. Namely the processes of pilot injection, evaporation, mixing and oxidation reactions during NVO recompression only provide useful work when they are given sufficient time to occur, that is at low engine speed. This theory is qualitatively supported and the contribution of work extraction during the NVO recompression is elaborated in the next section.

4.1.4 NVO Heat release

It was originally intended to analyze heat release during NVO recompression to assess the low temperature heat release (LTHR) characteristics of each fuel during that period. It was was thought that fuels with greater LTHR would might have a lower LLL, and earlier combustion phasing. However Rasweiller-Withrow heat release analysis is especially difficult during the NVO recompression due to changes in charge composition, temperature and pressure during injection and evaporation of pilot injection fuel. Apart from these sources of error, the analysis relies on the derivative of the pressure signal. As such, noise is "amplified". Ordinarily this noise is still negligible compared to the pressure signal and heat release during the main combustion event

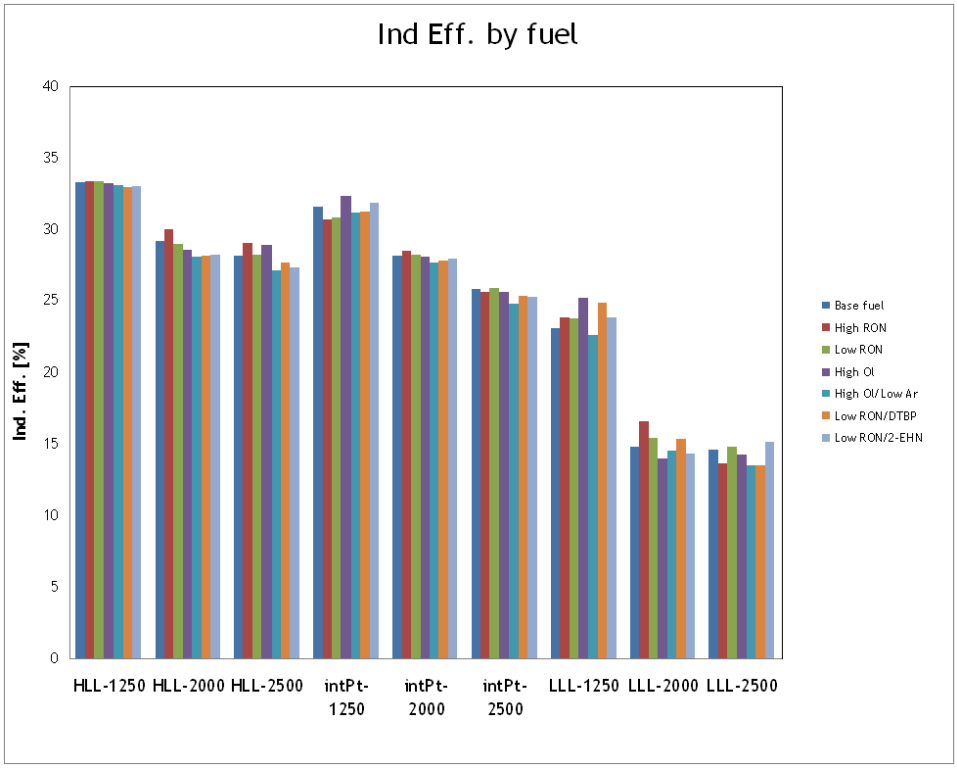

Figure 4-10: Indicated fuel conversion efficiency by fuel and operating point

may be calculated with acceptable error. However during NVO recompression, heat release is usually 30-40 times smaller, which means that noise here introduces unacceptable error into calculated NVO heat release. Nevertheless it is useful to apply the heat release analysis to observe qualitative changes and trends while remaining aware of the fact that the absolute quantitative results are in error.

One of the most common implementations of the Rasweiller-Withrow method for SI combustion utilizes an empirical finding, namely that changes in the specific heat ratio due to composition and temperature changes during combustion are offset by heat transfer out of the charge. In practice this means that a single, constant polytropic index can be used to characterize the compression process experienced by the charge caused by combustion, as opposed to the separate and simultaneous compression process caused by piston motion.

The physics and charge composition of CAI combustion are different than SI combustion. However, in some respects CAI presents a simpler case for analysis. For

lean (λ=1.3) dilute combustion the change in specific heat ratio due to pilot injection is minimal. Using reasonable estimates for gas properties from regression of actual cylinder pressure data, along with cylinder pressure and geometry data during NVO recompression it is possible to estimate heat release rate during NVO. Fig. 4-11 shows the noisy nature of HRR analysis during NVO. Both figures are taken at 2000 RPM and identical valve timing. Fig. 4-11(a) shows heat release during NVO with no pilot injection. As expected its average value is nearly zero. The disturbance around 320 CAD in Fig. 4-11(b) is the pilot injection. Subsequent heat release is evident even if it there is difficulty in assessing its magnitude quantitatively. Figures 4-12,4-13,

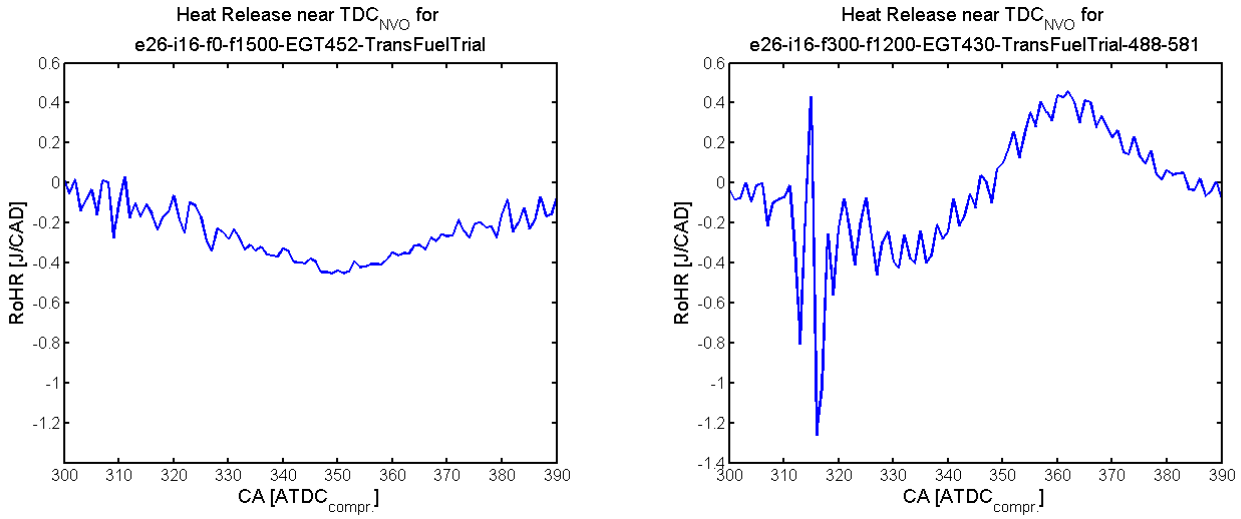

(a) Single injection

(b) Split injection

Figure 4-11: NVO heat release analysis for split and single injection at 1250 rpm

and 4-14 show the rate of heat release during the NVO recompression process for operating points near the LLL (i.e. split injection) at different engine speeds. All points had approximately the same pilot injection fuel mass. There is distinct heat release in all cases, but the magnitude of heat release decreases with increasing RPM. When the rate of heat release data is integrated, one obtains an estimate of the total heat release during NVO recompression. It must be emphasized that due to changes in gas properties, the calculated values for NVO heat release in Table 4.3 are approximate. From Table 4.3 it seems plausible that the difference between fuel conversion efficiencies of LLL operating points at different speeds is explained by

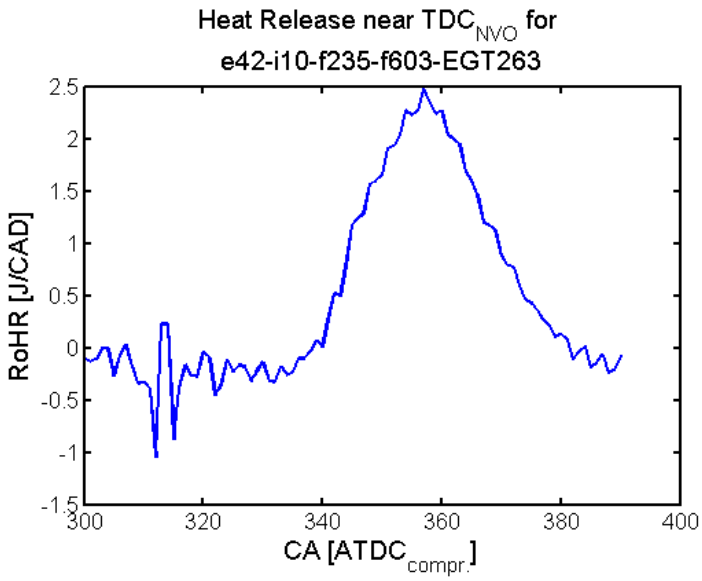

Figure 4-12: NVO heat release for split injection case at 1250 rpm

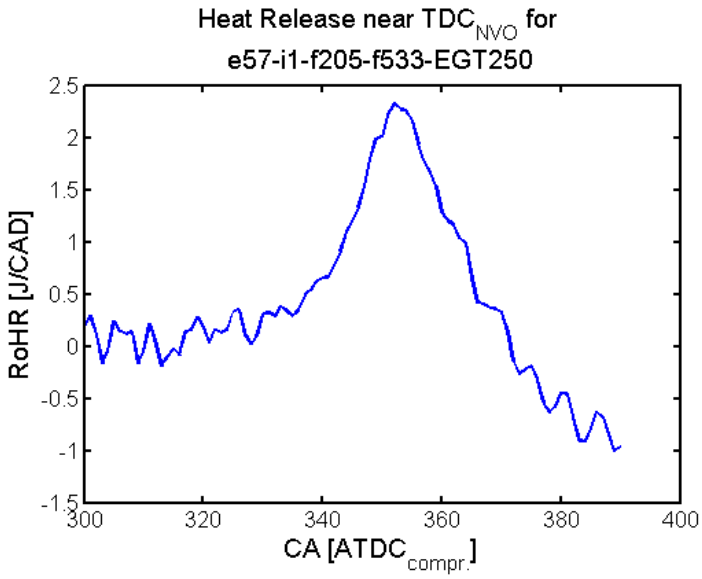

Figure 4-13: NVO heat release for split injection case at 2000 rpm

the heat release during NVO. At lower speeds, more heat release takes place, and therefore more thermal energy from the pilot injection can be extracted during the NVO expansion (i.e. intake) stroke. At higher speeds, insufficient time is available for evaporation, mixing and oxidation so heat release takes place later and provides less useful work during NVO expansion.

There are two other indirect indicators of heat release and work extraction during

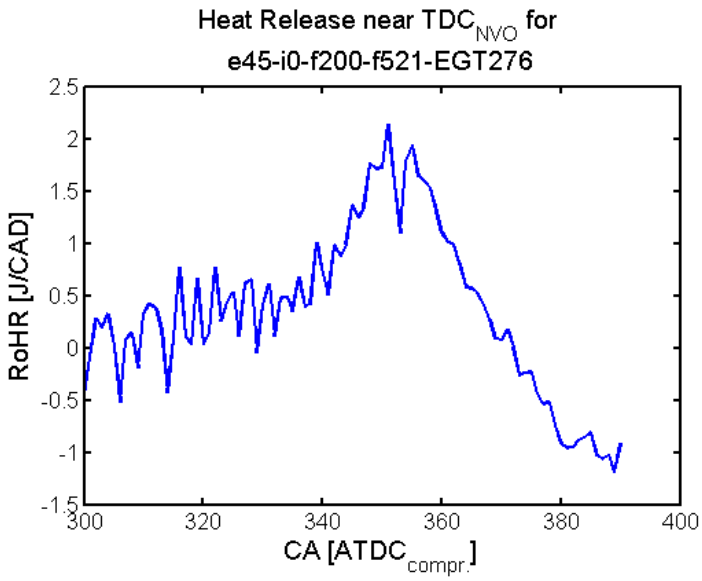

Figure 4-14: NVO heat release for split injection case at 2500 rpm

Table 4.3: Comparison of approximate NVO heat release at different speeds

Speed	m_{fuel} [mg]	γ	RGF [%]	Approximate NVO Heat Release [J]
1250	2.29	1.30	65	46.5
2000	2.01	1.24	72	25.1
2500	1.97	1.23	71	16.3

NVO. The first is PMEP and the second is p_{max} during NVO. Fig. 4-15 shows the PMEP organized by operating point and separated by fuel. The sign convention is such that positive PMEP is work done by the engine for the intake and exhaust strokes, and negative PMEP is work extracted by the engine during the intake and exhaust strokes.

Pumping work is a major source of inefficiency for the engine. The figure shows that PMEP is approximately constant for all interior and HLL points for all speeds. PMEP is slightly elevated at 2000rpm, but from Fig. 4-4 we see that EV is advanced so that simply reflects the greater pumping work to compress trapped residuals, some of which is lost as heat transfer. The interesting trend for LLL points is a dramatic decrease in PMEP compared to the relatively constant value at other operating conditions. Apart from greater exhaust valve cam phaser advance than the interior points, LLL points differ from other operating points in their use of a dual injection strategy.

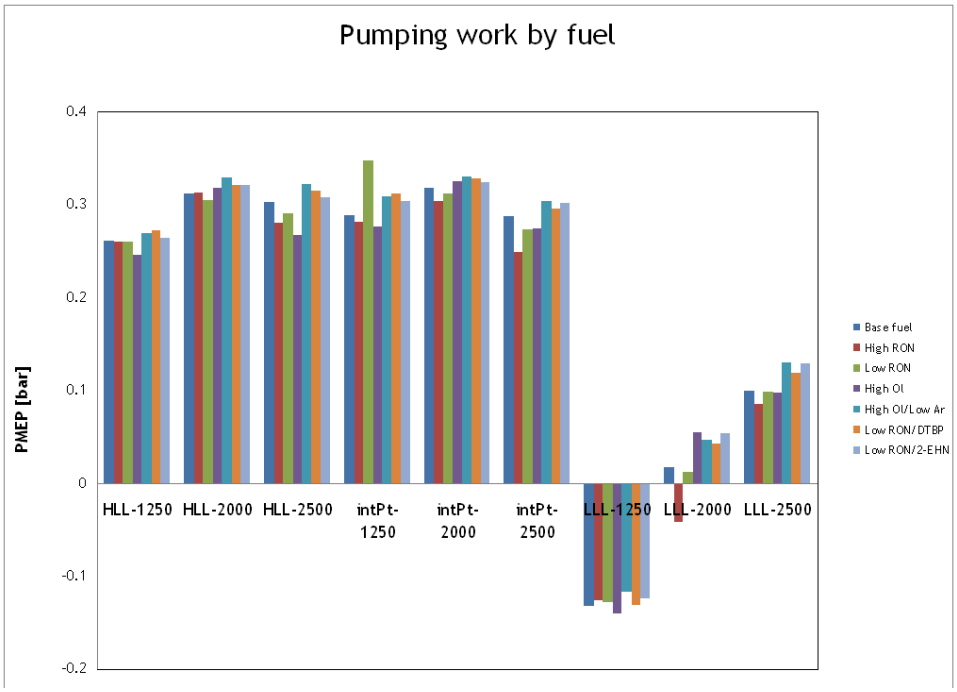

Figure 4-15: PMEP by fuel and operating point

The decrease in PMEP is mainly due to heat release from the pilot injection and the resulting work extraction during NVO. The PMEP of LLL points follows the same trend as the magnitude of heat release during NVO, shown in Table 4.3. The error in calculating PMEP is a few percent. With the exception of Low RON fuel at the interior point at 1250 RPM and the High RON fuel at the LLL at 2000 rpm all fuels fall within the error of these measurements.

Comparing pressure trace data for experiments with identical valve timing, and nearly constant fuel amount it is observed that p_{max} during NVO increases when pilot injection is present. This happens at low and high engine speed, at high and low loads as shown in Table 4.4. If charge cooling were the main mechanism for reducing PMEP then peak pressure would decrease. Since it increases, it is concluded that work extraction reduces PMEP. This work extraction is less efficient than the main combustion event because temperatures and pressures in cylinder are lower during NVO than main combustion, due to the lower effective compression ratio (EVC to TDC compared to IVC to TDC). This explains the decrease in conversion efficiency attributed to the split injection strategy. The reason why PMEP is lowest at low

Table 4.4: Operating point comparison, the role of injection strategy

Parameter	**Single inj.**	**Split inj.**		**Single inj.**	**Split inj.**
RPM	1247	1248		2496	2496
λ	1.30	1.20		1.30	1.32
EV adv [CAD]	26	26		47	47
IV adv [CAD]	16	16		1	1
NIMEP [bar]	3.88	3.48		1.40	0.68
$(p_{cyl})_{max}$ [bar]	37.55	40.77		30.49	23.10
CA(p_{max}) [ATDC]	13.2	7.5		6.2	7.1
PMEP [bar]	0.284	0.090		0.287	0.086
Pilot inj. [μs]	0	300		0	193
Main inj. [μs]	1500	1200		700	470
m_{fuel} [mg/cycle]	14.1	14.3		6.5	6.3
VE [%]	50.7	47.3		23.4	23.1
Ind. Eff. [%]	33.2	29.5		25.8	13.0
RGF [%]	39.6	41.9		67.0	71.7
NVO $(p_{cyl})_{max}$ [bar]	11.01	11.55		17.90	19.02
NVO CA(p_{max}) [ATDC]	361.4	362.6		361.8	362.4

RPM, i.e. most work extracted, is that flow losses across valves are lowest, time for evaporation and mixing of pilot fuel injection is longest and and a greater total fuel mass is injected in the pilot injection making for NVO work extraction at higher temperatures and pressures than occurs at higher RPM.

The influence of pilot injection timing is explored to investigate its effect on heat release during NVO. Holding fuel amount and valve timing constant, pilot injection timing is made progressively earlier. At both engine speeds, earlier injection time allows more time for evaporation, mixing and oxidation. Hence the magnitude of heat release increases with earlier pilot injection as seen in Fig. 4-16. Table 4.3 shows that the composition at all three speeds is approximately equal. The difference in the polytropic index must then be due to a difference in heat transfer or gas temperature with higher engine speed at higher temperature. This implies that at high RPM, the effect of increased temperature of in-cylinder gases (due to reduced heat transfer and greater RGF) is overcome by the reduced reaction time since fixed injecting timing was used for all experiments. It suggests that early injecting timing might be used to improve conversion efficiency at LLL operating points.

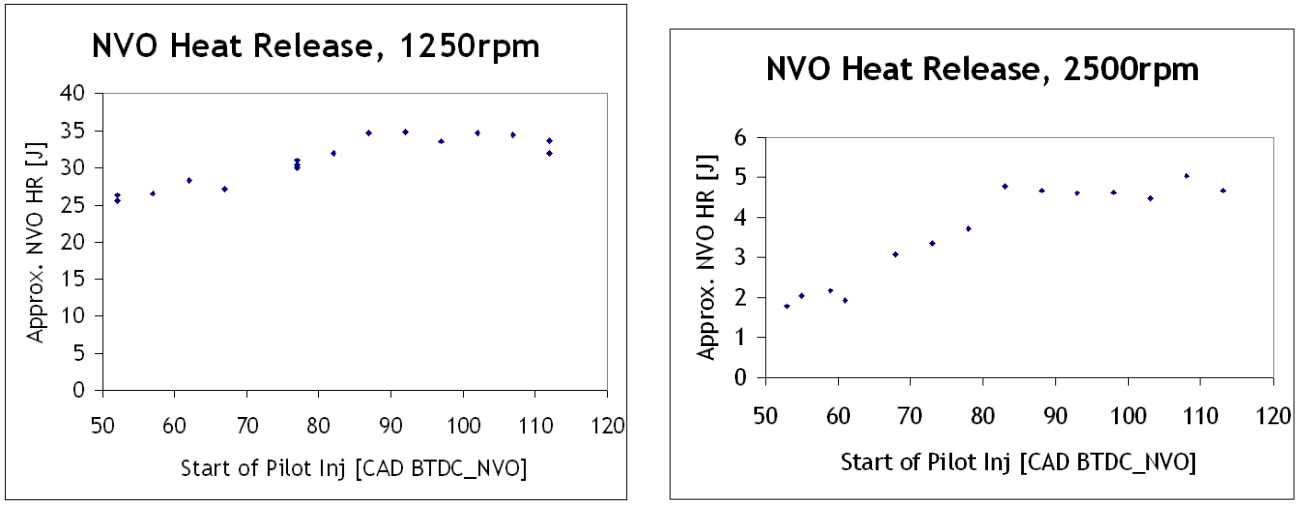

(a) 1250 rpm

(b) 2500 rpm

Figure 4-16: Effect of pilot injection timing on NVO heat release

4.2 Fuel effects

4.2.1 Combustion phasing

Combustion phasing has a direct impact on conversion efficiency. If combustion occurs too early, extra work must be expended for the piston to compress the in-cylinder gas whose pressure and temperature are increasing due to chemical heat release. If combustion occurs too late, the reacting mixture is cooled by expansion, which retards the reaction and reduces the mixture pressure. The initiation/timing of combustion is a function of temperature, pressure and mixture chemistry. Numerous factors affect combustion phasing through temperature and pressure such as valve timing and intake air temperature. There are other factors that affect combustion phasing as well, such as spark timing and equivalence ratio. Many of these are held constant in this work to isolate the role of fuel chemistry in combustion phasing.

The measure of combustion phasing used in this work is CA50. This is the crank angle corresponding to when 50% of the in-cylinder charge has burned. This is extracted from heat release data from the Rasweiller-Withrow method. A complete set of combustion phasing results for all fuels organized by operating point, and by speed is available in Appendix A. With reference to those plots, the trends in combustion

phasing are discussed.

The most advanced combustion phasing occurs for HLL operating points at 2500 rpm. In this configuration time for heat transfer is minimized and chemical heat release is maximized meaning reaction kinetics are most rapid. The most retarded combustion phasing occurs for interior operating points at 1250 rpm. In this configuration, time for heat transfer is maximized with an intermediate fuel mass, and no NVO reactions to keep the charge hot during recompression.

Comparing combustion phasing for HLL and interior points across engine speeds, it is noted that combustion phasing advances with increasing RPM. This is explained by higher in-cylinder temperatures resulting from increased friction and reduced time for heat transfer. Higher in-cylinder temperature results in faster reaction kinetics. Combustion phasing is not very sensitive to engine speed at the LLL with perhaps a slight retardation at high RPM, which may be a result of the greater RGF at high RPM. The insensitivity to RPM is a trade-off of competing influences. Near the LLL the split injection strategy and the accompanying heat release during NVO recompression result in a charge pre-heating effect. As noted in the discussion of PMEP, this heat release is strongest at 1250 rpm and diminishes at higher engine speeds. At higher engine speeds the lost heat release is compensated by decreases in heat transfer losses. The net result is that the charge remains at a nearly constant temperature, which all other factors being equal results in a nearly constant combustion phasing.

There is a positive correlation between combustion phasing and indicated efficiency as shown in Fig 4-17. The trend is stronger at the HLL (Fig 4-17(b)) than for interior points (Fig 4-17(a)).

Combustion phasing was never late enough to see declining efficiency with later phasing. This is because combustion occurs rapidly as soon as the charge has been raised to sufficient temperature and pressure for the autoignition reactions to initiate. CAI late into the expansion stroke would require extreme fuel autoignition delays, long enough to resist autoignition during the peak temperatures and pressures at TDC.

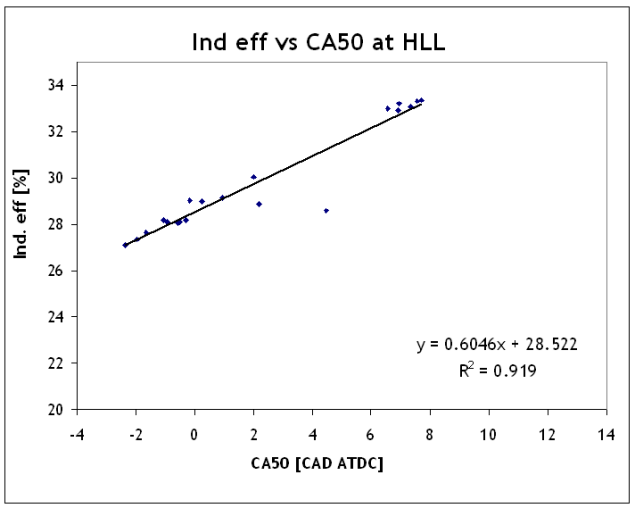

(a) Interior points

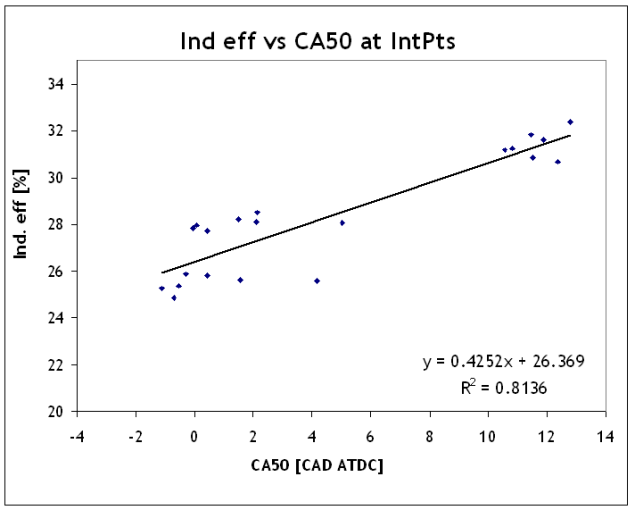

(b) HLL operation

Figure 4-17: Effect of combustion phasing on fuel conversion efficiency

Relation to fuel composition

The test fuels for this study were blended to hold RVP and RON approximately constant while varying the parameter of interest. The changes reported to composition in terms of %-Aromatic, %-Saturates and %-Olefin mask more complicated changes to the amount of each individual species. Even with complete knowledge of fuel composition, it is difficult to correlate autoignition behaviour and combustion dynamics with mixture components. Non-linearities crop up for reacting mixtures due to interactions between simultaneous and competing kinetic mechanisms for each mixture component in the reacting mixture.

Qualitatively we may see from the plots in Appendix B that there appears to be a weak positive correlation between later combustion phasing and aromatic content, and also a weak positive correlation between later combustion phasing and olefin content except the High Olefin/Low Aromatic fuel which shows a significantly earlier phasing than the High Olefin fuel. These trends disagree with previous phases of this project completed by Andreae, but he comments that the trends observed ran contrary to his own expectations.[14] The results here agree with results reported elsewhere, and expectations based on the high RON (i.e. high autoignition resistance) of olefin and aromatic components.[23, 24] Since the fuels have comparable olefin

Table 4.5: Combustion phasing by fuel

Earliest phasing	Low RON + 2-EHN
	Low RON + DTBP
	High Ol/Low Ar
	Low RON
	Base fuel
	High RON
Latest phasing	High Olefin

content, and aromatics are generally known to have high autoignition resistance, the disparity between the High Olefin and High Olefin/Low Aromatic fuel is most likely explained by the greater fraction of saturates in the High Ol/Low Ar fuel. Compared to olefins, saturates generally have lower autoignition resistance except heavily branched saturated hydrocarbons which can have comparable autoignition resistance.

There appears to be a weak correlation between earlier combustion phasing and higher %-Saturates content. The effect is strongest for Low RON fuels treated with the DTBP and EHN additives.

The most pronounced differences in combustion phasing seem to manifest themselves at high engine speed, at all operating points. The increase in friction and reduction in heat transfer losses mean that the charge is hottest here. The high temperatures accelerate the kinetics and accentuate any fuel to fuel variations. The ranking of fuels by combustion phasing is relatively constant, and given in Table 4.5. The range of different combustion phasing between fuels does not translate into significant differences in engine fuel conversion efficiency.

4.2.2 Combustion duration

In addition to their impact on combustion phasing, the chemical reaction kinetics of the fuel determine the overall fuel consumption rate. Burn duration is an important parameter because it can impact conversion efficiency. A fuel that has very late phasing may still have good efficiency if its burn duration is short compared to a fuel with earlier phasing but a longer burn duration. Burn duration also influences

pressure rise rate, which limits the utility of CAI combustion at high loads. For the present work, burn duration is measured by a parameter called 10-to-90 burn duration, or BD1090. It represents the number of crank angles between the point at which 10% of the fuel mass is burned to the point at which 90% of the fuel mass is burned. Equivalently $BD_{10-90} = CA90 - CA10$; with CA90 and CA10 estimated from Rassweiler-Withrow heat release data. The relationship between PRR and burn duration is shown in Fig. 4-18. Interior points show a largely linear relationship

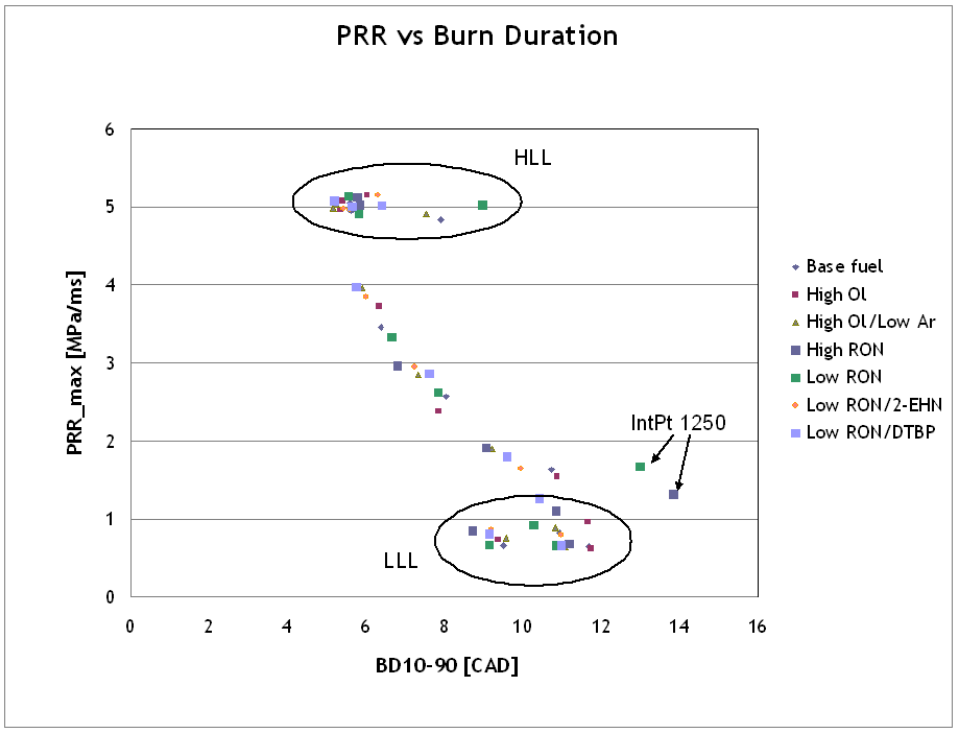

Figure 4-18: PRR vs burn duration

between burn duration and pressure rise rate. HLL points, whose PRR is essentially prescribed fall approximately on this line. Burn duration of points at the LLL depend heavily on RPM. Burn duration organized by operating point is shown in Fig. 4-19. The figures in Appendix A are also useful as they indicate combustion duration (black line between CA10 and CA90) in addition to the combustion phasing (red marker at CA50). From the figure it is apparent that the High RON consistently shows the longest burn duration. At 2000 rpm and 2500 rpm, burn duration shortens (i.e. combustion is more rapid) with increasing load. In these cases, increased fuel heat

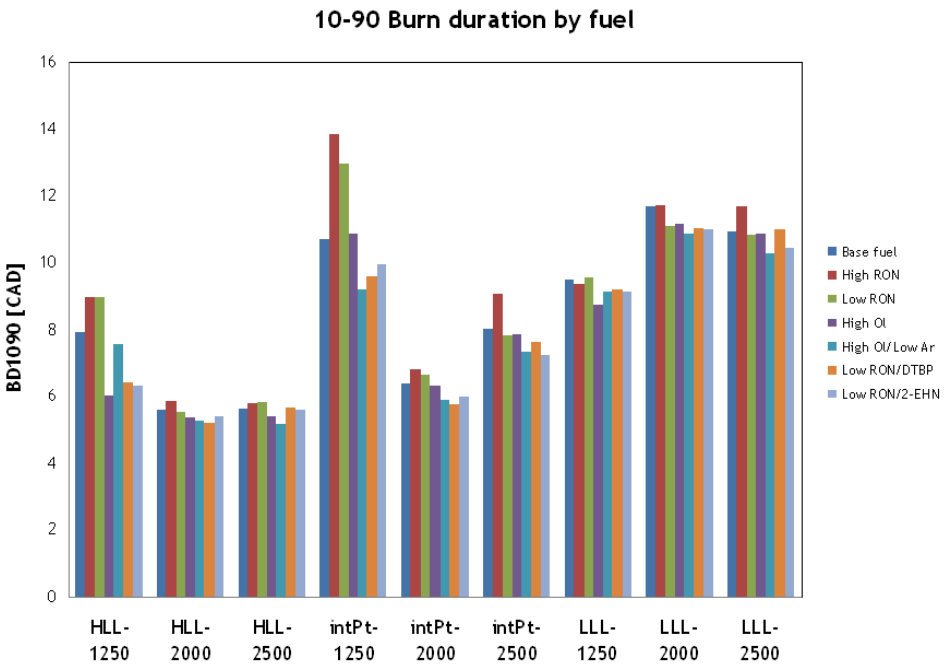

Figure 4-19: Burn duration by operating point and fuel

release results in faster reactions, evidently enough to compensate for the increased fuel mass. At 1250 rpm there is a slight increase in burn duration from the LLL to the interior operating point. This observation may be attributed to the significant heat release from the pilot injected fuel during NVO recompression, so that the main fuel combusts in a hotter environment.

BD1090 can be scaled with engine speed to give an estimated burn duration time. Fig. 4-20 shows that burn duration decreases with speed and load except at 1250 rpm for the reasons explained in the preceding paragraph. The decrease in burn duration between the intermediate operating point at 2000 rpm and the HLL at 2500 rpm, which occur at approximately the same load indicates the role of reduced heat transfer and increased turbulent mixing on enhancing combustion reaction rates. Fuel mass and rpm-scaled BD1090 can be used to compute an approximate average fuel burn rate for each fuel. The result is plotted in Fig. 4-21. The plot shows that fuel burn rate increases with load at all speeds although the effect is most pronounced at high speeds. Fig. 4-21 also shows that fuel consumption rates increase with

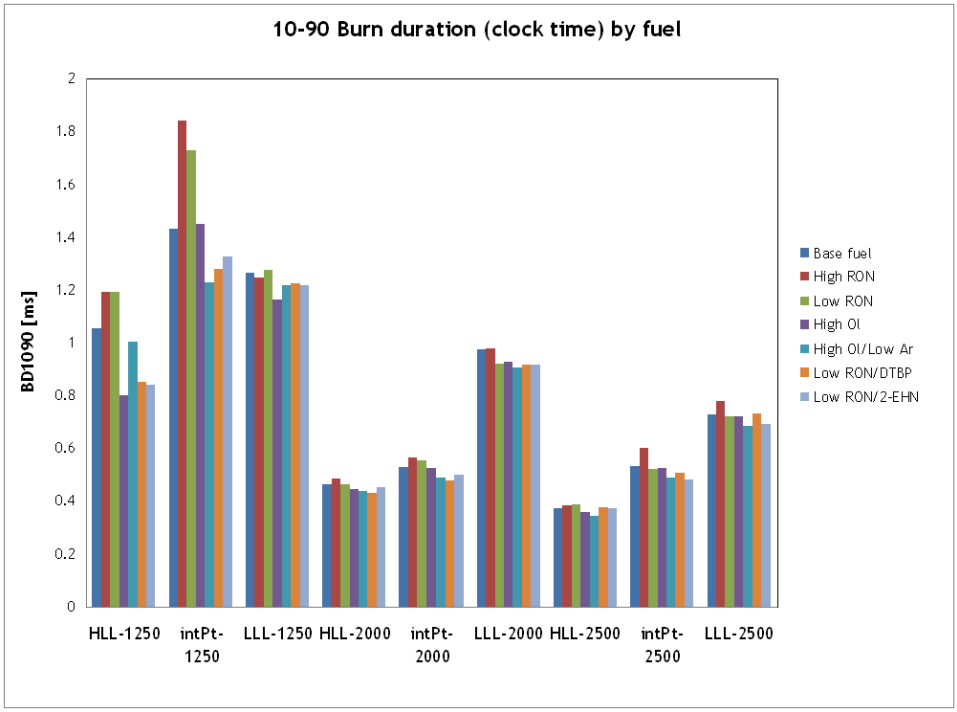

Figure 4-20: Burn duration time by operating point and fuel

engine speed. The average fuel burn rate is approximately constant for HLL points at 2000 rpm and 2500 rpm and approximately 40% greater than the average fuel burn rate at 1250 rpm. A plausible explanation is that the burn rate is controlled by temperature gradient; i.e. the combustion is a result of sequential ignition of the thermally stratified charge. Thus when the load increases, the burn duration is fixed, but the amount of fuel being burned increases. Therefore the burn rate increases with load. Since the thermal boundary layer is thicker at lower engine speed, the degree of temperature stratification is more pronounced at 1250 rpm (compared to 2500 rpm); hence the burn rate is much slower.

Relation to combustion phasing

The connection between conversion efficiency, combustion phasing and combustion duration was mentioned earlier. Here the relationship between combustion phasing and combustion duration is investigated. At the HLL, Fig. 4-22(a) shows that combustion duration is insensitive to combustion phasing except at 1250 rpm where

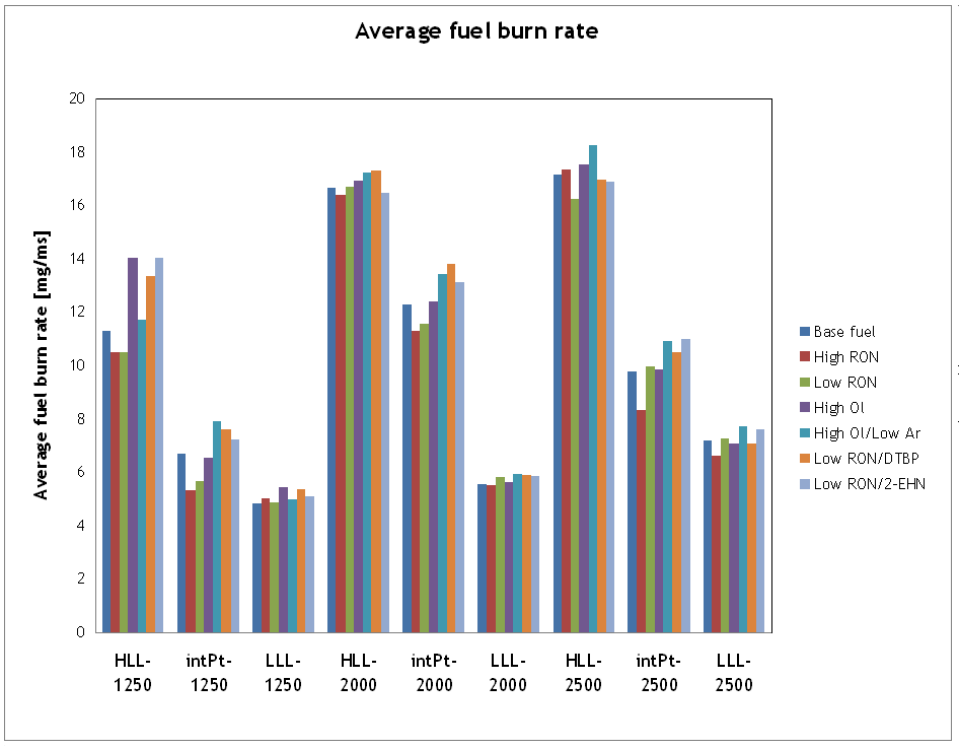

Figure 4-21: Average fuel burn rate

CA50 is beyond 6 CAD ATDC; then it appears that later phasing correlates with longer burn durations. Because the charge is cooler at 1250 rpm than other engine speeds, combustion reactions start later. Then the combustion reactions are impeded by expansion cooling caused by piston motion. This behaviour is also present for the intermediate load point data in Fig. 4-22(b). It is also noted here that High RON and Low RON fuels have longer than expected burn durations and High Olefin content fuel typically has the latest combustion phasing at a given operating point. At the HLL, burn duration is much less sensitive and does not show any discernible relationship to combustion phasing.

Relation to fuel composition

Given the relationship between PRR and burn duration, and since the PRR is deliberately limited at high loads, and shows a common minimum at low loads largely independent of fuel and engine speed (see Fig. 4-18), the focus for fuel-based differences in BD1090 is placed on interior operating points. A collection of BD1090 plots

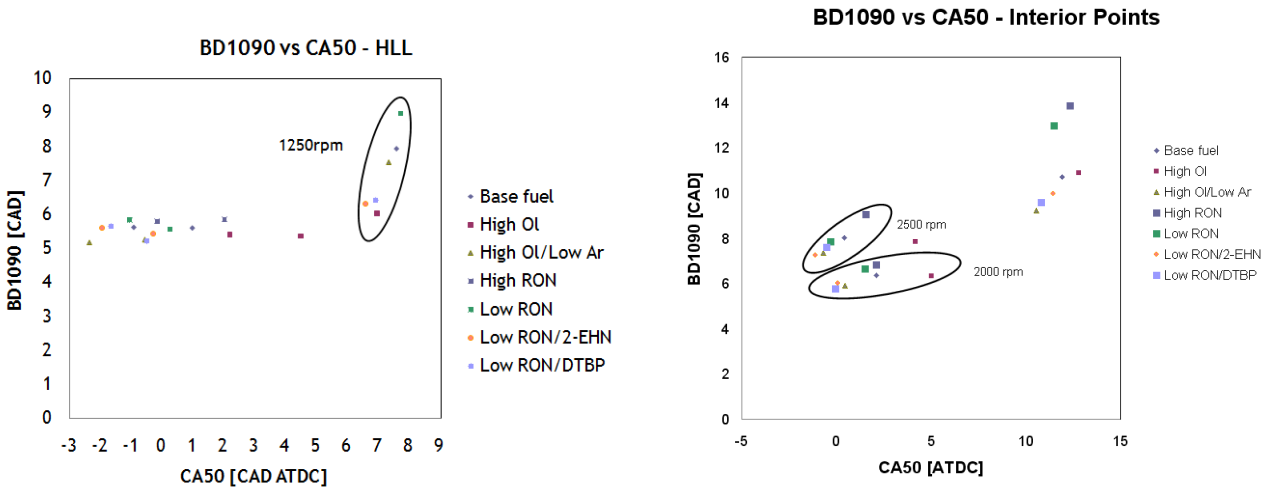

(a) HLL

(b) Interior points

Figure 4-22: Burn duration vs combustion phasing at HLL and interior points

versus fuel composition are presented in Appendix D. Fig. D-2 shows that at low RPM, burn duration of LOW RON fuels with cetane modifiers is noticeably shorter than burn duration of Low RON fuels although this effect is diminished at higher RPM. With the exception of cetane modifiers, burn duration does not show any dis-

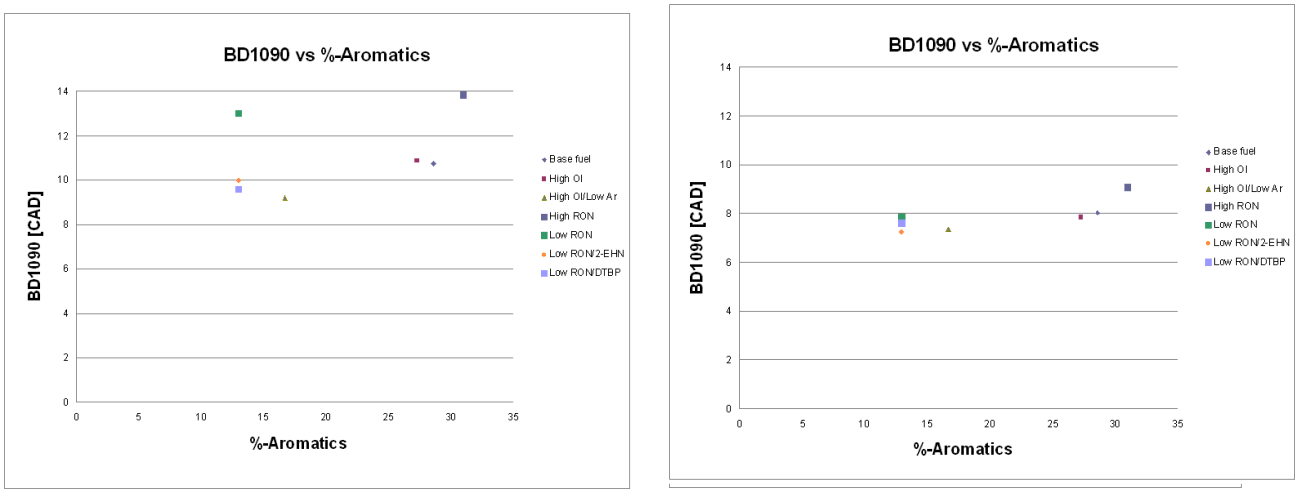

(a) 1250 rpm

(b) 2500 rpm

Figure 4-23: Burn duration vs %-Aromatic content at interior operating points

cernible trend in sensitivity to saturate aromatic, saturate or olefin content. This implies that for the fuels tested, burn duration for interior points is more dependent

on the in-cylinder state, than on fuel composition.

4.2.3 Pressure rise rate

Since maximum pressure rise rate is prescribed at the high load limit, the comparison of pressure rise rates between fuels will be confined to the interior points and points near the LLL. Fig. 4-24 shows pressure rise rate by operating point and fuel. Fuels

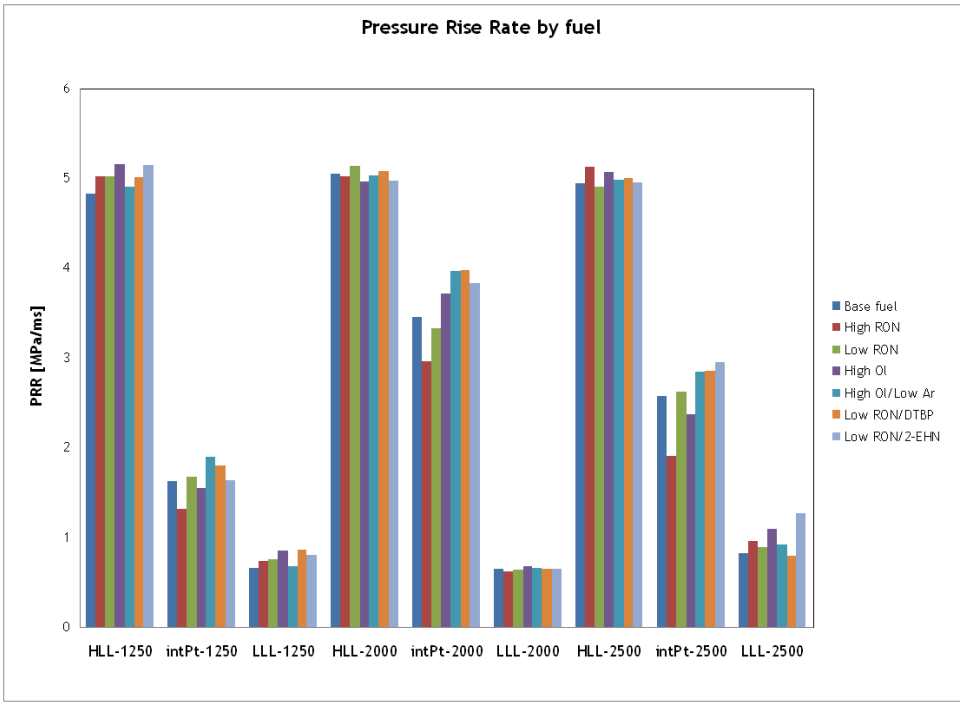

Figure 4-24: In cylinder PRR organized by fuel and operating point

display a fairly consistent PRR at the low load limit. PRR reflects the rate of chemical reaction. The PRR at the LLL is considered to be the slowest viable reaction rate for self-sustaining stable CAI combustion. There is some differentiation between fuels at the 2500 rpm LLL point with High Olefin and 2EHN treated fuels showing higher than average PRR.

At interior points, the High RON fuel shows the lowest pressure rise rates. High OI/Low Ar and the fuels treated with 2EHN and DTBP show slightly higher than average PRR. If pressure rise rate is interpreted as an indicator of fuel reaction rate, the low PRR of the High RON fuel agrees with its tendency to resist autoignition in

SI combustion.

For interior points, the average PRR increases from 1250 rpm to 2000 rpm, then decreases from 2000rpm to 2500rpm. This behaviour is plausibly explained by additional heat loss experienced by the charge at 1250 rpm. The lower in-cylinder temperature reduces reaction rates. However this is not the entire explanation, otherwise the PRR at 2500 rpm would be greater than at 2000 rpm which is not the case. The explanation is that the NIMEP value at 1250 rpm is substantially higher at the intermediat points than those at higher speeds; thus RGF is approximately 25% lower at 1250 rpm than 2000 rpm and 2500 rpm. The mixture is composed of more comparatively cool fresh air and less hot trapped residuals. The reduced in-cylinder temperatures lead to lower reaction rates and hence lower PRR.

PRR increases with engine load at all engine speeds, so to assess and compare the reactivity of different conditions on an even basis, the PRR is normalized by fuel mass. The result is Fig. 4-25.

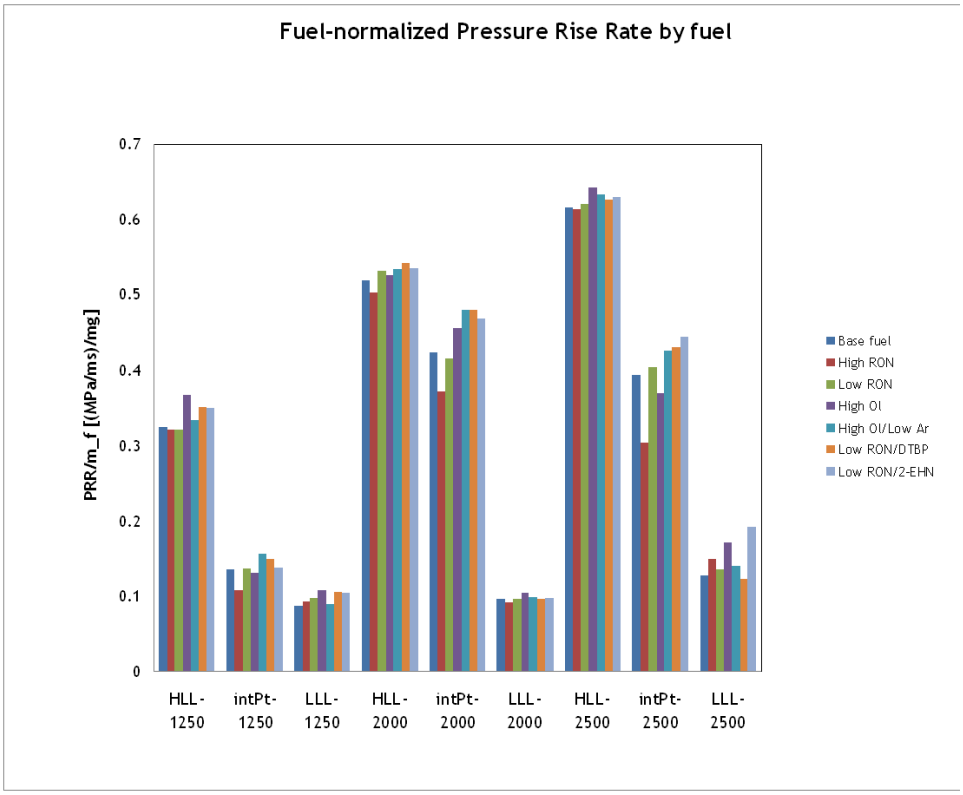

Figure 4-25: In cylinder PRR normalized by fuel mass

Fig. 4-25 shows that normalized PRR at the HLL increases with engine speed. This trend is the result of decreased heat transfer. The mixture, though it contains less fuel is hotter so it reacts more rapidly. This plot, which effectively cancels the influence of NVO heat release also shows an increase in normalized PRR at the LLL as well, albeit far more gradual than at the HLL. At interior operating points the PRR is lowest at 1250 rpm as a result of increased heat transfer and lower RGF. It is approximately equal for higher engine speeds although 2000 rpm shows slightly greater PRR than 2500 rpm because that test point is closer to the HLL at 2000 rpm than the interior point at 2500 is to its HLL point.

Since the PRR is deliberately limited at high loads, and shows a common minimum at low loads independent of fuel and engine speed the focus for fuel-based differences is placed on interior operating points. A complete set of graphs of PRR broken versus fuel composition is persented in Appendix C.

At all interior points PRR_{max} increases with %-Saturates, decreases with %-Aromatic and is relatively insensitive to %-Olefins. The ranking of highest PRR for fuels with similar compositions is not constant between loads, or by implication speeds for this set of 3 interior points. These findings are interesting because while fuel Olefin content helps determine phasing it seems to play less of a role in determining reaction rate, as inferred from PRR_{max}.

4.2.4 RON sensitivity

One of the most common parameters for characterizing a fuel for SI combustion is the octane number (ON). There are two different octane numbers that find common use in North America, the Research Octane Number (RON) and the Motor Octane Number (MON). To determine octane number, fuels are tested in specialized research engines under prescribed conditions. The conditions from the RON test differ from those of the Motor Octane Number (MON) test. RON is more representative of typical engine operating conditions and MON represents more severe service at higher speed and temperature. In terms of combustion phasing, burn duration and load limits, CAI combustion was found to be relatively insensitive to RON for the conditions tested

with this engine. The result is somewhat counterintuitive because RON is one of the key parameters used to describe auto-ignition behaviour for gasoline fuels. In order to explain the engine's seeming indifference to fuel RON, it is instructive to explain how the RON is measured. The candidate fuel is run in a special research engine. With test conditions being closely controlled, as prescribed by either the RON test or MON test, the compression ratio of the test engine is increased until the engine knocks. Then the test is repeated with a fuel that is a binary blend of n-heptane and iso-octane. The test fuel is assigned an octane number corresponding to the percentage of iso-octane in the mixture that knocks at the same compression ratio and test conditions as the test fuel did. n-heptane is known to have poor autoignition resistance is assigned an octane number of zero. Iso-octane, which has comparatively better autoignition resistance is assigned an octane number of 100. Thus the higher proportion of iso-octane in the blend with the same autoignition properties as the test fuel, the greater the test fuel's resistance to autoignition. Since these two bracketing cases are assigned, it is possible for a fuel to have an octane number less than zero or greater than 100 if it displays worse or better autoignition behaviour than n-heptane and iso-octane respectively. The key observation is that RON and MON are measures of autoignition behaviour (i.e. knock) due to compression of the end gas in normal SI combustion. The temperature and pressure trajectories experienced by the end gas in the specialized research engine in the octane rating procedure are substantially higher than those found in the ignition process of a CAI engine. Therefore the RON rating may be more dependent on the ignition behaviour in the high temperature range of the fuel and the CAI characteristic may be more dependent on that in the lower temperature range. The CAI charge is lean and considerably more dilute than the SI charge in the RON and MON tests. Thus the relevance of the fuel RON value is further weakened.

4.3 Load limits

4.3.1 HLL results

Much effort at MIT and elsewhere has been directed at characterizing the HLL and extending it to maximize the portion of a mixed-mode drive cycle spent in CAI operation mode. Wildman, Andreae and others have reported that there is a high load misfire limit, however for all conditions and fuels tested with this engine, the HLL was due to PRR_{max}. It is possible that higher loads would be attainable before the misfire limit if PRR constraints were relaxed. To that end, linear regression was performed on experimental points on both sides of the existing HLL for a variety of fuels.

Fig. 4-26 shows the increase of PRR with load near the HLL at 2000 rpm and 2500 rpm.

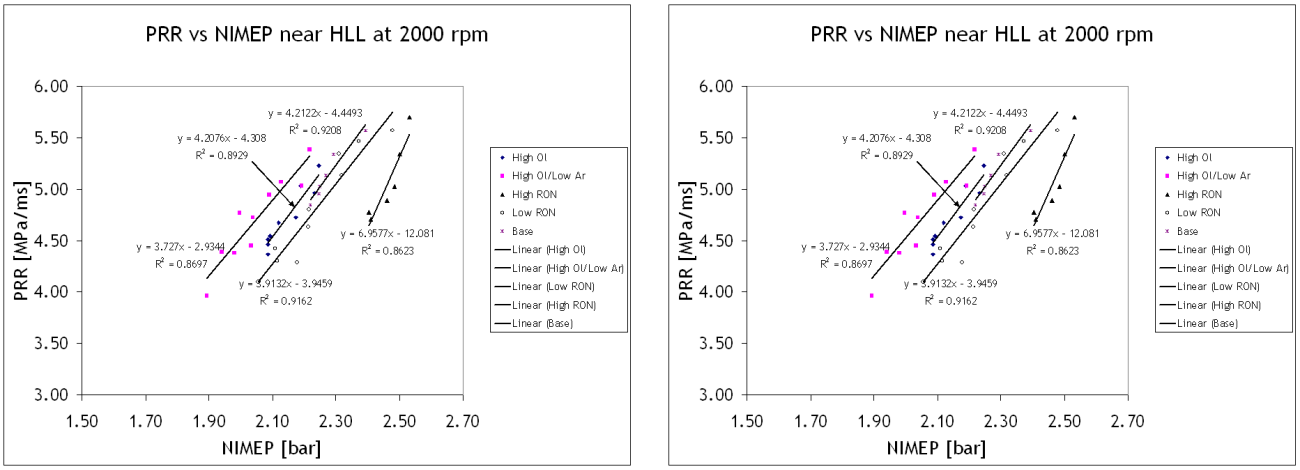

(a) 2000 rpm

(b) 2500 rpm

Figure 4-26: Change in PRR_{max} with load near the HLL at 2000, 2500 rpm

Taking an average value at 2000 rpm, with some fuel dependence and reasonable R^2 values for the linear fits:

$$\left(\frac{\partial(PRR_{max})}{\partial(NIMEP)}\right)\Bigg|_{nearHLL} \approx 4.6\frac{MPa/ms}{bar}$$

At 2500 rpm, with some fuel dependence and reasonable R^2 values for a linear fit

$$\left(\frac{\partial(PRR_{max})}{\partial(NIMEP)}\right)\Bigg|_{nearHLL} \approx 5.10\frac{MPa/ms}{bar}$$

Differences in the above mentioned partial derivatives between fuels were small but distinct. At 1250 rpm PRR seems to increase more rapidly in the vicinity of the HLL but Fig. 4-27 shows the data is less coherent than at 2000 rpm or 2500 rpm.

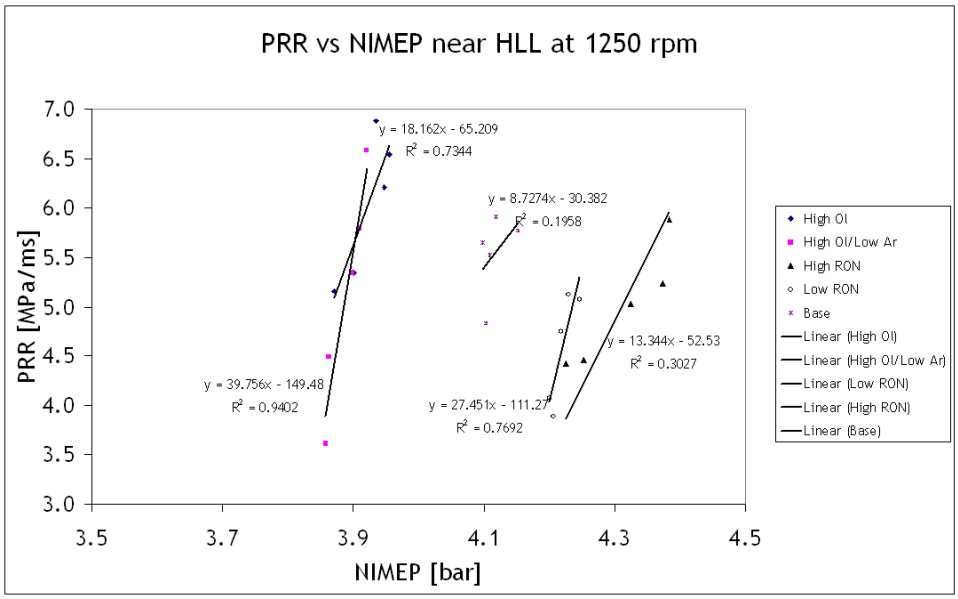

Figure 4-27: Change in PRR_{max} with load near the HLL at 1250 rpm

For this engine, PRR=5 MPa/ms already results in heavy audible knock, which indicates that without a novel method for mitigating PRR_{max} the HLL for this engine operating on these fuels is rather firmly limited by NVH concerns.

The HLL of each fuel at all three engine speeds is given in Table 4.6. Fuels are ranked from lowest to highest where highest is most desirable. This summary demonstrates that the High RON fuel is consistently a top performer whereas the Low RON fuel degrades as RPM increases. Similarly, the High Olefin fuel has the lowest HLL at 1250 rpm and the second best at 2500 rpm. The differences are small however. At all speeds tested the load range (HLL-LLL) was less than 13% of the HLL NIMEP at that speed. The maximum load limit difference of HLL for different fuels is 0.45 bar NIMEP at 1250 rpm.

Table 4.6: HLL ranked by fuel for each speed

Fuel	**HLL-1250**		Fuel	**HLL-2000**		Fuel	**HLL-2500**
High Ol	3.87		Low RON/2-EHN	2.17		High Ol/Low Ar	1.76
Low RON/DTBP	3.89		Low RON/DTBP	2.18		Low RON/2-EHN	1.78
Low RON/2-EHN	4.02		High Ol/Low Ar	2.19		Low RON/DTBP	1.83
High Ol/Low Ar	4.03		High Ol	2.23		Low RON	1.84
Base fuel	4.10		Low RON	2.32		Base fuel	1.87
High RON	4.32		Base fuel	2.35		High Ol	1.89
Low RON	4.32		High RON	2.48		High RON	2.01

Table 4.7: LLL ranked by fuel for each speed

Fuel	**LLL-1250**		Fuel	**LLL-2000**		Fuel	**LLL-2500**
High Ol/Low Ar	1.43		High Ol	0.76		Low RON/DTBP	0.72
Base fuel	1.46		Low RON/2-EHN	0.79		High RON	0.72
Low RON	1.54		High Ol/Low Ar	0.81		High Ol/Low Ar	0.74
Low RON/2-EHN	1.54		Base fuel	0.83		High Ol	0.76
High RON	1.55		Low RON	0.86		Base fuel	0.79
High Ol	1.66		Low RON/DTBP	0.86		Low RON	0.80
Low RON/DTBP	1.68		High RON	0.93		Low RON/2-EHN	0.83

4.3.2 LLL Results

Because of the substanctial throttle loss of SI operation at low load, the low CAI fuel conversion efficiency (15%) at LLL points at 2000 rpm and 2500 rpm is still a considerable improvement over SI combustion at those loads. Moreover some preliminary experiments show that high speed LLL conversion efficiency could likely be improved by earlier pilot injection at high RPM to improve NVO heat release.

The LLL of each fuel at all three engine speeds is given in Table 4.7. Fuels are ranked from lowest to highest where lowest is most desirable. This summary shows no consistent pattern in behaviour. In all cases the LLL of the highest LLL is within 22% of the lowest LLL at a particular speed. That range is deceptively large because of the small magnitude of the loads involved and the uncertainty in calculated NIMEP. The maximum load limit discrepancy of LLL for different fuels is 0.26 bar NIMEP at 1250 rpm. Cetane additives were considered as a potential method for extending the LLL by enhancing low temperature reactivity. In fact the expected behaviour was to translate the entire operating window to lower loads, including a reduced HLL. It

appears that the load envelope contracts slightly at low RPM and remains relatively unchanged with respect to the Low RON fuel at higher speeds. It is possible that the cetane improvement behaviour relies on kinetics that are simply not active at the temperatures and pressures in CAI combustion.

4.4 Practical considerations

4.4.1 Interior point results

In contrast with HLL and LLL tests, which focus on what range of loads is available, the fixed speed-load targets of the interior operating points give a sense of how the differences in fuel composition may impact the engine control strategy needed to achieve a specified speed-load target. The interior points were originally selected to be well inside the load limits to eliminate the "edge effects" such as combustion instability associated with near-boundary operation.

Table 4.8 gives the valve timing used to achieve the speed-load target with each fuel. The conclusion is that, notwithstanding differences in the location of load limits, engine operation within the load limits is insensitive to fuel. This is an important finding for practical implementation of CAI combustion.

Table 4.8: Camshaft phaser position at interior operating points

	EV adv [CAD]			IV adv [CAD]		
	1250	**2000**	**2500**	**1250**	**2000**	**2500**
Base fuel	38	55	47	10	1	1
High Ol	36	55	49	6	0	1
High Ol/Low Ar	37	55	48	5	0	1
High RON	35	54	48	10	0	2
Low RON	35	56	47	6	0	1
Low RON/2-EHN	37	53	47	5	1	0
Low RON/DTBP	36	54	47	5	1	0
Min	35	53	47	5	0	0
Average	36.3	54.6	47.6	6.7	0.4	0.9
Max	38	56	49	10	1	2

4.4.2 Load limits

Fig. 4-28 is a plot of the load limit of each fuel grouped by engine speed. The operating range does not differ substantially between fuels. Therefore very little overall CAI operating range would be lost calibrating the engine to the worst case HLL with the worst case LLL at each RPM to construct a constrained operating regime that guarantees stable CAI operation over the range of market fuel properties expected.

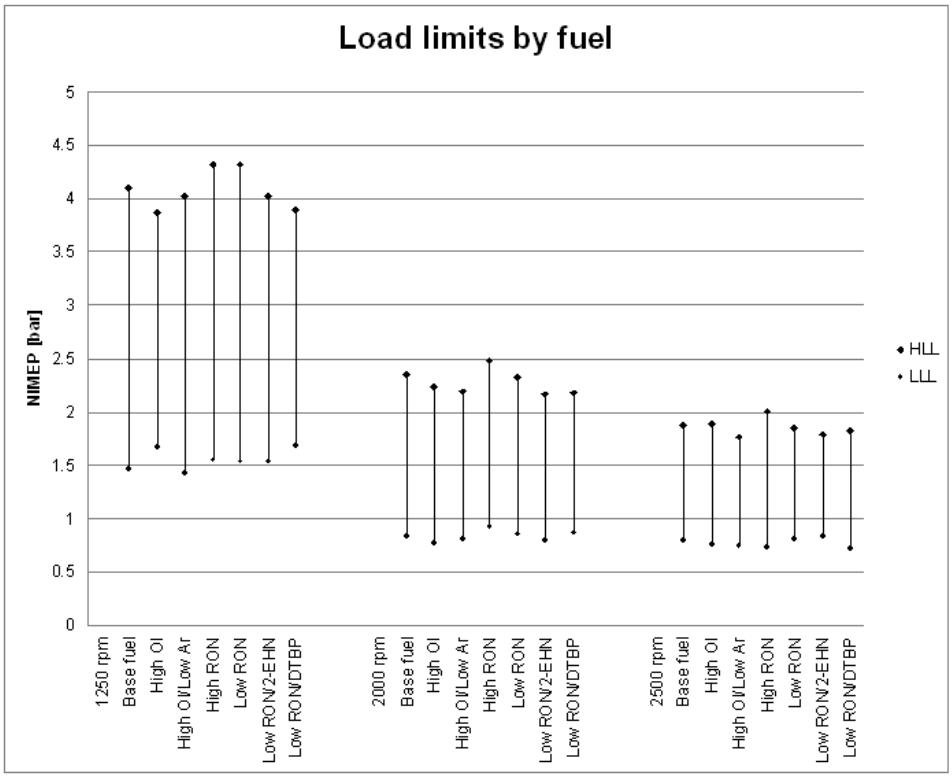

Figure 4-28: Load limits by fuel

The data from Fig. 4-28 can be replotted to emphasize the magnitude of the operating range. Fig. 4-29 shows that High RON fuel has the best operating range of all fuels and conditions tested.

The superiority HLL performance of High RON fuel is fortunate. CAI combustion is amenable to higher compression ratios than typical SI engines, however compression ratio on mixed mode engines is limited for knock considerations when operating in SI mode. A mixed mode engine like this one, High RON fuel would mean a wider CAI

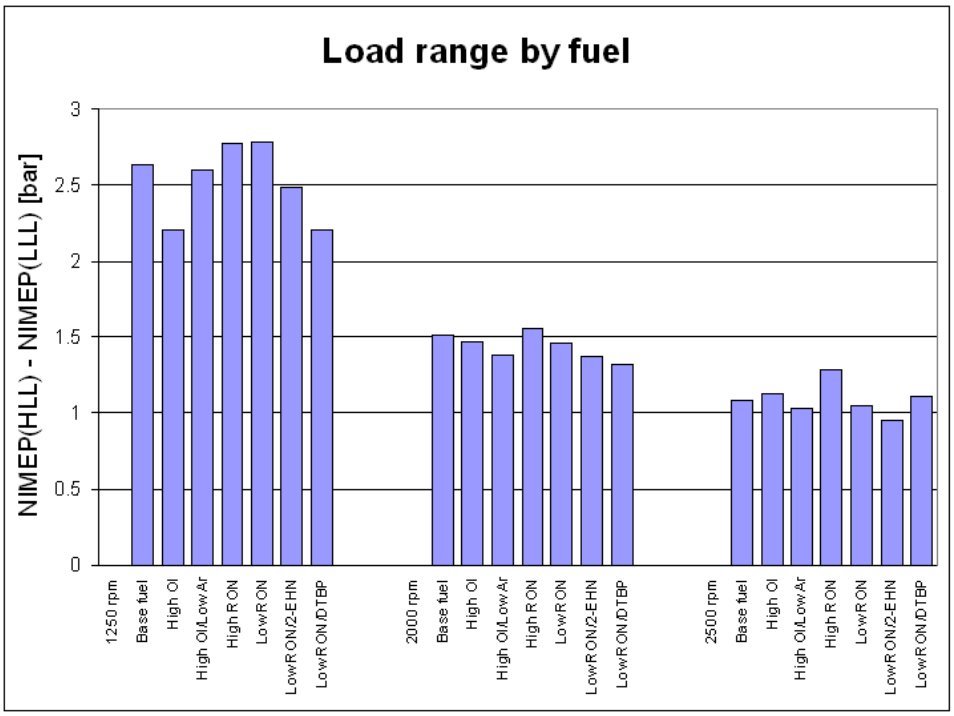

Figure 4-29: Range of loads available by fuel

combustion range and also be tolerant of higher compression ratios in SI mode due to the superior autoignition resistance of High RON fuel. By operating on fuels with behaviour similar to the High RON fuel tested here, this engine could be optimized and potentially profit from the thermodynamic benefits of high compression ratio in both modes.

Following a discussion of what loads are achievable it is appropriate to discuss the means by which they are achieved, and in particular what differences exist between fuels. The useful conclusion from Tables 4.9 and 4.10 is that cam phaser timing is insensitive to fuel. The High Olefin fuel and the fuels with cetane improvers appear to deviate most significantly from the underlying trends. It should be noted that these fuels are the least representative of true market-available fuels.

In the preceding tables it should be noted that CAI engine operation using NVO is far more sensitive to exhaust valve timing than intake valve timing. The effect of EV timing on VE and RGF is many times greater than the effect of IV timing.

Drawing an analogy with engine knock in SI combustion, and the safety margin

Table 4.9: Camshaft phaser position at HLL operating points

	EV adv [CAD]			IV adv [CAD]		
	1250	**2000**	**2500**	**1250**	**2000**	**2500**
Base fuel	22	44	38	20	1	3
High Ol	23	46	40	19	0	2
High Ol/Low Ar	23	47	40	19	0	2
High RON	17	41	35	25	0	7
Low RON	17	45	42	25	0	1
Low RON/2-EHN	22	47	40	20	0	2
Low RON/DTBP	25	48	39	17	1	3
Min	17	41	35	17	0	1
Average	21.3	45.4	39.1	20.7	0.3	2.9
Max	25	48	42	25	1	7

Table 4.10: Camshaft phaser position at LLL operating points

	EV adv [CAD]			IV adv [CAD]		
	1250	**2000**	**2500**	**1250**	**2000**	**2500**
Base fuel	44	57	47	10	1	2
High Ol	39	60	49	5	0	1
High Ol/Low Ar	44	60	50	8	0	0
High RON	44	57	48	10	5	2
Low RON	44	58	48	9	5	0
Low RON/2-EHN	40	60	48	3	5	0
Low RON/DTBP	39	59	48	4	1	1
Min	39	57	47	3	0	0
Average	42.0	58.7	48.3	7.0	2.4	0.9
Max	44	60	50	10	5	2

applied to spark timing at low engine speed and high load, it is likely that the load limits explored here would be "padded" in the engine control strategy of a practical SI-CAI multi mode implementation. In that case, the valve timing strategy, can be managed without considering fuel effects. A necessary qualification of that conclusion is that the market fuel test matrix did not include ethanol blends which are becoming increasingly prevalent, nor did it include other oxygenated fuels that may appear in the marketplace in the foreseeable future.

4.4.3 Misfire recovery

One of the major differences between this engine and the engines used for previous phases of research is mixture preparation. GDI opens up possibilities for injection

in the NVO recompression process. The strategy is used in the present work for extension of the LLL. In an engine equipped with GDI, the latent heat of vaporization for evaporating fuel is drawn from the in-cylinder charge instead of the walls of the intake manifold as in PFI. This cooling presents a problem to misfire recovery.

It was found that when the engine misfired near the LLL, spontaneous recovery was not always possible unless fuel injection was temporarily switched off. The pressure trace near the LLL under these conditions showed lower pressures than expected. Following complete extinction (not just intermittent/unstable combustion) the split injection strategy excessively cools the in cylinder charge, lowering its temperature and pressure to a point that precludes autoignition. The lower the load the greater the difficulty in restarting combustion even with spark assist. After several cycles without combustion the cylinder contains excess fuel due to the high proportion of trapped residuals between cycles. If fuel injection is suspended for a few cycles it is observed that the pressure trace "recovers" to its motoring value, at which point combustion resumes immediately upon reactivation of fuel injection. The unburned hydrocarbon emissions during misfire would be unacceptable, but so would the torque fluctuation resulting from misfire and cylinder deactivation even for a few cycles. This highlights the need for a robust control strategy that minimizes low load misfire. There was no difficulty in recovering from misfire in single injection mode whatever the load, although spontaneous misfire recovery was fastest at high engine speed. It is thought that spark assist aids the misfire recovery process.

4.5 Accuracy and repeatability

Fuel contamination

A rigorous fuel-switching procedure was developed to minimize the potential for contamination between fuels. The protocol involved evacuation, purging with N_2, changing components such as filters, flushing with new fuel and finally a run-in period between fuels to ensure that the operating fuel was unadulterated test fuel. The

effectiveness of the switching procedure in avoiding contamination was measured indirectly in the following way. An SI test of maximum spark advance before knock onset is conducted with fixed intake temperature and pressure. Similar to the HLL of CAI combustion, knock is defined for this experiment as PRR exceeding 5MPa/ms. The knock limit is approached and receded several times to obtain an average value for maximum spark advance. Then the fuel is switched, per the switching procedure, to one with a significantly different RON (usually higher). The test is repeated and the new maximum spark advance is noted (usually more advanced). Then the fuel is switched back to the original per the switching procedure and the spark advance is recorded a third time.

The results of the first test would identically match the first test if fuel switching was perfect. Any degree of contamination would result in a spark advance for the third test somewhere between the first and second tests. This experiment was conducted with Low RON fuel (89.4 RON) and High RON fuel (97.4 RON). The difference in spark timing for the first and third tests was less than 5% of the difference between the first and second tests. In other words, the fuel switching method is adequate to prevent fuel contamination.

Pressure measurements

The accuracy of manufacturer-supplied calibrations for intake manifold, exhaust, cylinder and fuel pressure sensors were verified using sensors of known accuracy or deadweight pressure testers.

Air-fuel ratio

The Horiba λ meter was calibrated periodically using a three-point calibration as per the manufacturer recommended calibration procedure. Such a calibration utilizes test gases at three different, known concentrations of O_2. The fuel H/C ratio did not vary significantly over the range of fuels tested. The fuel's C/O ratio was identically zero for all fuels tested as well so no adjustment to either factor was required.

Fuel injector calibration

Fuel mass is calculated from fuel injector pulse width and fuel injection pressure using an experimental pulsewidth-mass correlation. Fuel mass is used with equivalence ratio and fuel stoichiometry to calculate air mass. These quantities are subsequently used in the estimation of volumetric efficiency, residual gas fraction and indicated efficiency. Hence it is critical that calculated fuel mass is accurate.

Sources of uncertainty within the correlation experiment such as evaporation of fuel (and subsequent loss from the collection vessel), condensation of water from the ice bath were quantified and found to be less than 1% for the test protocol used. Fuel pulse width correlations for different gasoline test fuels did not differ within the uncertainty of the correlation. Correlations for fuel blends containing ethanol and butanol are expected to differ appreciably from that of gasoline.

Qualitative validation of the correlation can be obtained by testing injection strategies using two rapid, adjacent injections (to mimic one single injection) whose respective pulsewidths vary but whose total fuel mass is predicted by the correlation to remain constant. During this experimentation λ is observed to remain constant, and for constant valve timing this strongly implies that fuel mass is indeed constant. This does not indicate the absolute accuracy of the correlation, but that it consistently predicts the trend in the amount of fuel delivered per unit pulsewidth.

Day-to-day repeatability

It is known that CAI combustion is sensitive to ambient conditions such as humidity and atmospheric pressure that were not explicitly controlled in this experiment. Identical data points were repeated on different days with engine operating parameters such as speed, fuel mass, valve timing, coolant and intake temperatures held constant. The resultant load, λ, combustion phasing and duration for the same point on different days can be interpreted as a measure of baseline variability and imprecision in measurements and calculations. A summary of average day-to-day differences is presented in Table 4.11, which shows that findings in a particular configuration

Table 4.11: Repeatability of measured or derived quantities on different days

Parameter	**Average %-diff from nominal**
RPM	$< \pm 0.1\%$
NIMEP	$\pm 3.0\%$
λ	$\pm 0.7\%$
m_{fuel}	$\pm 3.0\%$
VE	$\pm 2.0\%$
RGF	$\pm 3.0\%$
$\eta_{ind.}$	$\pm 2.0\%$

are consistent. The summary includes several repeatability trials, with each set of repeatability trials conducted at a different point to include different speeds, loads and fuels.

NIMEP calculations

NIMEP calculations involve cylinder pressure and volume data based on engine geometry and piston position. NIMEP calculations do not depend on accurate pegging of cylinder pressure because they are cyclic integrals so only phasing errors and signal drift or interference can cause errors in NIMEP calculations. Although the NIMEP is independent of long term drift of the pressure, signal drift is held in check through the time constant of the charge amplifier and the pressure transducer cable is specially shielded against interference, as are likely sources such as injector wires and spark plug wires.

The cylinder pressure transducer and charge amp system were frequently checked by analyzing motoring trace at moderate engine speed (2000 rpm) and WOT conditions with SI camshafts and timing. Under these conditions, if compression were quasi-static and adiabatic the polytropic index of compression would be equal to the specific heat ratio, γ, which for air at ambient temperatures is 1.4. The value for the measured motoring trace should differ from γ_{air} to account for the effects of heat and mass loss through cylinder walls and valve seats respectively. From experience it know expected that the polytropic index will be between 1.34 and 1.36 for compression and 1.38 to 1.40 on expansion. Greater losses would decrease the value on

compression, and increase the value on expansion.

The alignment of the crankshaft encoder and the engine geometry is verified before and after every test by recording a motoring trace at WOT and moderate engine speeds. The limited resolution of +/- 1 CAD limits the accuracy of NIMEP calculations for which phasing between p_{cyl} and cylinder volume (calculated from encoder angle) is critical. Previous experience suggests an error of about 5% on NIMEP for each CAD of phasing error. Crankshaft encoder phasing is verified using the motoring technique described above. The location of peak pressure as well as the shape of a p-V diagram plotted in log-log near TDC can help verify proper phasing.

Heat release calculations

The Rassweiler-Withrow heat release method gives an approximate way to calculate apparent heat release. It explicitly combines chemical heat release with heat transfer, and ignores crevice effects. This assumption probably introduces less error for CAI than SI because of the lower peak combustion temperatures and pressures associated with CAI combustion. The algorithm includes code to automatically detect the start and end of combustion (CA0 and CA100 respectively) based on changes to the cylinder pressure and volume. The detection was tuned using SI and CAI combustion traces for a variety of speeds and loads, compared against manual selection of CA0 and CA100. The algorithm also automatically detected the appropriate polytropic constant used in the method. When it comes to burn duration (BD1090) and combustion phasing (CA50) the RW method is not extremely sensitive to values chosen for CA0 and CA100 because combustion starts slowly, rapidly accelerates then finishes "asymptotically" as reactant concentration diminishes.

Chapter 5

Summary and conclusions

Robust, stable spark assisted CAI combustion using trapped residuals was demonstrated on a prototype engine at various speeds and loads. This GDI-equipped platform is used to investigate the effects of market fuel variations of hydrocarbon fuels on engine behaviour, and compare this modern engine with previous phases completed with port-fuel-injected hardware.

One key finding is that changes in cylinder heat transfer and volumetric efficiency with valve timing and engine speed affect combustion phasing and burn duration to a much grater extent than the variations in fuel composition expected in the marketplace. The heat transfer effects and volumetric efficiency have a direct impact on the thermal and mechanical state of the charge. For the fuels tested, the chemical processes for CAI combustion are sufficiently similar that the temperature dependence dominates the chemical dependence. That explains why engine operating parameters such as valve timing are approximately the same for all fuels at a given operating point, because only small changes are necessary to adjust for differences in fuel properties.

Heat transfer from cylinder contents changes with engine speed. At lower engine speeds there is more time for heat transfer. At high engine speeds there is less time for heat transfer. The time effect dominates over the increases in heat transfer rate with speed so that the cumulative heat loss is higher at low engine speed.

Volumetric efficiency affects the temperature in cylinder because intake air is

cool compared to trapped residuals. Improved volumetric efficiency improves the gas exchange process across both valves resulting in less residual gas and more fresh air.

5.1 The effect of GDI

The use of multiple injections per cycle stabilized combustion at low loads through heat release during the NVO recompression. The low load injection strategy used for this work was a 30%/70% split by mass for pilot and main injections, timed symmetrically with end of injection at 50 CAD $BTDC_{exh}$ and 50 CAD $ATDC_{exh}$. At all engine speeds tested, indicated conversion efficiency was lower for split injection than single injection. This decrease in efficiency is due to the poor fuel conversion efficiency of the fuel burned during the NVO recompression cycle, especially at higher engine speeds.

5.2 Operation near the high load limit

The highest load achievable in CAI operation was limited by the NVH constraint applied to pressure rise rate. The high load limit decreased rapidly with increasing engine speed. At high speed, heat transfer from the charge decreases and volumetric efficiency decreases. These result in a hotter charge whose kinetics are more rapid. This is supported by pressure rise rate data normalized by fuel mass, which increases with engine speed. All fuels demonstrate advancing combustion phasing with increasing engine speed. The differences between fuels in terms of combustion phasing and burn duration were most pronounced at high loads where temperatures are highest and kinetics most active. High olefin content fuels consistently demonstrates the latest combustion phasing, and the Low RON blends treated with 2-EHN, DTBP and high Ol/low Ar show earliest phasing.

At the HLL, the burn rate averaged over the fuels is is approximately 50% lower at 1250 rpm than those at other speeds. The improved volumetric efficiency and higher heat transfer at low speeds result in a cooler charge which may result in a slower heat

release.

It was originally theorized that compression temperatures would be greatest for the interior operating points. The reasoning was that near the HLL there would be a small fraction of relatively hot residuals, and near the LLL there was a large fraction of relatively cool trapped residuals. Interior points would have intermediate quantity of moderate temperatures residuals and resulting in a maximum compression temperature. Judging by the burn duration, the average fuel burn rate and the pressure rise rate the hottest temperatures for the operating points tested are found closer to the HLL. Here chemical heat release dominates enthalpy from trapped residuals. It is possible the optimum lies between the operating points tested, and that is supported by simulation work done in previous phases of this study. It was found that the reaction rates for the 2000 rpm interior point are greater than the 1250 HLL. The 1250 HLL point has considerably more fuel heat release, but also more heat transfer losses and a cooler charge which would diminish reaction rates. Moreover, the reaction rates are limited at 1250 by the enforced PRR limit, whereas the interior point at 2000 rpm. As mentioned, the thermodynamic properties of the charge at 1250 rpm limit the maximum permissible reaction rate to a lower value than what is acceptable at 2000 rpm and above.

The High RON fuel demonstrates the highest HLL across all speeds tested but the margin is slim. The HLL for all fuels tested fall within an HLL window of 4.08 bar $\pm$ 0.23 bar NIMEP at 1250 rpm decreasing to 1.86 bar $\pm$ 0.12 bar NIMEP at 2500 rpm.

Under the engine operating conditions tested, there is very little opportunity to extend the HLL by relaxing the PRR constraint. Each additional 1 bar of NIMEP would result in an approximate increase of 4.7-5.10 MPa/ms of the pressure rise rate.

5.3 Operation near the low load limit

Operation at low loads is limited by combustion stability. Low chemical heat release generates cooler residuals that bring insufficient enthalpy for charge preheating for

autoignition. Operation at low loads can be stabilized through multiple injections. Heat release from a pilot injection before TDC during NVO generates much needed enthalpy and dramatically stabilizes combustion.

Combustion phasing and burn duration are consistent for LLL points across the range of engine speeds tested. Contrary to results at other operating points, the earliest phasing and shortest burn duration occur at 1250 rpm. In this case, the low temperatures that result from improved volumetric efficiency and greater heat transfer losses are offset by the greater NVO heat release.

Practical extension of the LLL is limited by injector performance. For the operating conditions and injection strategy employed in this work, the LLL was reached at around the minimum repeatable fuel quantity. It is possible that cycle to cycle variations in injector performance initiated instability near the LLL.

5.4 Inside the operating region

For the range of points and fuels tested, CAI combustion and engine operation not least sensitive to fuel effects inside the operating region at points far from the HLL and LLL. At these interior points, load targets can be reached using minor adjustments of the valve timing. This is because for this set of test fuels, the range of combustion behaviour does not vary enough to appreciably alter the engine output.

5.5 Fuel chemistry effects

Attempts to correlate macro behaviour such as combustion phasing, burn duration and pressure rise rate with fuel properties such as aromatic content, olefin content, saturates content and RON were largely inconclusive. It is thought that these classifications do not provide adequate resolution on fuel composition. Lumping heavily branched saturated hydrocarbons together with long straight saturated chains ignores the role that branching plays in autoignition behaviour. The useful conclusion is that the engine is insensitive to fuel effects for the range of hydrocarbon fuels chosen,

namely those representative of expected market fuel variation shown to be significant in previous phases of this project.

There were some fuel-specific findings.

- The High RON fuel consistently had among the longest burn durations at all operating conditions, which explains why it had the highest HLL and broadest operating range.

- The high olefin fuel had latest phasing which is consistent with the strong autoignition resistance of many olefins. The high olefin/low aromatic fuel had the earliest phasing because its low aromatic content was offset by increased saturates which have comparatively weaker autoignition resistance.

- Low RON fuel treated with the 2-EHN additive had among the earliest combustion phasing, the effect of which was most pronounced at 2500 rpm.

- The nearly total inactivity of DTBP may be attributable to the low pressure CAI combustion environment. It is known that DTBP decomposition is highly pressure dependent.

- Although increasing RON correlated reasonably with combustion later phasing, differences in phasing were within the margin of error in the calculated combustion phasing for low RON and base fuels.

- In general it is concluded that RON is a poor indicator of fuel behvaiour for CAI combustion. RON does not show any strong connection to pressure rise rate or LLL performance. RON differences that would result in significantly different SI operation showed little overall impact on CAI combustion.

- Cetane improvers not only failed to shift the operating regime of CAI combustion, but actually reduced the operating range under some circumstances. The role of cetane improvers in CAI combustion should be subjected to further study.

5.6 Practical operation

For the range of market fuels tested, load limits are relatively insensitive to fuels. The range of HLL and LLL over the fuels tested are small enough that valve timing calibration based on the worst case HLL and worst case LLL at each engine speed would not pose a severe constraint on the range of operation.

Exhaust valve timing required more cam advance at 2000 rpm than either 1250 rpm or 2500 rpm. This indicates the need for more trapped residuals. This could be explained by a manifold acoustic resonance at or near 2000 rpm which would improve volumetric efficiency at that speed. For the fixed stoichiometry of the test program, more exhaust residuals were required. Admittedly, a practical CAI implementation would not necessarily restrict the air-fuel ratio as was done in this test program. This is a finding of interest because volumetric efficiency and valve timing have a more profound impact on CAI combustion characteristics and engine operation than they do in SI mode. Because of the short valve lift and duration in CAI operation, the breathing of the engine is more prone to acoustic effects.

It is found that for operation near the LLL with different fuels, the difference in cam timing required for each fuel is less than for operation near the HLL. This is fortunate because CAI enjoys a greater comparative efficiency advantage over SI at low loads than it does at part loads and this reduced sensitivity means the practical minimum load (actual+safety factor) can be closer to the actual minimum. Of course the question of whether it's better to extend the HLL or LLL must account for the amount of time spent at each operating point over a drive cycle, and when and how mode switch are conducted. Those considerations are interesting but beyond the scope of this work. The differences in required cam timing are more significant at low engine speed and become more consistent at higher RPM.

It is found that the range of viable air/fuel ratios widens at higher speed and load because a hotter mixture has wider combustible limits. Combustion stability issues were encountered when coolant temperature was not sufficiently high. In that case wall quenching and heat transfer loss from the charge increased until autoignition

was impossible for a mixture that experienced stable combustion at higher coolant temperatures. It is therefore qualitatively concluded that a practical implementation of CAI would require a UEGO to truly optimize control. A conventional oxygen sensor used for SI mode would be inadequate to compensate for these effects in CAI mode.

The use of trapped residuals to preheat and dilute the incoming charge requires high residual gas fractions. This strong dependence on the combustion history means that perturbations have a long settling time compared to conventional combustion. The long settling time manifested itself in two separate instances. The first is the case of charge cooling due to pilot injection leading to permanent extinction of LLL combustion following a misfire. The second case was misfire or partially incomplete combustion followed by oscillatory and sometimes divergent disturbances. The partial misfire increases the amount of unburned mixture in the subsequent cycle whose augmented chemical heat release advances the combustion of the cycle that follows. Advanced phasing leads to more work extraction, cooler residuals and later phasing. Later phasing can lead to misfire, or the perturbation can settle out. These cases are admittedly extreme but these scenarios were observed on a limited number of occasions by this author and others.

The final comment on the practical exploitation of this engine concerns the fuel injectors. For the given injector pressure and 30%/70% mass split injection scheme the injectors were at their practical performance limit in terms of repeatable minimum pulsewidth. Extension of the LLL requires increasing NVO heat release. This requires a more even fuel split, higher injection pressures or refined injector design, or a fuel that is more reactive at low temperatures.

5.7 Future work

There is potential for research into the role of GDI in extending the HLL. An advanced injection strategy using charge cooling and charge stratification might allow for high load extension. Charge cooling to reduce temperatures in cylinder and by extension

control reaction rates and the PRR. Charge stratification might influence PRR by altering the local reactivity of mixtures that more or less simultaneously react. It is not known whether charge stratification would be achievable repeatably in practice, or whether stratification effects for a spray guided injector would be erased by random turbulent mixing.

The role of injection strategy near the LLL was explored to learn what role pilot injection timing had on heat release during the NVO period. There is some potential to extend the LLL by altering the pilot/main timing and split. A more even distribution would improve pilot injection repeatability, and earlier pilot injection would improve NVO heat release at high RPM.

The inefficacy of cetane additives to alter CAI combustion characteristics invites further work. Future work is planned for similar fuel blends with additives in greater concentrations. Another avenue is to test the same fuels with different intake air temperature to see if the low temperature reactivity they demonstrate in Diesel fuel combustion is being masked in CAI combustion for which the temperature and pressure regime may be impairing or deactivating certain critical kinetic pathways.

The final avenue of future research is to include bio-fuels. The North American market is moving towards gasoline blends with increasing ethanol content. Compared to gasoline, ethanol has a high autoignition resistance, low volumetric energy content and high heat of vaporization. The reaction kinetics of ethanol are also fundamentally different because of ethanol's OH functional group. These raise interesting possibilities in a GDI engine where for exhample enhanced charge cooling can be used to offset higher compression ratios. Another bio-fuel candidate for later testing is butanol. Butanol has a similar energy content to gasoline but none of the handling or material compatibility concerns of ethanol. Although it has lower autoignition resistance and latent heat of vaporization than ethanol, it will still be an attractive candidate for future market fuel blends if industrial synthesis can be effectively scaled.

Appendices

This page intentionally left blank

Appendix A

Combustion phasing and duration results

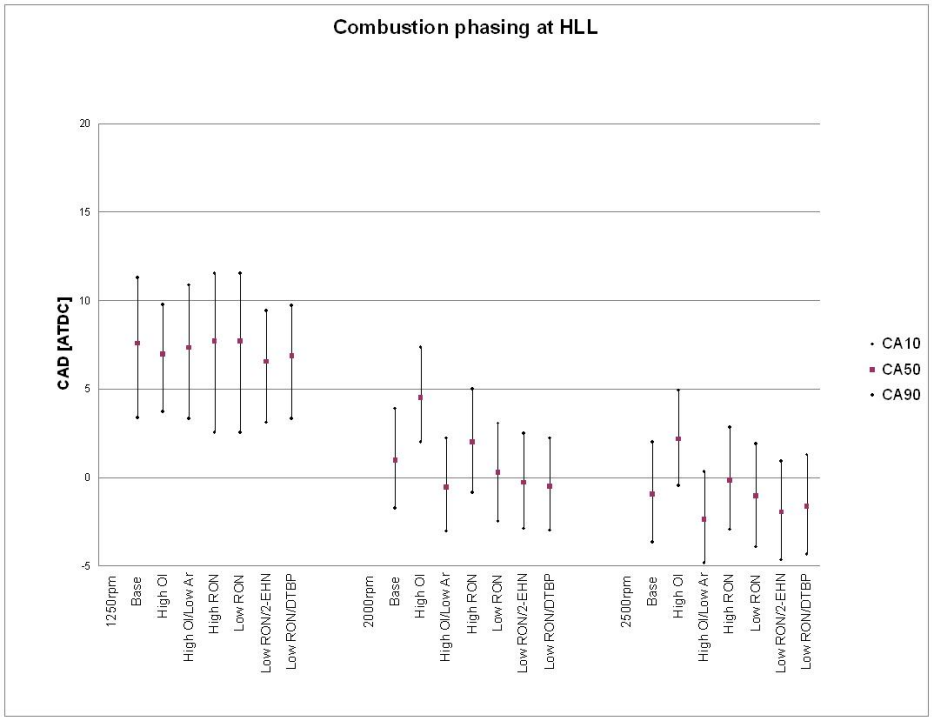

Figure A-1: Combustion phasing and duration for HLL operating points

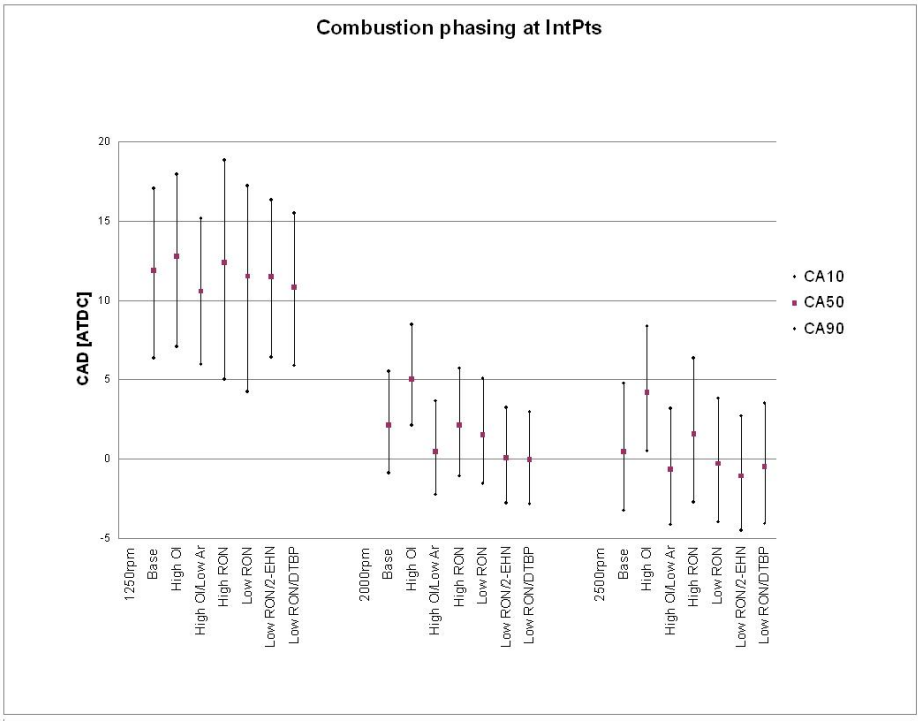

Figure A-2: Combustion phasing and duration for interior operating points

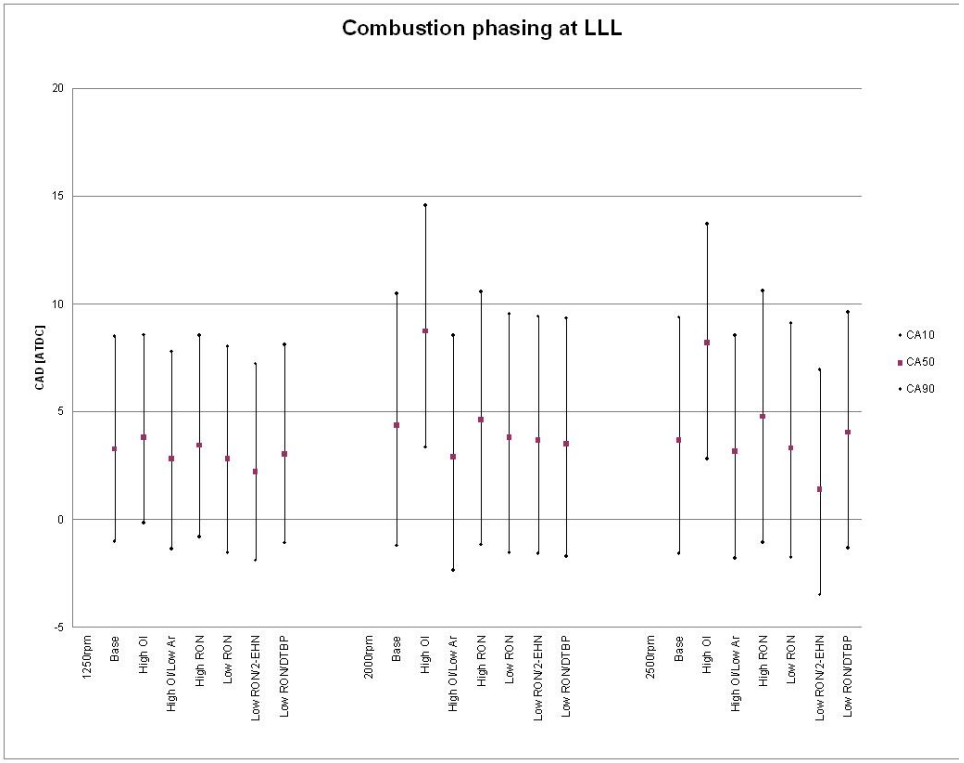

Figure A-3: Combustion phasing and duration for LLL operating points

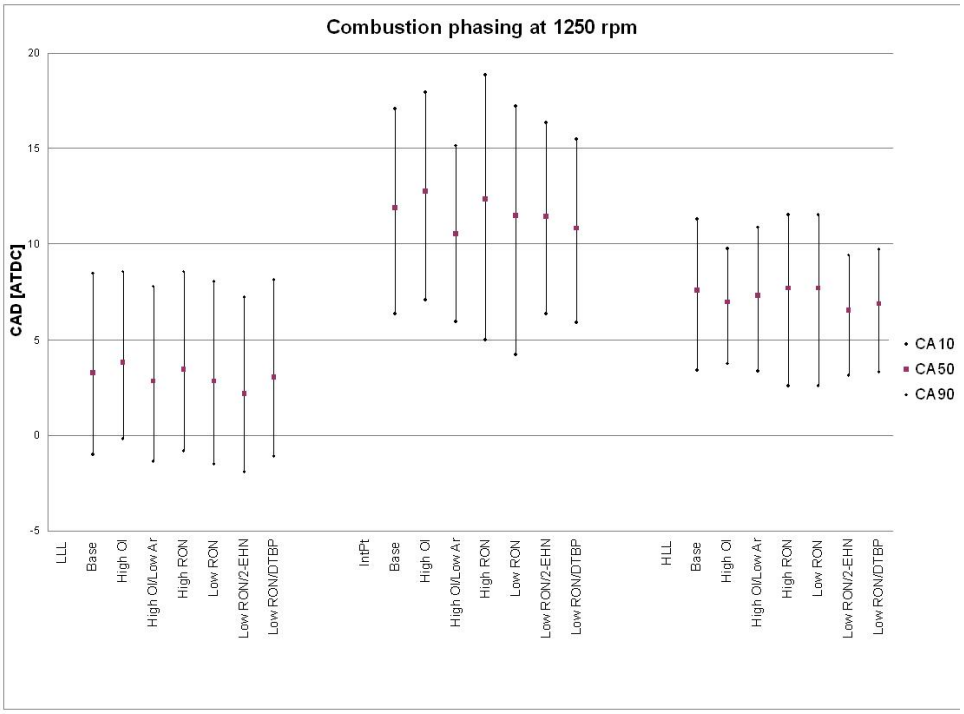

Figure A-4: Combustion phasing and duration at 1250rpm

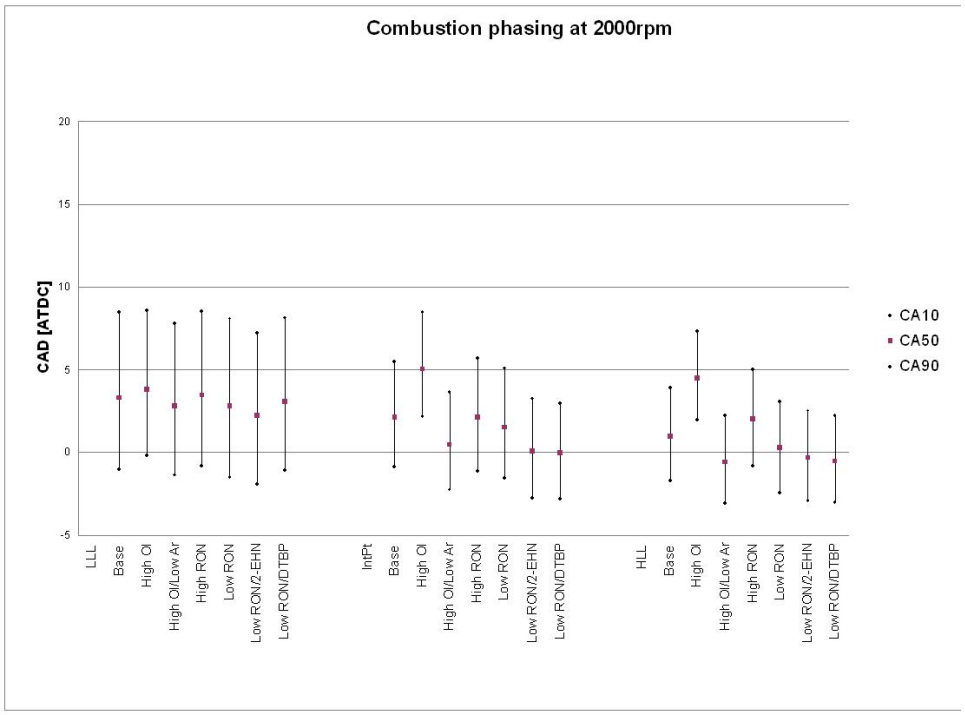

Figure A-5: Combustion phasing and duration at 2000rpm

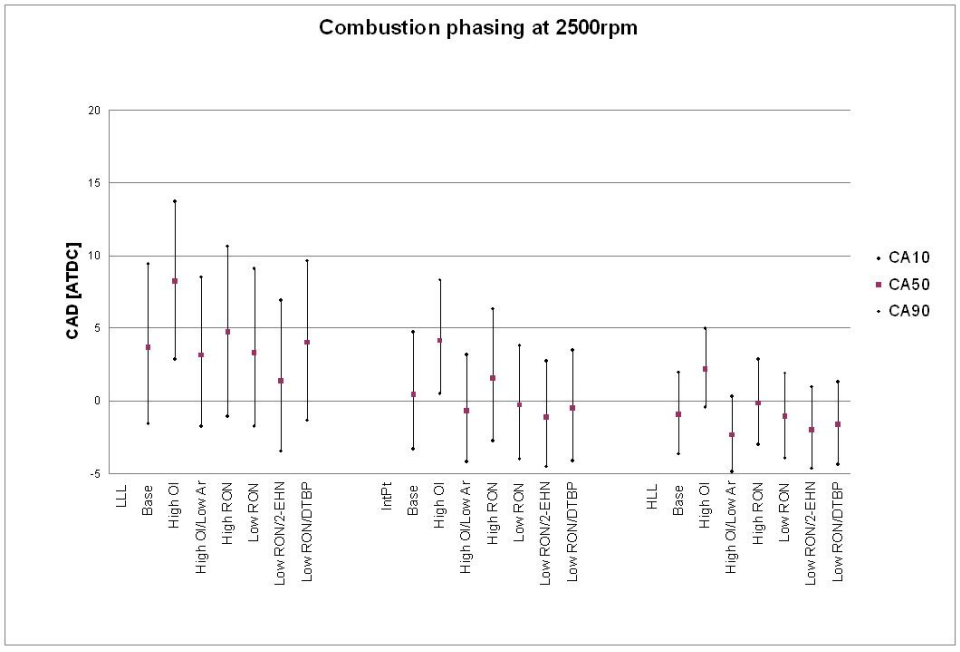

Figure A-6: Combustion phasing and duration at 2500rpm

Appendix B

Combustion phasing vs fuel composition

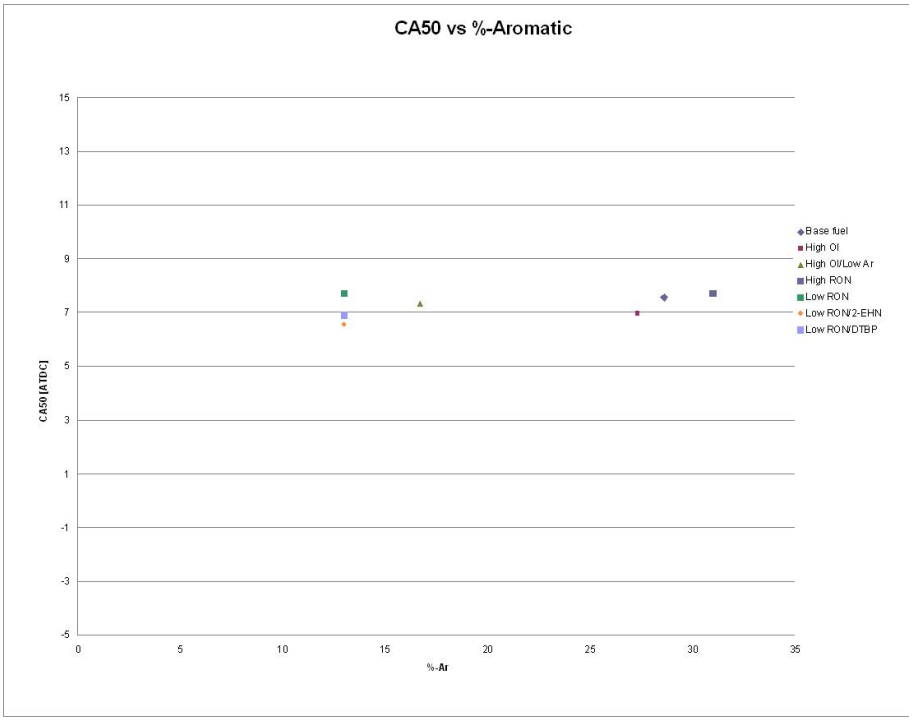

Figure B-1: Combustion phasing vs aromatic content at the 1250 rpm HLL

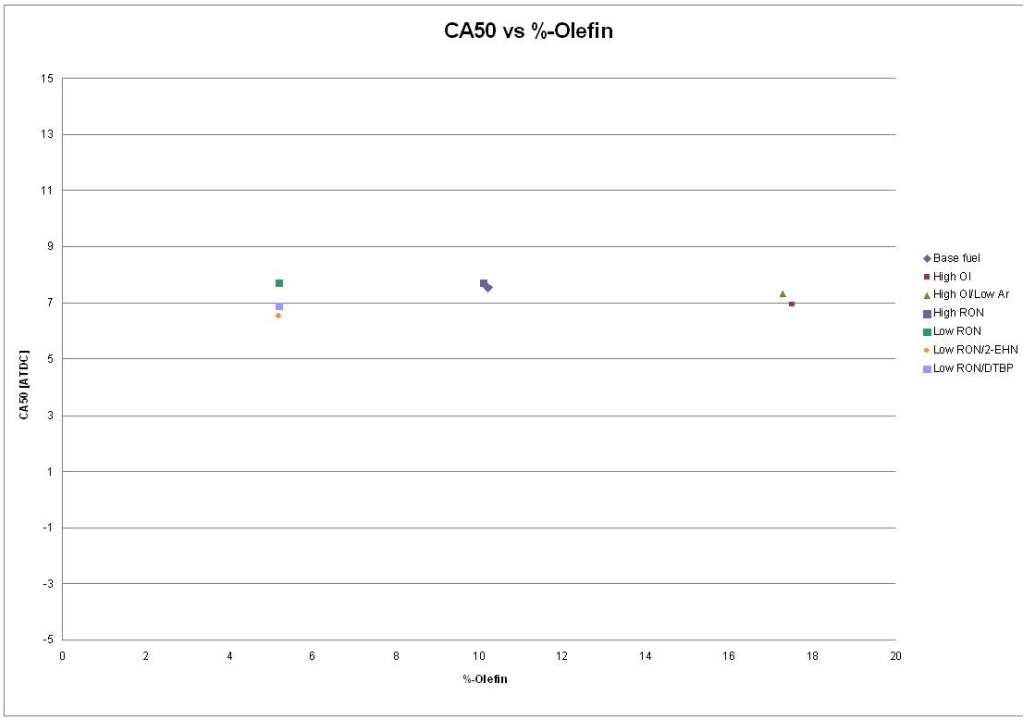

Figure B-2: Combustion phasing vs olefin content at the 1250 rpm HLL

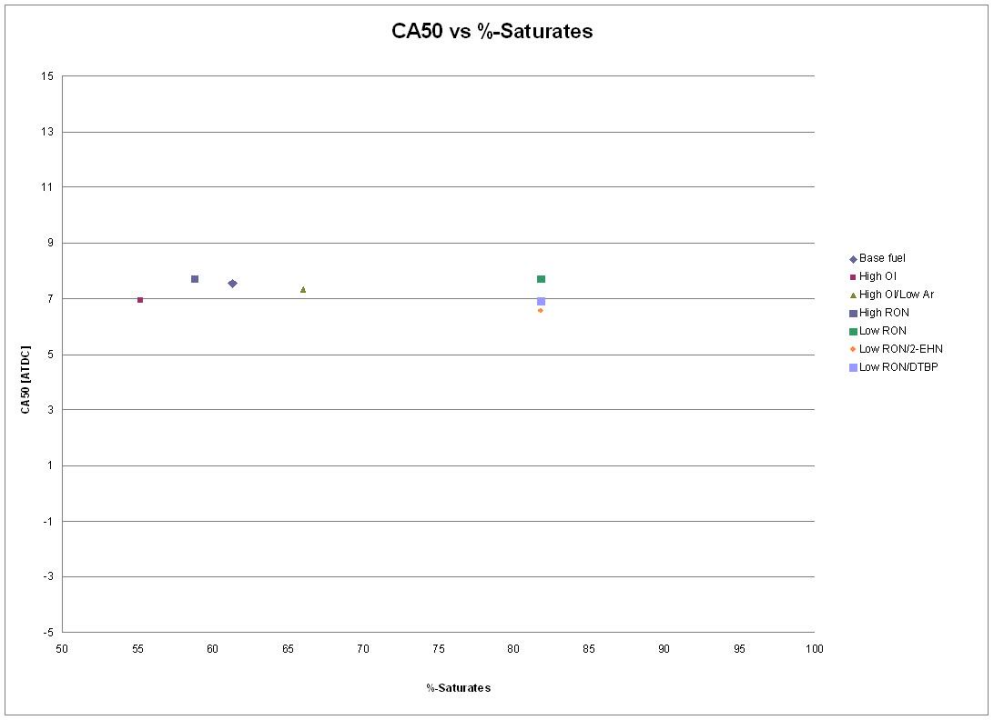

Figure B-3: Combustion phasing vs saturates content at the 1250 rpm HLL

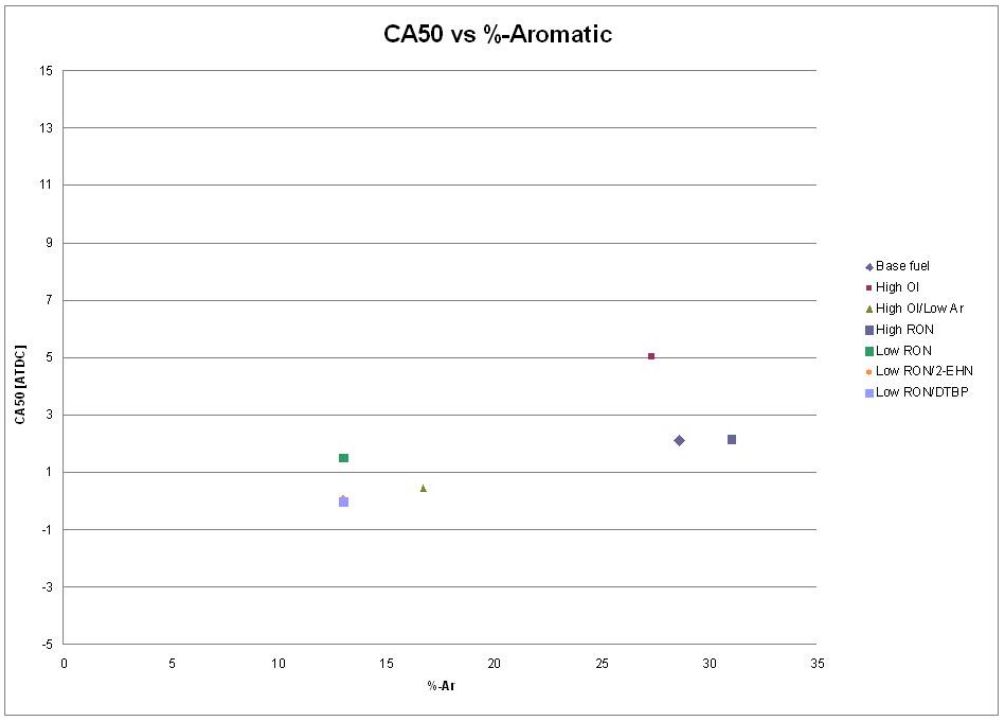

Figure B-4: Combustion phasing vs aromatic content at 2000 rpm interior point

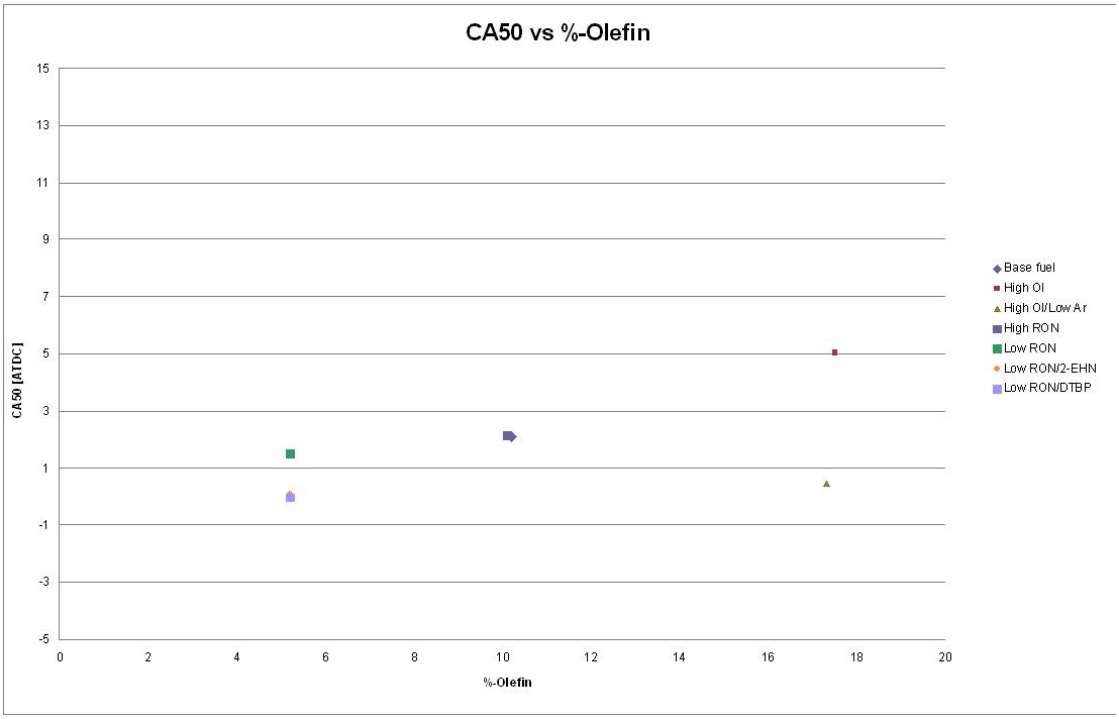

Figure B-5: Combustion phasing vs olefin content at 2000 rpm interior point

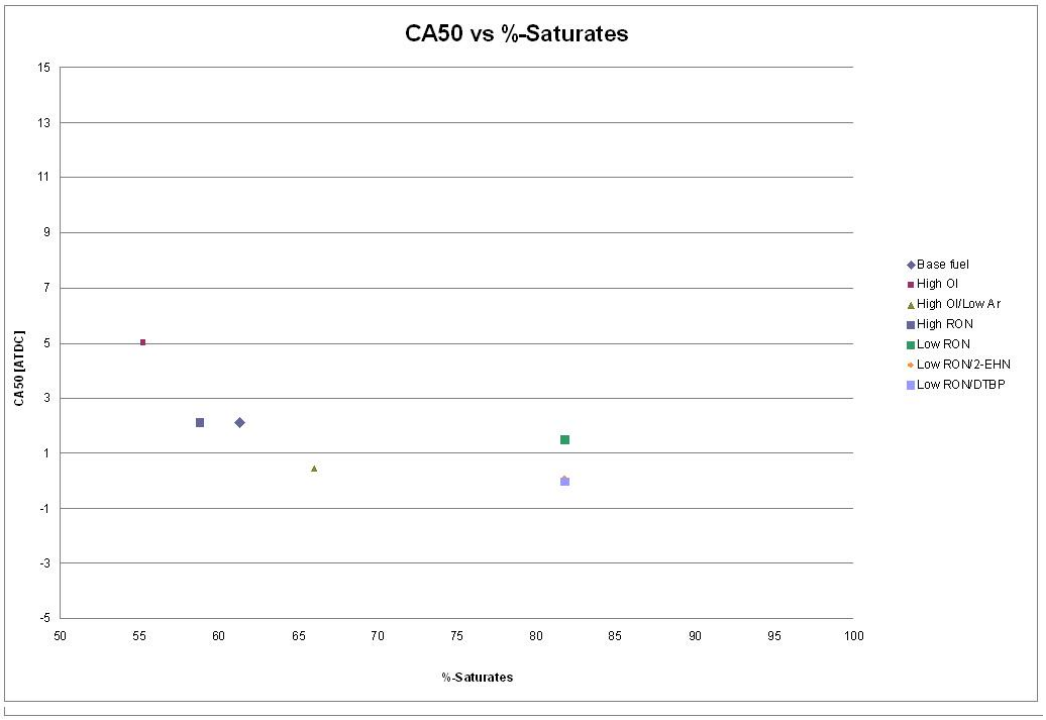

Figure B-6: Combustion phasing vs saturates content at 2000 rpm interior point

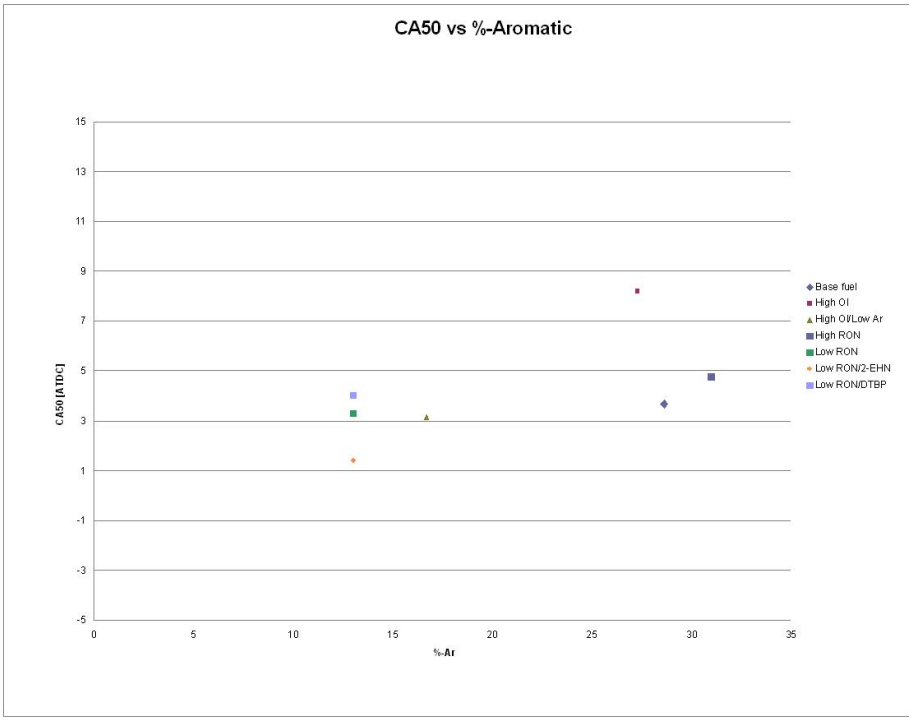

Figure B-7: Combustion phasing vs aromatic content at the 2500 rpm LLL

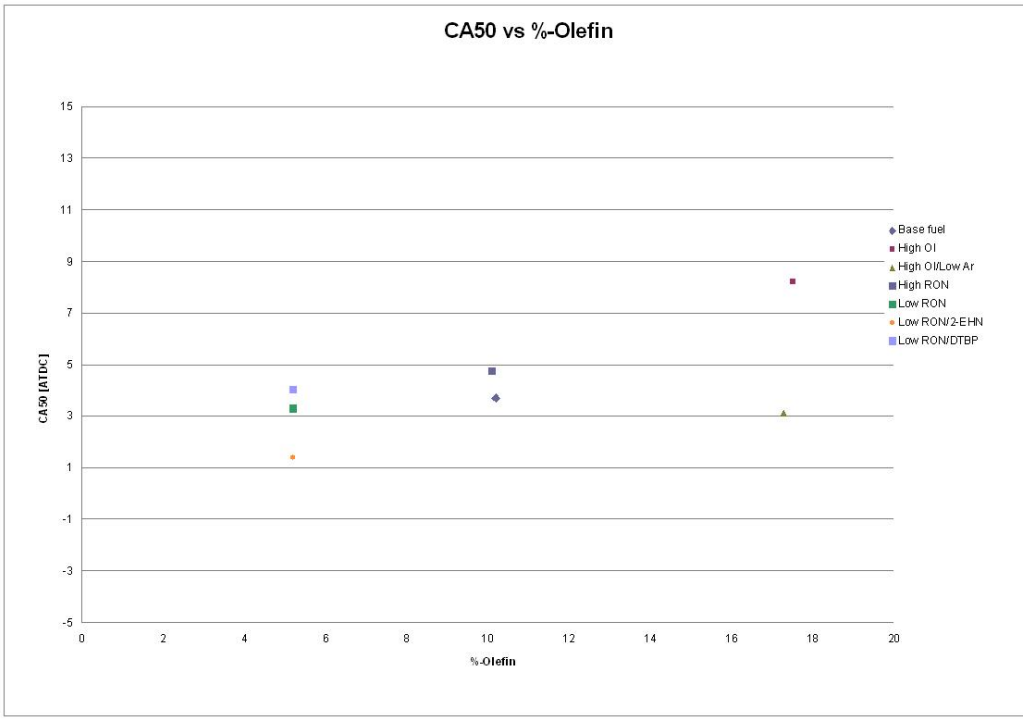

Figure B-8: Combustion phasing vs olefin content at the 2500 rpm LLL

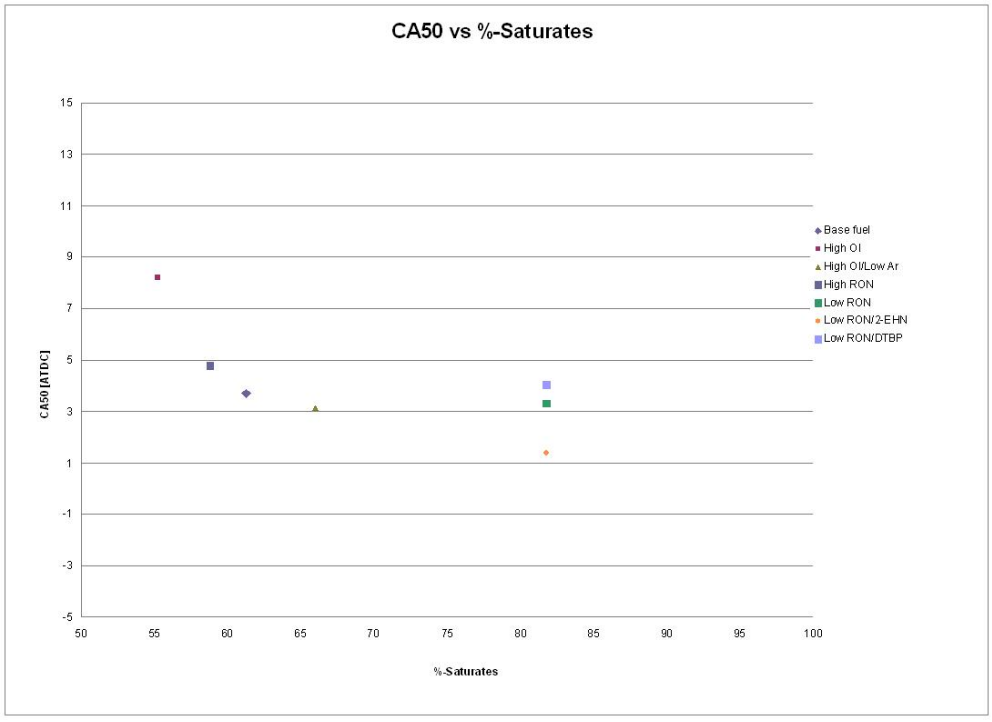

Figure B-9: Combustion phasing vs saturates content at the 2500 rpm LLL

Appendix C

PRR vs fuel composition at interior points

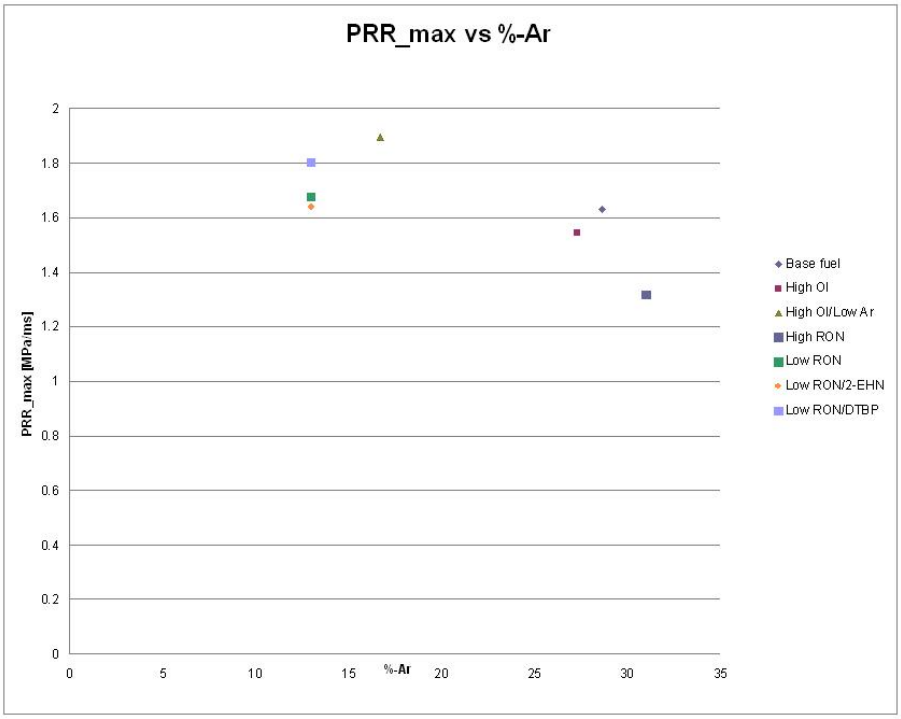

Figure C-1: PRR vs aromatic content at the 1250 rpm interior points

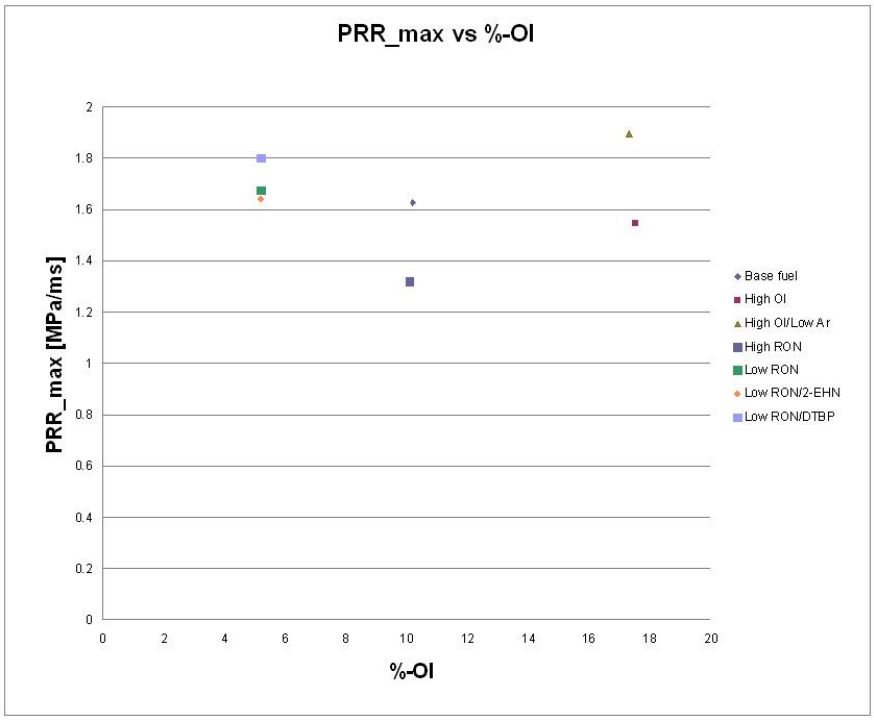

Figure C-2: PRR vs olefin content at the 1250 rpm interior points

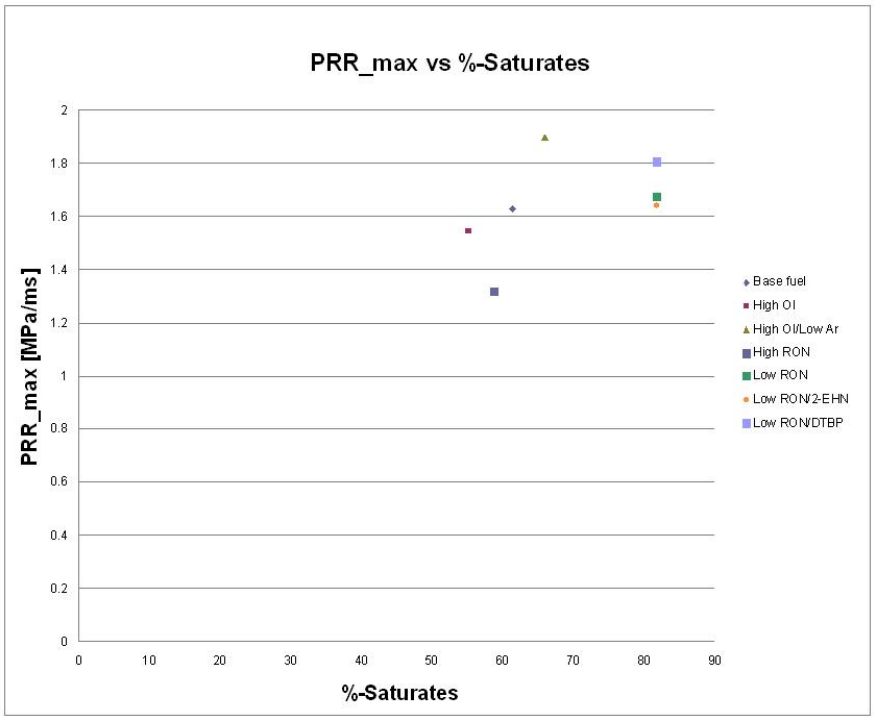

Figure C-3: PRR vs saturates content at the 1250 rpm interior points

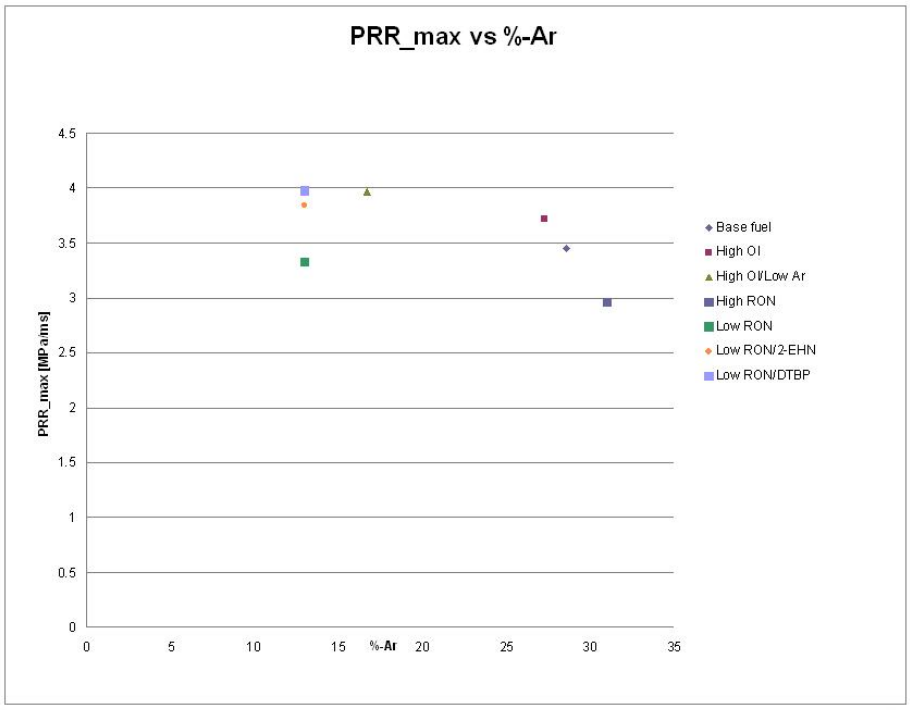

Figure C-4: PRR vs aromatic content at the 2000 rpm interior points

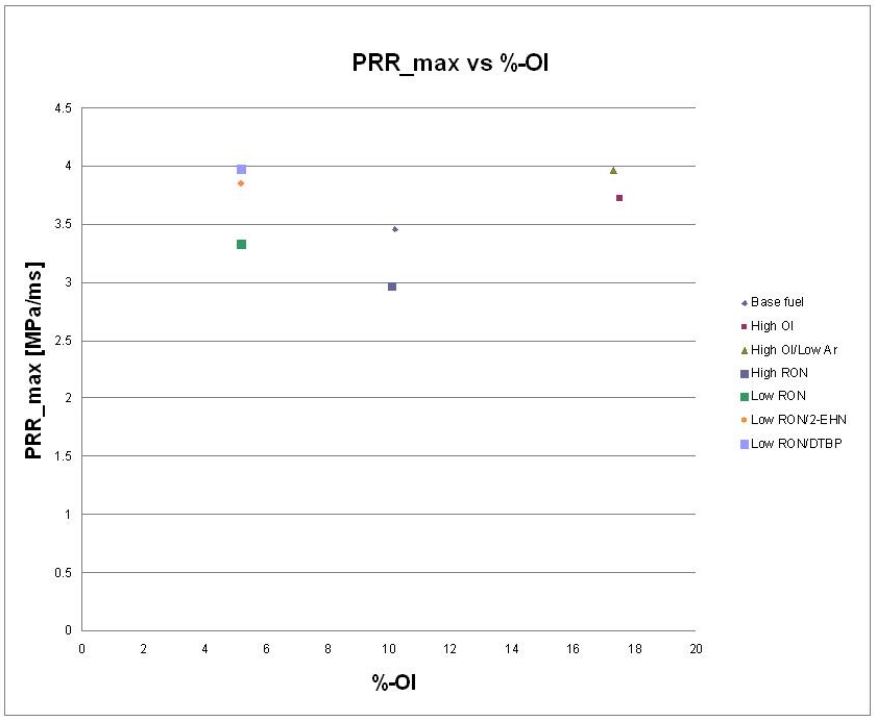

Figure C-5: PRR vs olefin content at the 2000 rpm interior points

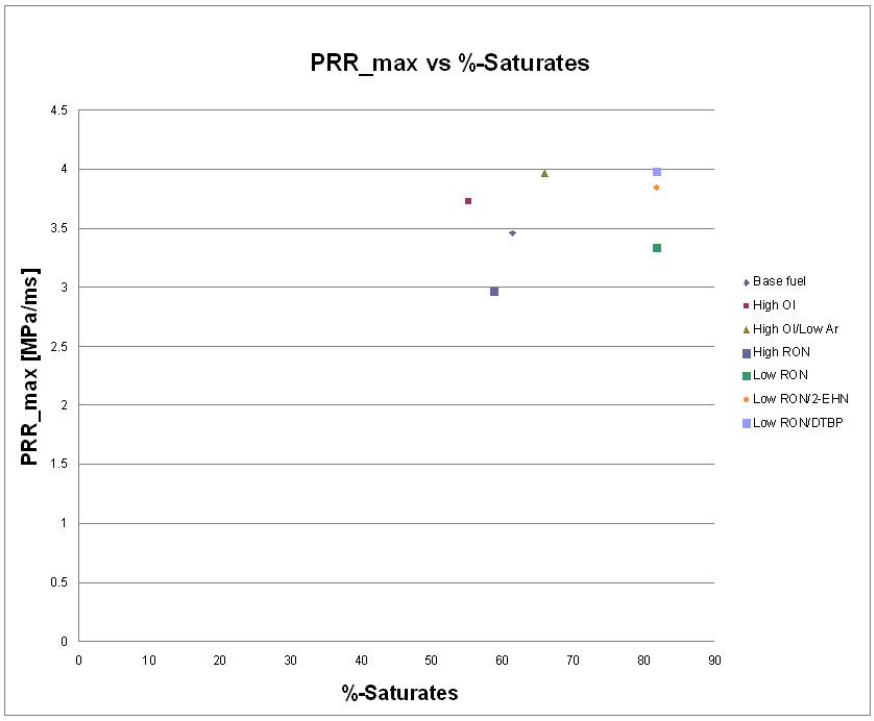

Figure C-6: PRR vs saturates content at the 2000 rpm interior points

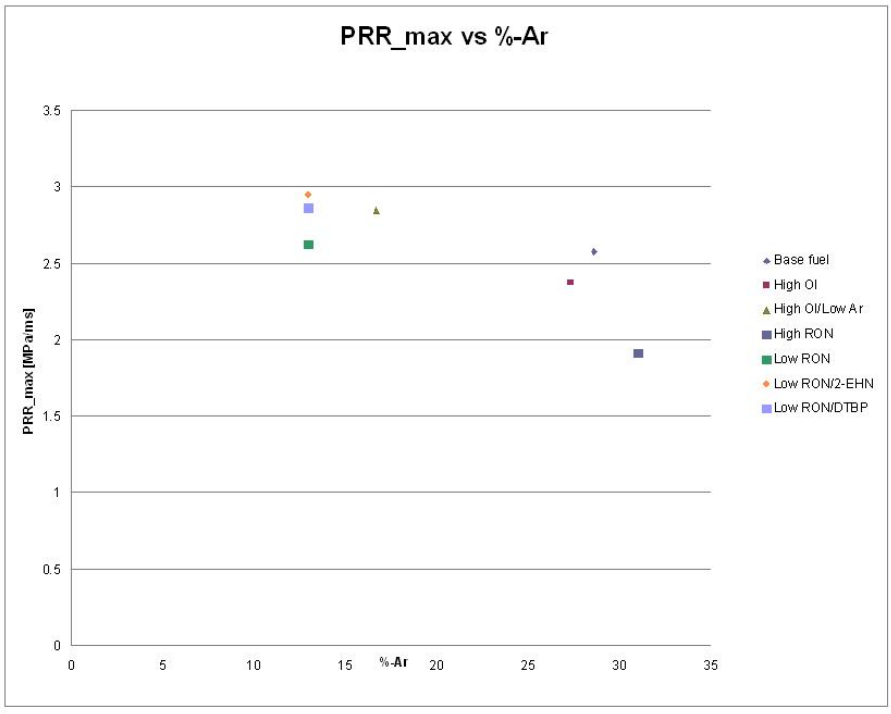

Figure C-7: PRR vs aromatic content at the 2500 rpm interior points

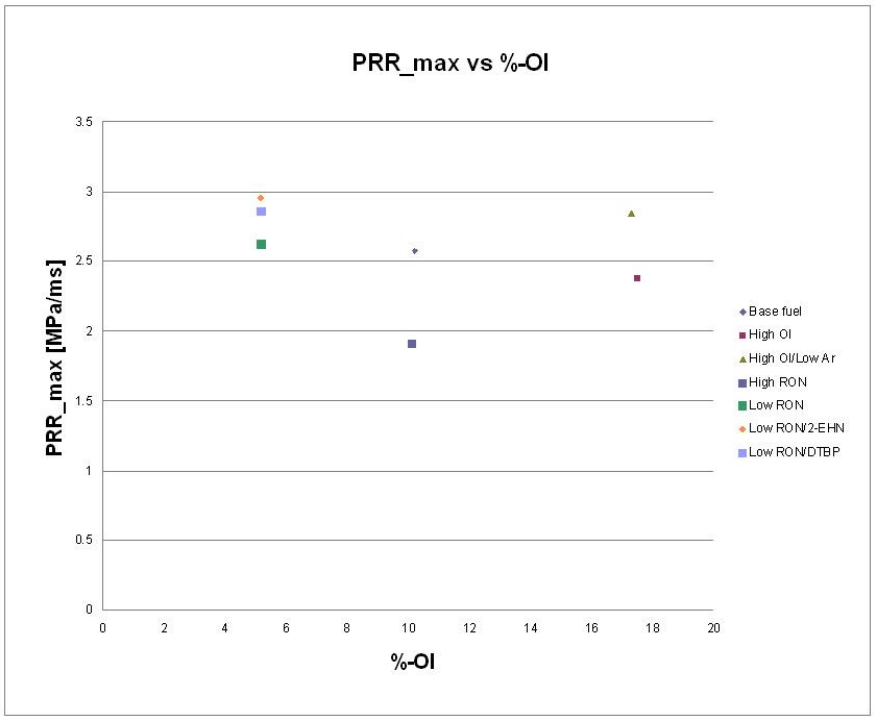

Figure C-8: PRR vs olefin content at the 2500 rpm interior points

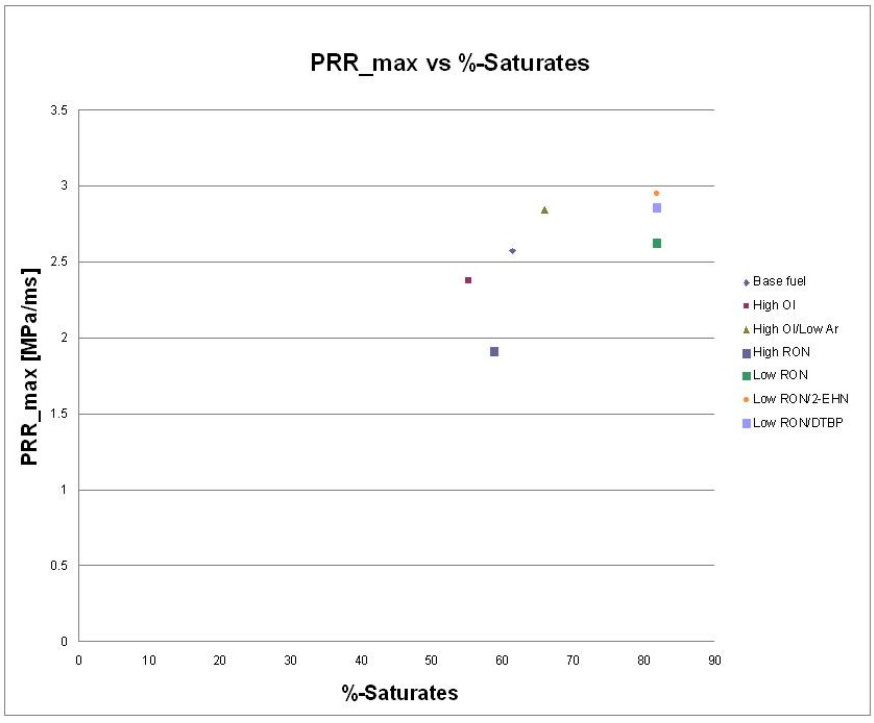

Figure C-9: PRR vs saturates content at the 2500 rpm interior points

Appendix D

BD1090 vs fuel composition at interior points

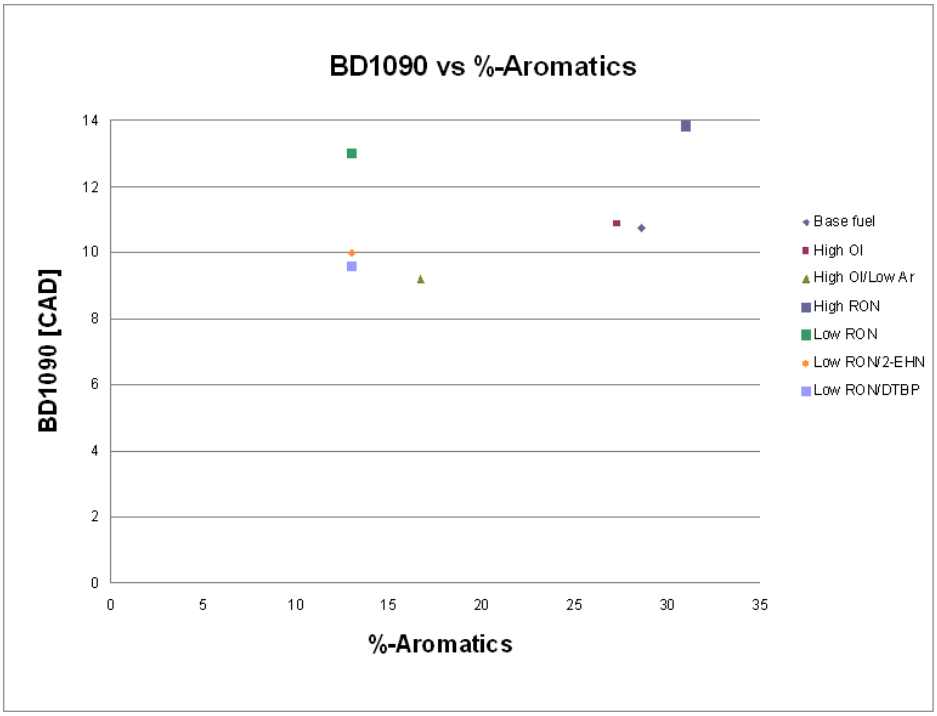

Figure D-1: BD1090 vs aromatic content at the 1250 rpm interior points

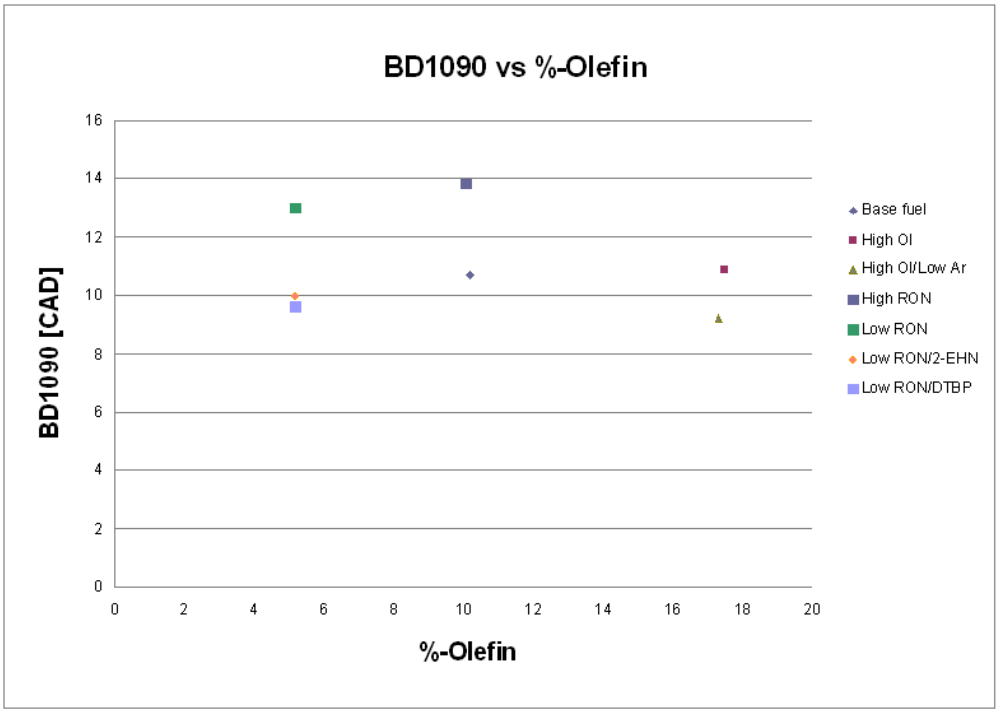

Figure D-2: BD1090 vs olefin content at the 1250 rpm interior points

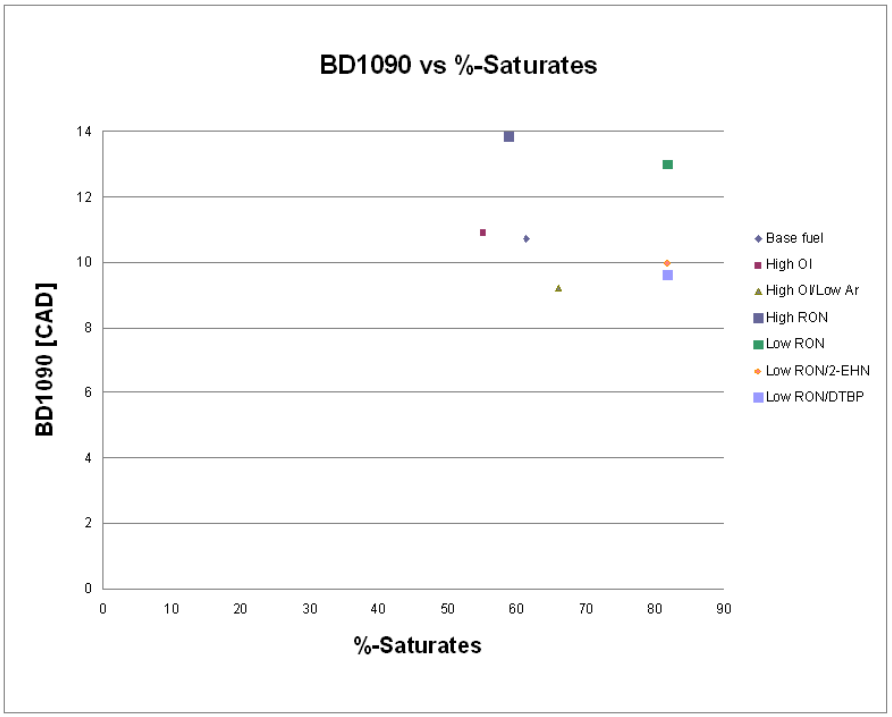

Figure D-3: BD1090 vs saturates content at the 1250 rpm interior points

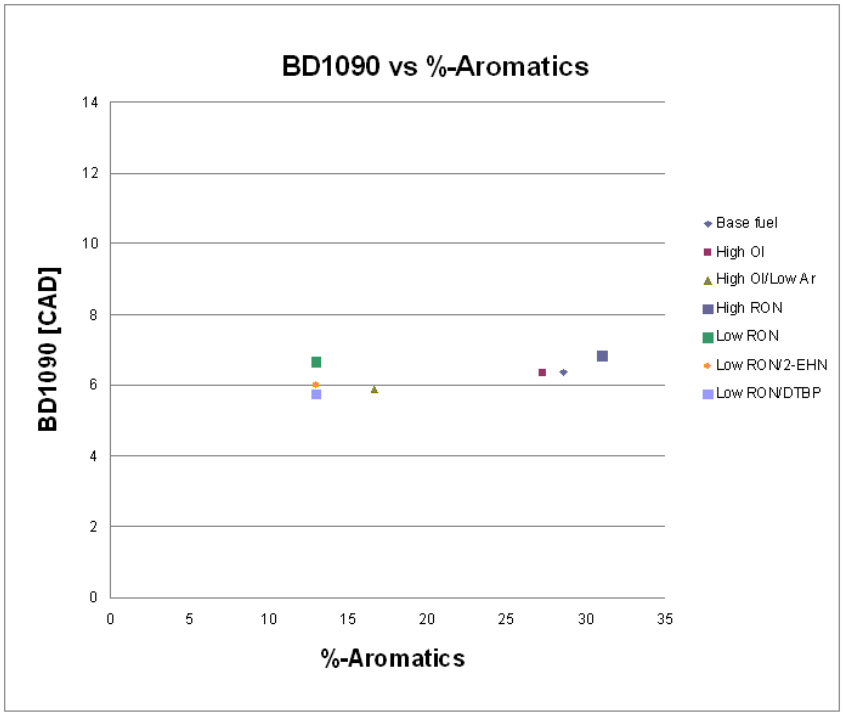

Figure D-4: BD1090 vs aromatic content at the 2000 rpm interior points

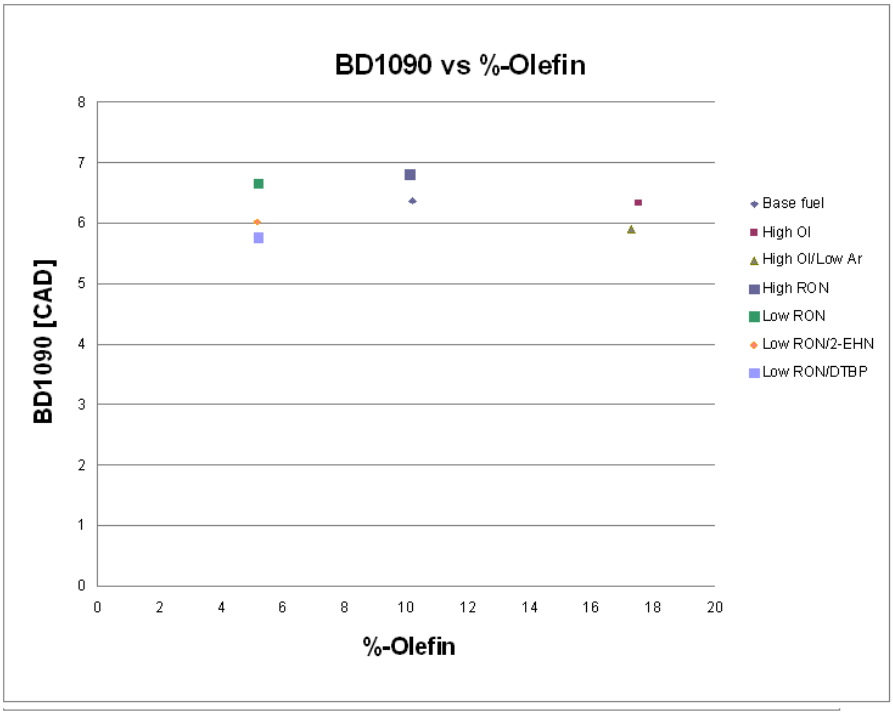

Figure D-5: BD1090 vs olefin content at the 2000 rpm interior points

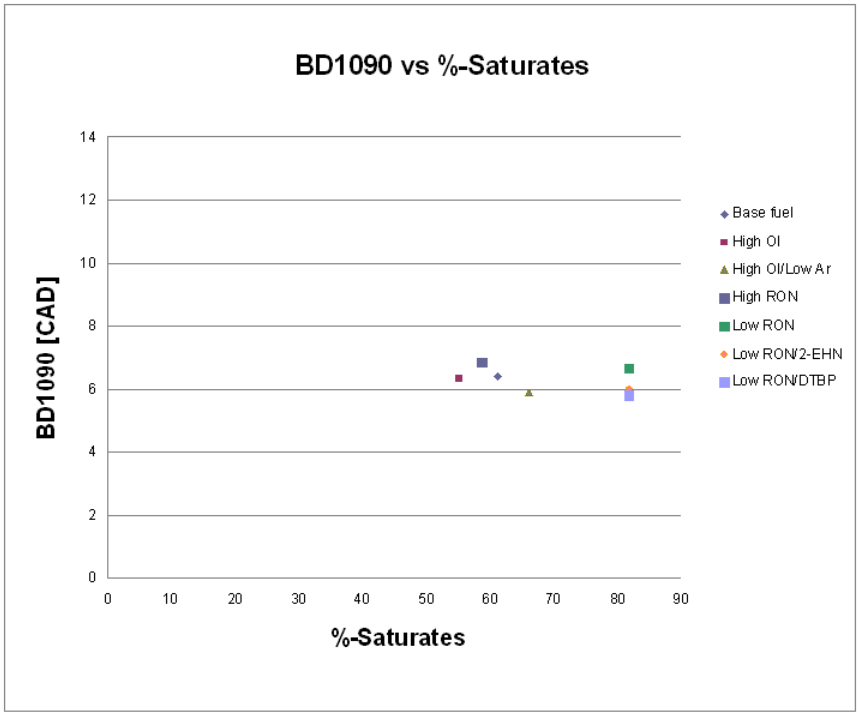

Figure D-6: BD1090 vs saturates content at the 2000 rpm interior points

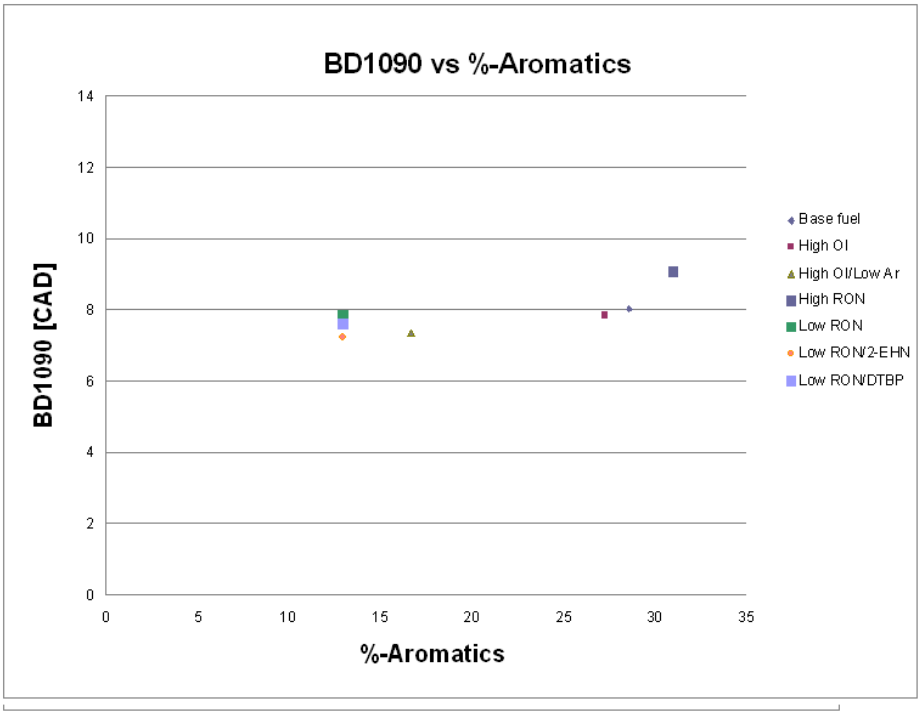

Figure D-7: BD1090 vs aromatic content at the 2500 rpm interior points

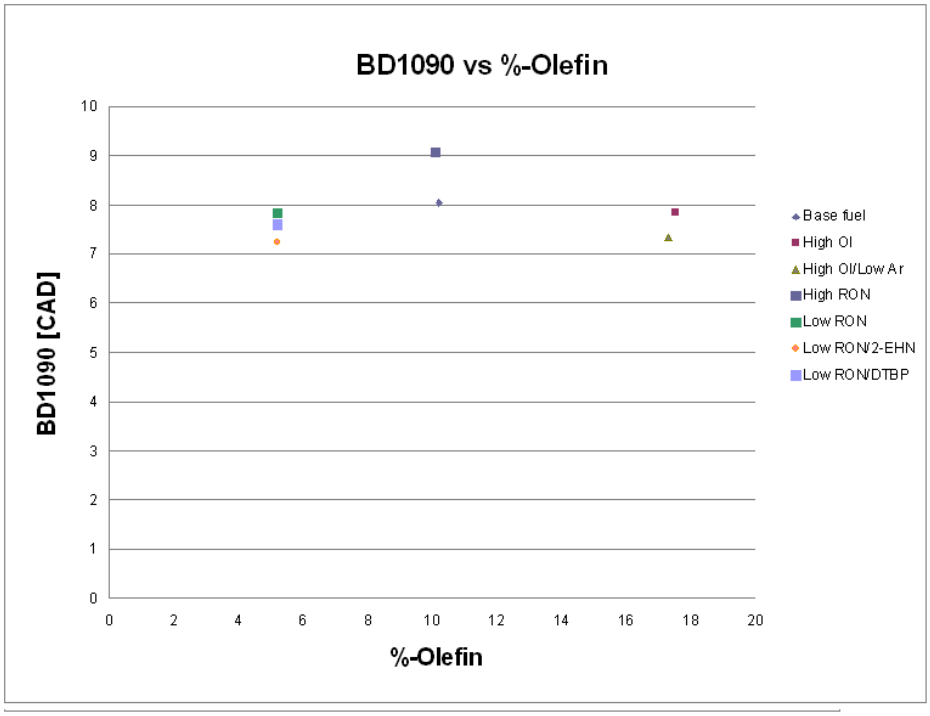

Figure D-8: BD1090 vs olefin content at the 2500 rpm interior points

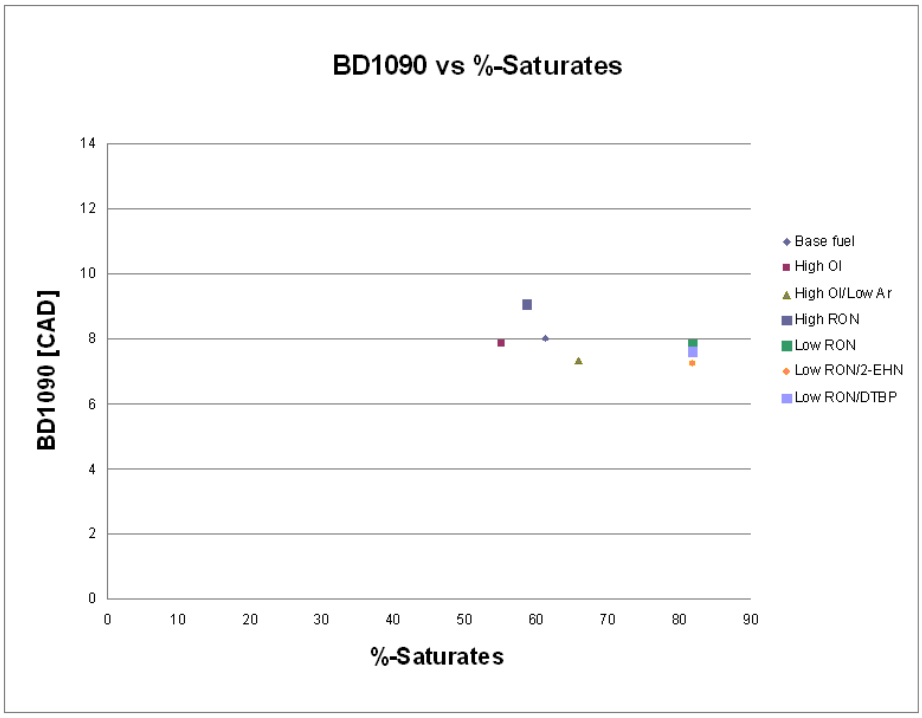

Figure D-9: BD1090 vs saturates content at the 2500 rpm interior points

Bibliography

[1] Fuquan Zhao. *Homogeneous Charge Compression Ignition (Hcci) Engines: Key Research and Development Issues*. SAE International, illustrated edition edition, March 2003.

[2] Magnus Christensen, Patrik Einewall, and Bengt Johansson. "Homogeneous Charge Compression Ignition (Hcci) Using Isooctane, Ethanol and Natural Gas– A Comparison With Spark-Ignition Operation." sae 972874. 1997.

[3] Daniel Dahl, Mats Andersson, Andreas W. Berntsson, Ingemar Denbratt, and Lucien Koopmans. "Reducing Pressure Fluctuations at High Loads by Means of Charge Stratification in HCCI Combustion with Negative Valve Overlap." SAE 2009-01-1785. 2009.

[4] Nebojsa Milovanovic, Dave Blundell, James Turner, and Stephen Gedge. "Cam Profile Switching (CPS) and Phasing Strategy vs Fully Variable Valve Train (FVVT) Strategy for Transitions between Spark Ignition and Controlled Auto Ignition Modes." SAE 2005-01-0766. 2005.

[5] Per Risberg, Gautam T. Kalghatgi, and Hans-Erik Angstrom. "The Influence of Egr on Autoignition Quality of Gasoline-Like Fuels in HCCI Engines." SAE 2004-01-2952. 2004.

[6] Magnus Sjoberg, John E. Dec, Aristotelis Babajimopoulos, and Dennis N. Assanis. "Comparing Enhanced Natural Thermal Stratification Against Retarded Combustion Phasing for Smoothing of HCCI Heat-Release Rates." SAE 2004-01-2994. 2004.

[7] Magnus Sjoberg, John Dec, and Wontae Hwang. "Thermodynamic and Chemical Effects of EGR and Its Constituents on HCCI Autoignition." SAE 2007-01-0207. 2007.

[8] Magnus Sjoberg, John E. Dec, and Nicholas P. Cernansky. "Potential of Thermal Stratification and Combustion Retard for Reducing Pressure-Rise Rates in HCCI Engines, Based on Multi-Zone Modelling and Experiments." SAE 2005-01-0113. 2005.

[9] Tomonori Urushihara, Kouichi Yamaguchi, Koudai Yoshizawa, and Teruyuki Itoh. "A Study of a Gasoline-Fueled Compression Ignition Engine-Expansion

of HCCI Operation Range Using Si Combustion as a Trigger of Compression Ignition." SAE 2005-01-0180. 2005.

[10] Magnus Christensen, Bengt Johansson, Per J. H. Amneus, and Fabian Mauss. "Supercharged Homogeneous Charge Compression Ignition." SAE 980787. 1998.

[11] Craig Wildman. *High load limits of the controlled autoignition engine*. PhD thesis, MIT, Cambridge, MA, 2009. Thesis (Ph. D.)–Massachusetts Institute of Technology, Dept. of Mechanical Engineering, 2009.

[12] Kathi Epping, Salvador M. Aceves, Richard L. Bechtold, and John E. Dec. "The Potential of Hcci Combustion for High Efficiency and Low Emissions." SAE 2002-01-1923. 2002.

[13] Jari Hyvonen. "Operating Conditions Using Spark Assisted HCCI Combustion During Combustion Mode Transfer to SI in a Multi-Cylinder VCR-HCCI Engine." SAE 2005-01-0109. 2005.

[14] Morgan M. Andreae. *Effect of ambient conditions and fuel properties on homogeneous charge compression ignition engine operation*. Thesis. Thesis (Ph. D.)–Massachusetts Institute of Technology, Dept. of Mechanical Engineering, 2006.

[15] Nathan Anderson. Examination of the high load limit of an HCCI engine. Thesis. Thesis (S.M.)–Massachusetts Institute of Technology, Dept. of Mechanical Engineering, 2008.

[16] Andreas Berntsson. *HCCI combustion using Charge Stratification and Spark-assistance*. PhD thesis, Chalmers University of Technology, Gothenburg, Sweden, 2009.

[17] Andreas W. Berntsson and Ingemar Denbratt. "Optical Study of HCCI Combustion Using NVO and an SI Stratified Charge." SAE 2007-24-0012. 2007.

[18] Lucien Koopmans, Ingemar Denbratt, and Ove Backlund. "Cycle-To-Cycle Variations: Their Influence on Cycle Resolved Gas Temperature and Unburned Hydrocarbons From a Camless Gasoline Compression Ignition Engine." SAE 2002-01-0110. 2002.

[19] Lucien Koopmans, Ingemar Denbratt, Hans Strm, Staffan Lundgren, and Ove Backlund. "Demonstrating a SI-HCCI-SI Mode Change on a Volvo 5- Cylinder Electronic Valve Control Engine." SAE 2003-01-0753. 2003.

[20] Halim G. Santoso, Jeff Matthews, and Wai K. Cheng. "Managing SI/HCCI Dual-Mode Engine Operation." SAE 2005-01-0162. 2005.

[21] Martin Weinrotter, Kurt Iskra, Ernst Wintner, Theo Neger, Jimmy Olofsson, Marcus Alden, Hans Seyfried, Max Lackner, Franz Winter, Anders Hultqvist, Andreas Vressner, and Bengt Johansson. "Optical Diagnostics of Laser-Induced and Spark Plug-Assisted HCCI Combustion." SAE 2005-01-0129. 2005.

[22] Morgan M. Andreae, Wai K. Cheng, Thomas Kenney, and Jialin Yang. "On HCCI Engine Knock." SAE 2006-01-0633. 2006.

[23] David E. Stikkers. Octane and the environment. *The Science of The Total Environment*, 299(1-3):37 – 56, 2002.

[24] George Douglas Hobson. *Modern Petroleum Technology*. Institute of Petroleum, Great Britain, 1984.